ISSN 0911-5730
UVSOR-14
April 1987

UVSOR
ACTIVITY REPORT
1986

Ultraviolet Synchrotron Orbital Radiation Facility
Institute for Molecular Science

CONTENTS

Status of the UVSOR Facility in 1986

H. Inokuchi
UVSOR Facility, Institute for Molecular Science
Myodaiji, Okazaki 444

1. Introduction

UVSOR is a dedicated VUV synchrotron light source used for research in molecular science and related fields. It is a 600 MeV (max. 750 MeV) electron storage ring, which is injected by a 600 MeV synchrotron and a 15 MeV linac. UVSOR first became operational in November, 1983. At present, 10 beam lines are available to users. They cover wavelengths from the far infrared to the soft X-ray region. Plan views of the UVSOR Facility and of the storage ring with its associated beam lines and the intensity distribution of synchrotron radiation from the bending magnets are presented in Figures 1-3. The main parameters of the light source and a description of the beam lines are given in Tables I and II. The organization of the facility is described in the Appendix.

2. Status of UVSOR

The light source operated throughout 1986, except for a shutdown in March. The normal operating schedules remained the same as for the last year: that is with Monday for machine studies and Tuesday to Friday inclusive for users. Beam is available from 9:15 to 13:00 and from 13:15 to 18:00 with two injections per day. A total of 44 weeks operation will be available to users in the fiscal year 1986.

During the March shutdown several important improvements were made to the source. Valves were inserted on both sides of the RF cavity, the damaged inner surfaces of the ceramic perturbator chambers were re-coated with gold and manual valves were installed on all vacant synchrotron radiation ports. A maximum current of 500 mA at 600 MeV was achieved in April and the source has been operated at 750 MeV since June. The normal current after injection is 100 mA with a lifetime at that current level of about 2 hours. Single bunch operation was achieved on several occasions for

time resolved spectroscopy users. The current is normaly around 5 mA in single bunch mode with a pulse width of about 0.4 ns. An undulator, beam pipe and mirror chambers were assembled for a free electron laser (FEL) experiment and also the characteristics of the undulator have been measured.

On BL2A, BL2B2 and BL3B, gas phase experiments have been carried out throughout the year, while BL6A2, BL7A, BL7B, BL8A and BL8B2 have been used primarily for solid state experiments. Especially noteable achievements have been on BL7A, where K edge absorption spectra of light elements were measured with high resolution and also on BL8B2 where angle-resolved photoelectron spectroscopy studies of organic solids had begun. New entirely two beam lines were opened to users: they are BL3A1,which uses undulator radiation without a monochromator and BL6A1 which exploits the infrared part of the synchrotron radiation using a Martin - Puplett interferometer. BL1B, with a 1 m Seya-Namioka monochromator and BL8B1, with a 2.2 m Rowland circle grazing incidence monochromator were set up and preliminary commissioning is now underway. These beam lines are expected to be available to users from April, 1987. It was decided to utilize BL5B as a calibration port for plasma diagnostics devices under the direction of the Institute of Plasma Physics, Nagoya University.

Within the fiscal year 1986, 4 research programmes of "Joint Studies", 15 programmes of "Cooperative Research" and 52 programmes of "Use of Facility" will be undertaken, in addition to the research studies of the staff in Department of Molecular Assemblies at IMS. A Users' Meeting, and a workshop on Beam Dynamics and Free Electron Lasers were held and the 28th Okazaki Conference on "Solid State Chemistry with VUV Synchrotron Radiation "was held from 5-7 February, 1987.

Acknowledgments

The light source and the beam line instrumentation are working very well and the research programme at UVSOR continues to expand in scale and in quality. We would like to express sincere thanks both to in-house staff and to outside users for their excellent support.

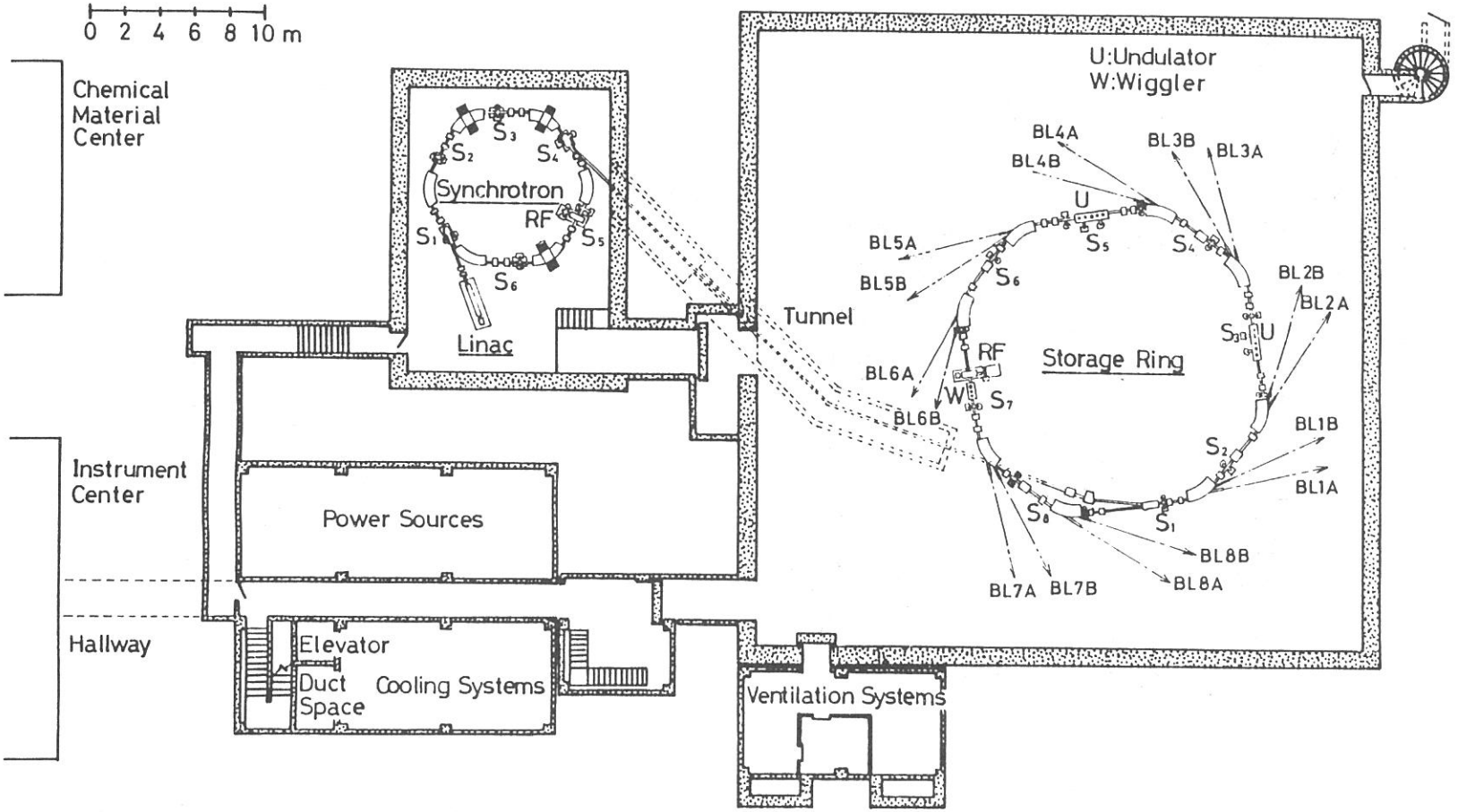

Fig. 1 Plan view of the basement of the UVSOR Facility.

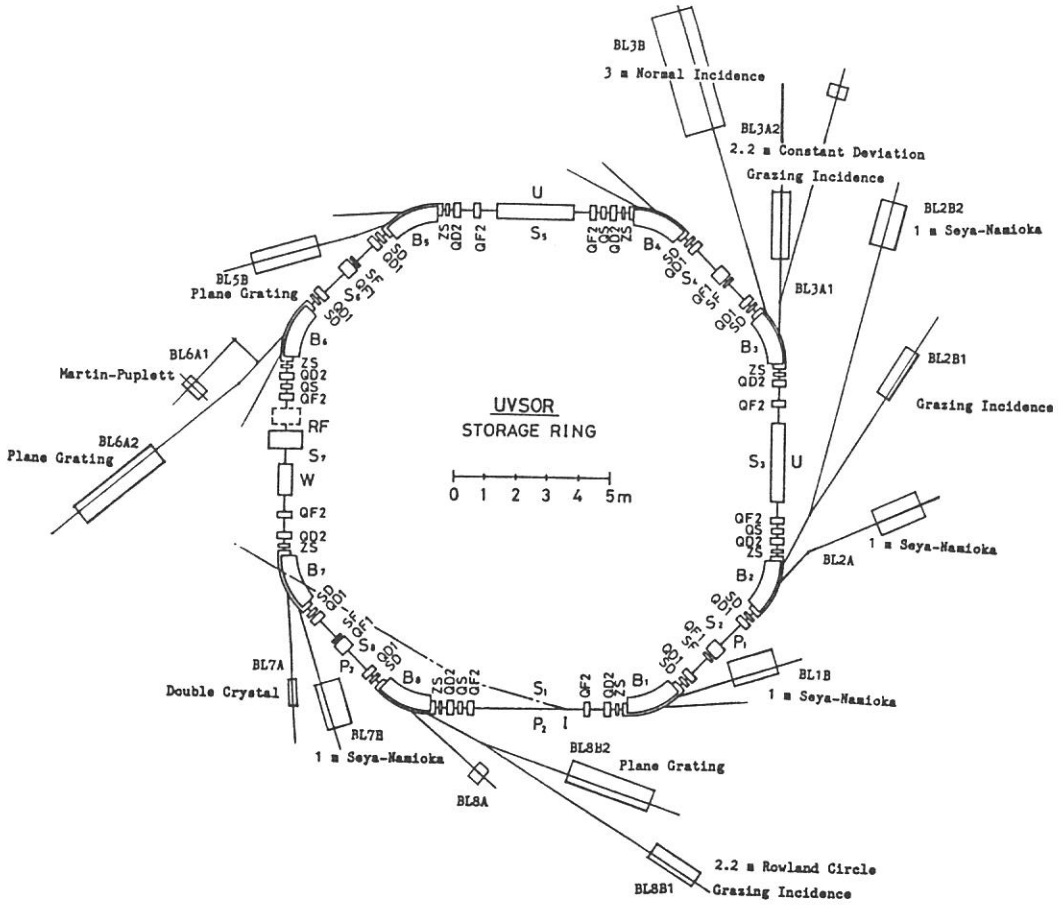

Fig. 2 Plan view of the UVSOR storage ring with associated beam lines.

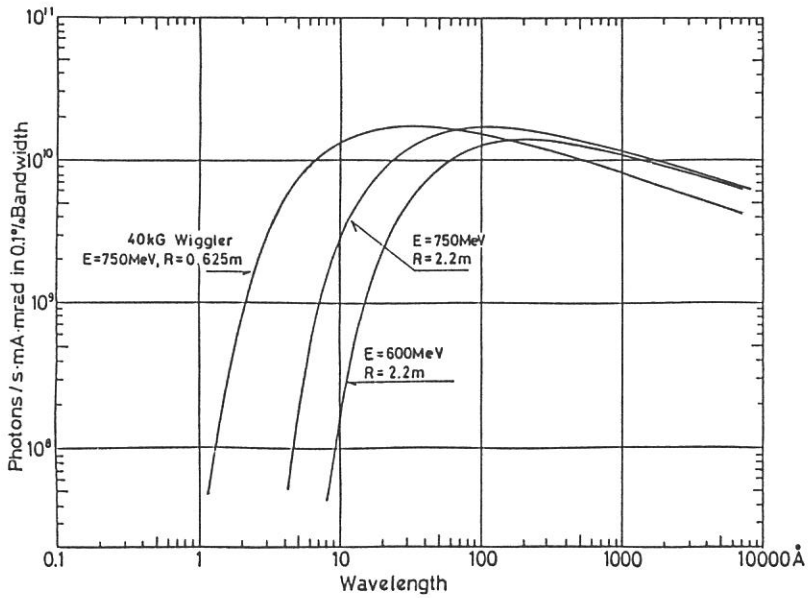

Fig. 3 Intensity distribution of the radiation from the UVSOR.

Table I Main Parameters of UVSOR

	Designed		Achieved	
Linac				
Energy	15	MeV	20	MeV
Frequency	2.856	GHz		
Synchrotron				
Energy	600	MeV	600	MeV
Current	50	mA	20	mA
Circumference	26.6	m		
Periodicity	6			
Bending Radius	1.8	m		
Tune (Q_H, Q_V)	(2.25, 1.25)			
Harmonic Number	8			
Radio Frequency	90.1	MHz		
Repetition Rate	1-3	Hz	2.5	Hz
Storage Ring				
Energy	600 (max. 750 MeV)	MeV	750	MeV
Critical Wavelength	56.9	A		
Current	500	mA	500	mA
Lifetime	1 (500 mA)	hr	2 (100 mA)	hr
Circumference	53.2	m		
Periodicity	4			
Bending Radius	2.2	m		
Bending Field	0.91	T		
Tune (Q_H, Q_V)	(3.25, 2.75)			
Harmonic Number	16			
Radio Frequency	90.1	MHz		
RF Voltage	75	kV		
Radiation Damping Time				
Horizontal	45.4	ms		
Vertical	40.9	ms		
Longitudinal	19.5	ms		
Emittance				
Horizontal	$8\pi\times10^{-8}$	m.rad	$16\pi\times10^{-8}$	m.rad
Vertical	$8\pi\times10^{-9}$	m.rad*		
Beam Size (at the Center of Bending Section)				
Horizontal ($2\sigma_H$)	0.64	mm		
Vertical ($2\sigma_V$)	0.46	mm*		
Bunch Length ($2\sigma_\tau$)	0.17	ns	0.4	ns

*10% coupling is assumed.

Table II Beam Lines at UVSOR

Beam Line	Monochromator, Spectrometer	Wavelength Region	Acceptance Angle(mrad) Horiz.	Vert.	Experiment
BL1B	1 m Seya-Namioka	6500-300 Å	60	6	Gas & Solid
BL2A	1 m Seya-Namioka	4000-300 Å	40	6	Gas
BL2B1**	Grazing Incidence				Gas
BL2B2	1 m Seya-Namioka	2000-300 Å	20	6	Gas
BL3A1	None (Filter, Mirror)		(U) 0.3	0.3	Gas & Solid
BL3A2*	2.2 m Constant Deviation	1000-100 Å	10	4	Gas & Solid
	Grazing Incidence		(U) 0.3	0.3	
BL3B	3 m Normal Incidence	4000-300 Å	20	6	Gas
BL5B*	Plane Grating	2000- 20 Å	10	2.2	Calibration#
BL6A1	Martin-Pupplet	5 mm-50 μm	80	60	Solid
BL6A2	Plane Grating	6500-80 Å	10	6	Solid
BL7A	Double Crystal	15-8 Å	2	0.3	Solid
		15-2 Å	(W) 1	0.15	
BL7B	1 m Seya-Namioka	6500-300 Å	40	8	Solid
BL8A	None (Filter)		25	8	Irradiation, User's Instr.
BL8B1	2.2 m Rowland Circle	440-20 Å	10	2	Solid
	Grazing Incidence				
BL8B2	Plane Grating	6500-80 Å	10	6	Solid

* : under construction. ** : under contemplation. # : Institute of Plasma Physics, Nagoya University. U : with an undulator. W : with a wiggler.

LIGHT SOURCE

FREE ELECTRON LASER EXPERIMENT AT UVSOR

Hiroto YONEHARA, Toshio KASUGA, Toshio KINOSHITA
and Masami HASUMOTO

Institute for Molecular Science, Myodaiji, Okazaki 444

Storage ring Free Electron Laser (FEL) experiment using the UVSOR is planned. The wavelength considered for this study is decided within visible light, especially 488 nm wavelength, for simplicity of the optical system. Parameters of this experiment are tabulated in Table 1. For this purpose a plane undulator was constructed, of which parameters are shown in Table 2. Effects of the undulator on the stored electron beam are studied and the required low energy operation of the ring for studying the FEL can be accomplished. And the beam lifetime of the single bunch beam of 10 mA is about 5 minutes, which is well agreed with the calculated value. The spectrum of the undulator radiation was analyzed by a monochromator Jobin Yvon (HR-320). And the intensity of the light was measured with a photo-multiplier which was placed at the outlet of the monochromator. This measurement was carried out with the undulator gap between 29.5 mm and 31.5 mm as shown in Fig. 1.

To measure the gain of the FEL, the laser light of 488 nm was run through the undulator duct from the other end of it, and aligned to overlap on the electron beam. At the same time, the circuit for the gain measurement, of which block diagram is shown in Fig. 2 , is tested.

Electron Energy	Number of Bunches	Current in a Bunch	Wavelength	Length of the Optical Cayity	Expected Gain
270 MeV	2	10 mA	488 nm	13.3 m	1 %

Table 1 ; Parameters of FEL at UVSOR

magnet	B_r (gauss)	N	K	λ_0
$SmCo_5$ (LM22) ($18.5^t x 18.5^h x 90^w$)	8700 ~ 8900	29	2.5 (gap=30)	74 mm

Table 2 ; Parameters of Undulator

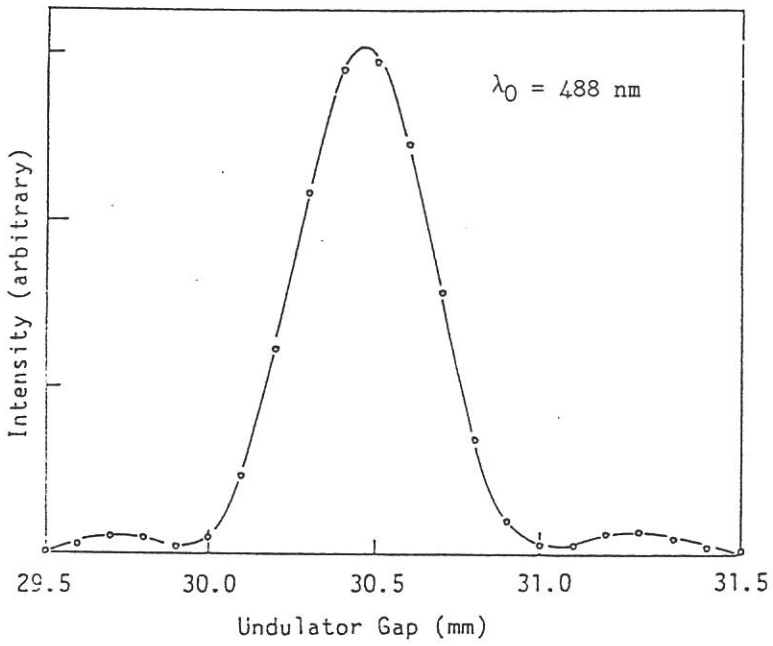

Fig. 1 ; Intensity Distribution vs. Undulator Gap

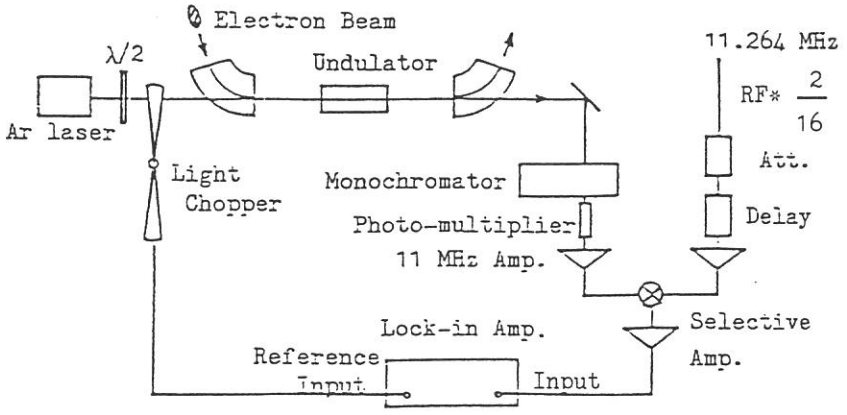

Fig. 2 ; Block Diagram of Gain Measurement

EQUIPMENT DEVELOPMENT

CONSTRUCTION OF AN APPARATUS FOR PHOTOCHEMICAL SURFACE REACTION STUDIES

Nobuo HAYASAKA,* Atsunari HIRAYA, and Kosuke SHOBATAKE
Institute for Molecular Science, Myodaiji, Okazaki 444 JAPAN
* Sponsorial Research Fellow from VLSI Research Center, Toshiba Corp., Komukai Toshiba-cho, Saiwai-ku, Kawasaki 210 JAPAN

Photo-assisted surface reactions on solid semiconductor materials have attracted considerable attention from the viewpoint of their applications to semiconductor processes. Much progress has been made using visible and UV light. Natural extension of these studies is to use vacuum UV light. However nothing is known about what would happen on solid surface when VUV light is irradiated upon it in a reactive gas atmosphere. We have thus constructed an apparatus to study photochemical surface reactions using synchrotron radiation as a light source.

Figure 1 is a schematic of the apparatus installed on beam line BL8A. It consists of two chambers, a reaction chamber(RC) and a differential pumping chamber (DPC), which are connected to each other via a channel (6mm diameter X 80mm long) (C). The RC is pumped by a 330 l/sec turbomolecular pump (TP) and the DPC by a 600 l/sec TP and a liq. N_2 cryopump (CP) as well. A thin Ti foil (T) fitted between the DPC and the beam line chamber serves both as a filter to select the wavelength range of the irradiated light and as a window to prevent reactive gas from going into the beam line.

Silicon samples (kept at ~ 27°C) (S) are held on a sample manipulator (SM) in the reaction chamber, the base pressure of which is 1.0×10^{-9}Torr. After the gate value GV-1 is closed, Cl_2 gas is constantly flowed upon the solid surface into the reaction chamber through a multichannel capillary array. The Cl_2 pressure in the reaction chamber ranged from 0.05 to 0.5 Torr and was controlled by a needle valve in the gas inlet line plus a choke valve between the RC and chlorine trap (T), which consists of a liq. N_2 cryopump followed by a chemical vacuum pump.

The UVSOR synchrotron is operated at 750 MeV beam energy. A Ti filter 500 Å thick which is transparent mostly in the extreme vacuum region 1-20 nm was used. When the filtered SR is admitted

spectrum of the glow was recorded in the visible and UV region as shown in Fig. 2. The strong lines are identified as Cl^+ transitions. Since the formation of Cl^+ ions was identified, a rectangularly netted Ni mesh (M) with 64% transmittance was positioned 0.6 cm upstream from the Si sample. The Ni mesh was biased up to $\pm$ 75 volts to observe the effect of an applied electric field on the Si etch rate.

From the absorption spectra of metallic Ti and the SR operated at 750 MeV, we have estimated the total number of photons irradiated upon the heavily phosphorous doped poly-crystalline silicon (n^+ poly-silicon) surface to be 5.2 x 10^{13} photons s^{-1} cm^{-2} per mA stored current and the average photon energy to be 322 eV. Etching experiments were normally done at a Cl_2 pressure of 0.3 Torr. The quantum yield for the removal of Si atoms was found to be 0.5 % when the Ni mesh was kept at ground, and that to be 1.0 % when the Ni mesh was positively biased at 75 volts, providing with a 900 $\pm$ 100 Å etch depth for 230 mA hr irradiation, as illustrated in the abstract of 28th Okazaki Conference of the present issue.

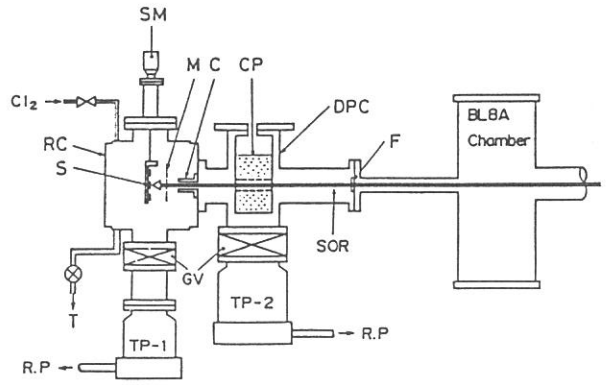

Fig. 1. Apparatus used for photochemical surface reaction studies. See the text for explanations except for R.P.: rotary pump; C: channel.

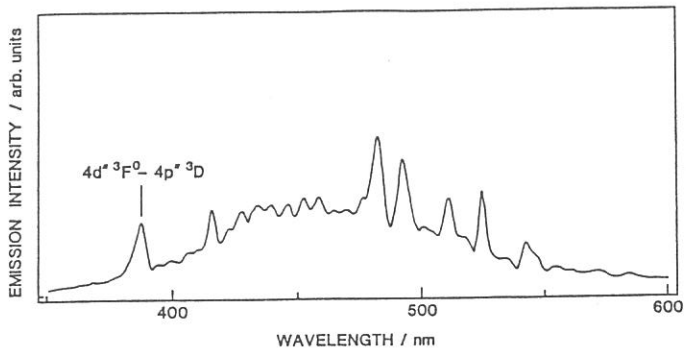

Fig. 2. Emission spectrum in the wavelenghth region 350-600 nm of the fluorescence from the light path of the SR (monochromator resolution: 3 nm).

ANGLE-RESOLVED UPS SYSTEM AT BL8B2

Kazuhiko SEKI*, Hitoshi FUJIMOTO, Takehiko MORI, and Hiroo INOKUCHI

*Institute for Molecular Science, Myodaiji, Okazaki 444
*Department of Materials Science, Faculty of Science, Hiroshima University, Hiroshima 730

An angle-resolving UPS system was constructed at BL8B2. The setup is shown in Fig. 1. Synchrotron radiation from UVSOR is monochromatized by the previously reported plane-grating monochromator[1] which supplies radiation in the energy range of 2 - 150 eV. The photoelectron spectrometer consists of a preparation chamber, a measurement chamber, and a transfer system. Each chamber is evacuated by a combination of an sputter ion pump, a turbomolecular pump, and a Ti getter pump, with a final pressure of 10^{-10} Torr range. A hemispherical electron-energy analyzer of 25 mm mean radius can be rotated around vertical and horizontal axes. The sample mounted on a

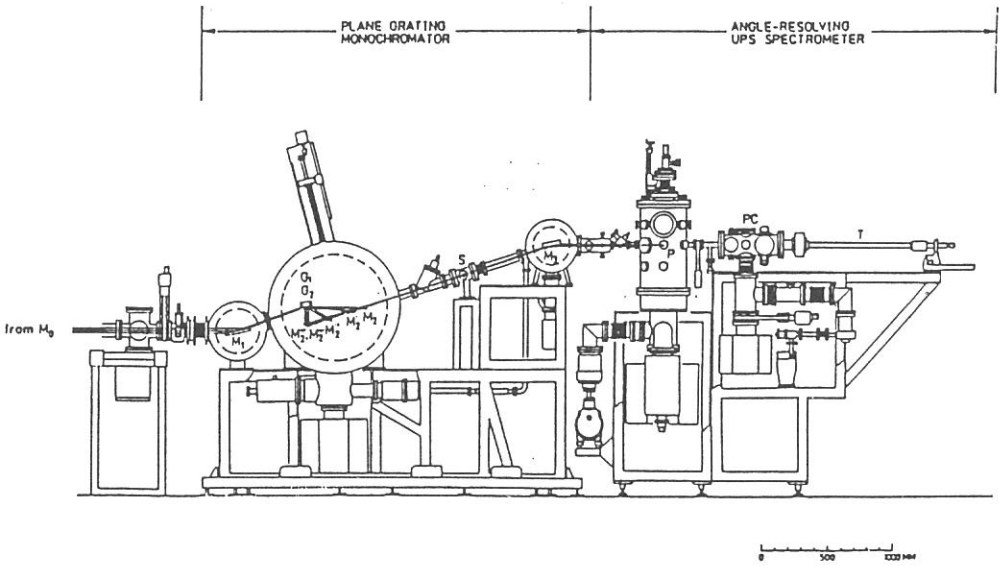

Fig. 1. Angle-resolving UPS system.

manipulator can be also rotated around two axes. The system is designed primarily for measuring various organic solids such as molecular crystals, polymers, and graphite intercalation compounds. The samples are prepared on a small disk of 12 mm in diameter by methods such as vacuum evaporation and cleavage. The total resolution was 0.2 eV, as determined by mesuring the Fermi edge of gold. In Fig. 2, we show a test spectrum of RbCl taken at various photon energies. Now the electronic structures of n-$CH_3(CH_2)_{34}CH_3$ and poly(phenylene sulfide) is being measured, the former being reported in another article of this report.

Reference

1) K. Seki, H. Nakagawa, K. Fukui, E. Ishiguro, R. Kato, T. Mori, K. Sakai, and M. Watanabe, UVSOR Activity Report 1984/85 p.35; Nucl. Instrum. Methods Phys. Res., A246, 264 (1986).

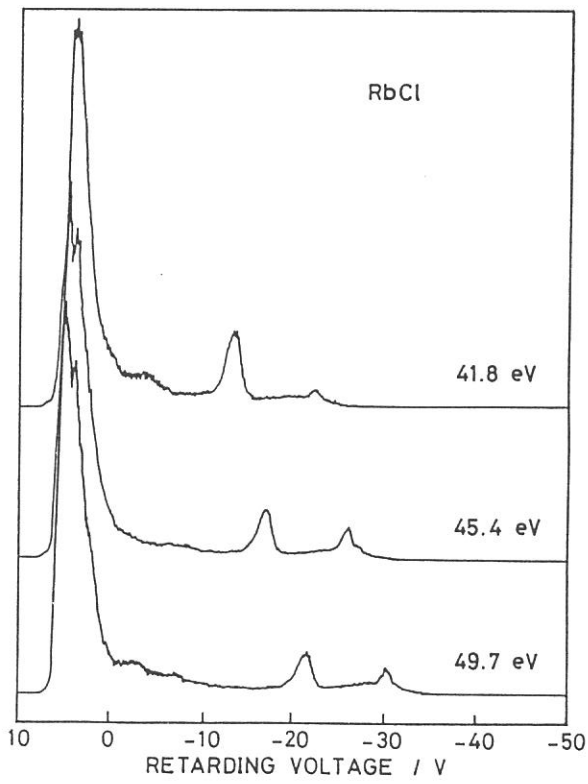

Fig. 2. Normal emission spectra of RbCl in retarding potential scale. The kinetic energy of photoelectrons increase from left to the right.

RESEARCH ACTIVITIES

VACUUM-ULTRAVIOLET ABSORPTION SPECTRA OF CCl_3F and CCl_2F_2

Toshio IBUKI, Atsunari HIRAYA* and Kosuke SHOBATAKE*
Institute for Chemical Research, Kyoto University, Uji, Kyoto 611
*Institute for Molecular Science, Myodaiji, Okazaki 444

Chlorofluoromethanes such as CCl_3F and CCl_2F_2 are typical aerosol propellants and refrigerants, and recently they have used as dry or plasma echants. The role of halogenated methanes in photochemistry in the upper atmosphere has been debated since the stratospheric ozone layer may or may not be depleted by Cl atoms released through solar photolysis of chlorofluoromethanes. Because of the importance of the ozone layer as solar UV-radiation shield, many investigations of their absorption or photoreactions have been carried out, mostly at $\lambda > 170$ nm.

Figures 1 and 2 show the absorption and fluorescence excitation spectra of CCl_3F and CCl_2F_2, respectively, using an apparatus at the BL-2A station of UVSOR. The valence shell configuration of CCl_3F is $(3e)^4(5a_1)^2(4e)^4(5e)^4(1a_2)^2$.[1] Chlorine lone pair orbitals are of a_2, e, e and a_1 symmetries, the ionization potentials of which are in order 11.76, 12.13, 12.96 and

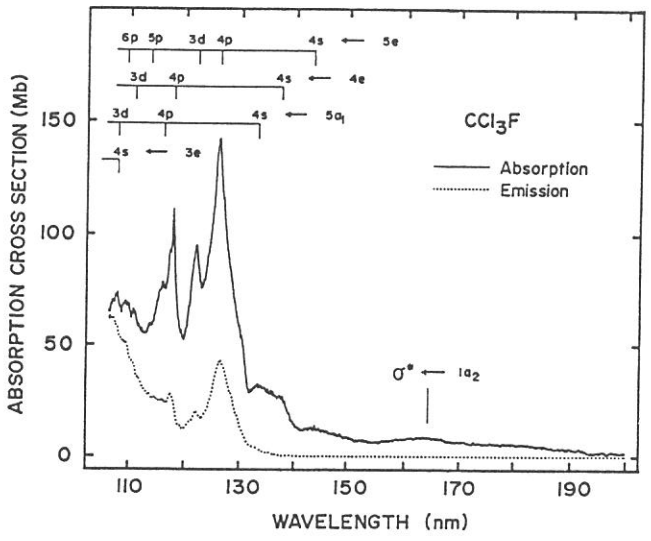

Fig. 1. Absorption and fluorescence excitation spectra of CCl_3F.

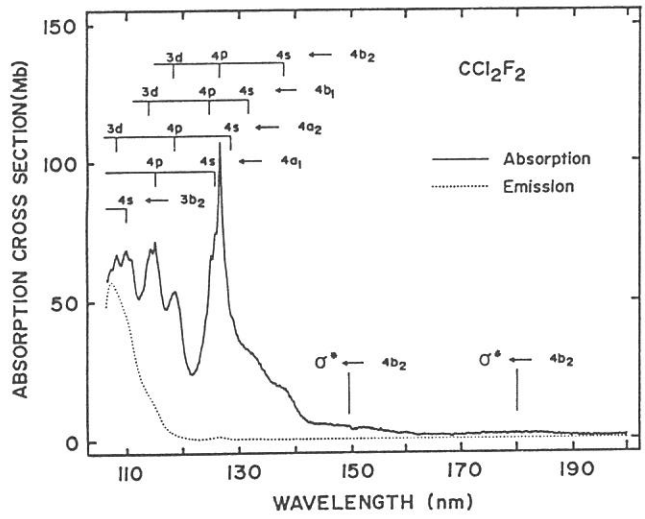

Fig. 2. Absorption and fluorescence excitation spectra of CCl_2F_2.

13.42 eV, respectively.[1] The next inner 3e orbital represents mainly the σ_{C-Cl} bonding electron with IP = 15.01 eV. Using these IP values, the Rydberg assignments are given in Fig. 1.

The electronic configuration of the outer shells of CCl_2F_2 is expressed as $(3b_2)^2(4a_1)^2(4a_2)^2(4b_1)^2(4b_2)^2$.[2] Adopting the published IPs of these orbitals,[2] the assignments of the Rydberg transitions are also given in Fig. 2.

The emitters are assigned as $CClF(\tilde{A}^1A'')$ and $CF_2(\tilde{A}^1B_1)$ radicals in the photodecomposition of CCl_3F and CCl_2F_2, respectively. The thresholds for the fluorescence strongly support the following processes:

$$CCl_3F + h\nu \rightarrow CClF(\tilde{A}) + 2Cl,$$
$$CCl_2F_2 + h\nu \rightarrow CF_2(\tilde{A}) + 2Cl.$$

The radiative lifetimes of the excited $\tilde{A}$ state of CClF and CF_2 are determined to be 650 ± 20 and 58 ± 2 ns, respectively.

References

1) M. R. Jardrny, L. Karlsson, L. Mattsson, and K. Siegbahn, Phys. Scri. 16, 235 (1977).

2) T. Cvitas, H. Güsten, and L. Klansinc, J. Chem. Phys. 67, 2687 (1977).

ABSORPTION AND FLUORESCENCE SPECTRA OF S_2Cl_2 AND $OSCl_2$

Ikuo TOKUE, Atsunari HIRAYA*, and Kosuke SHOBATAKE*

Department of Chemistry, Niigata University, Niigata 950-21
*Institute for Molecular Science, Myodaiji, Okazaki 444

Several photochemical studies have been made on S_2Cl_2[1] and $OSCl_2$[2,3] Time resolved spectroscopic studies of S_2Cl_2[1] in the near ultraviolet flash photolysis indicate that primary process is in the fission of the S-S bond following an $n-\pi^*$ or $n-\sigma^*$ transition:

$$S_2Cl_2 + h\nu \longrightarrow 2SCl. \qquad (1)$$

The excited states of SO, $A^3\Pi$ and $B^3\Sigma$, were found to be formed in the photodissociation of $OSCl_2$[3] at the Kr resonance lines. The primary process for producing of SO(A) near its threshold energy is

$$OSCl_2 + h\nu \longrightarrow SO(A) + 2Cl(^2P_{3/2}). \qquad (2)$$

In the present work, the photoabsorption cross section (c.s.) and fluorescence excitation spectrum of S_2Cl_2 and $OSCl_2$ in the vacuum ultraviolet (VUV) were measured. Fluorescence spectra from the excited fragments produced were observed in the 200-500 nm region in the experiment. All chemicals obtained commercially were vacuum-distilled and stored in a pyrex container. All data were measured at vapor pressure lower than 20 mTorr.

The photoabsorption c.s. of S_2Cl_2 as a function of wavelength in the 105-200 nm region are reproduced in fig. 1 with the fluorescence excitation spectrum. In the absorption spectrum several peaks are attributed to the HCl impurity; the concentration of HCl impurity is estimated to be $\simeq 5$ %. The experimental uncertainty in the absorption c.s. was estimated to be within ± 15 % of the given value. The fluorescence excitation spectrum in the 110-150 nm region follows closely the main features in the absorption c.s. Dispersed emission measured at the excitation wavelength of 113.0, 115.8 and 125.8 nm is shown in fig. 2. The spectral resolution of emission is 6 nm. Three emission bands are probably observed; namely, the relatively sharp bands centered at 256 and 316 nm and the broad band centered at 350 nm. Comparing with the assignment of the absorption spectrum by Donovan et al.[1], we concluded that the broad band centered at 350 nm is attributed to the $S_2(B-X)$ band. The threshold wavelength of incident photons for producing fluorescence measured by monitoring both the total emission and the emission at 320 ± 6 nm is 155.5 ± 0.6 nm; fluorescence from HCl impurity longer than 125 nm is negligible. The primary process for producing of $S_2(B)$ near

its threshold energy is

$$S_2Cl_2 + h\nu \longrightarrow S_2(B) + 2Cl(^2P_{3/2}). \qquad (3)$$

The minimum energy required for Reaction (3) is 7.99 eV(155.2 nm).

The photoabsorption c.s.and the fluorescence intensity of $OSCl_2$ as a function of wavelength in the 105-220 nm region have been measured. The absorption c.s. observed in the 115-135 nm region is found to be ≃ 25 % smaller than that reported by Okabe[3]. This is probably caused by the Cl_2, HCl and SO_2 impurities. The fluorescence excitation spectrum of $OSCl_2$ shows two peaks at 107 and 113 nm. The emission spectra with the spectral resolution of 6 nm were observed at the excitation wavelengths of 107±1 and 113±1 nm. The sharp band centered at 256 nm and the broad band in the 240-400 nm region are attributed to the SO(A-X) and SO(B-X) band, respectively. The threshold wavelengths of the excitation photons for producing the fluorescence measured by monitoring the total emission and the emission at 256±6 nm are 132.±0.6 and 130.6±0.6 nm, respectively. These are in good agreement with the value reported by Okabe[3].

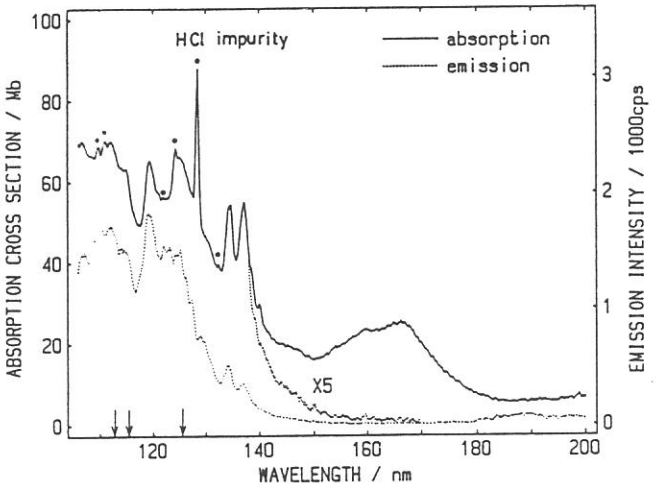

Fig. 1. The absorption c.s. and fluorescence excitation spectra of S_2Cl_2

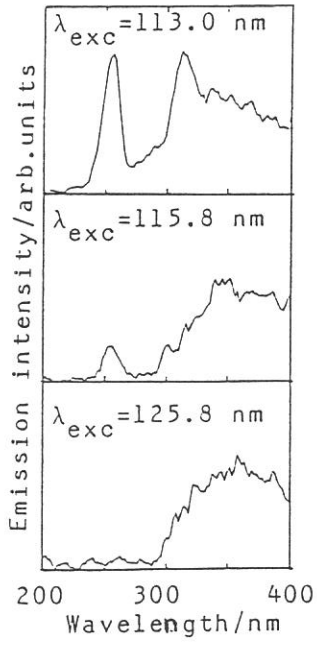

Fig. 2. Emission spectra produced from S_2Cl_2 at 113.0, 115.8 and 125.8 nm excitations

References

[1] R.J.Donovan, D.Husain and P.T.Jackson, Trans. Faraday Soc. 64, 1798 (1968); R.J.Donovan, D.Husain and C.D.Stevenson, ibid. 66, 1(1970).

[2] R.J.Donovan, D.Husain and P.T.Jackson, Trans. Faraday Soc. 65, 2930(1969).

[3] H. Okabe, J. Chem. Phys. 56, 3378(1972).

ISOTOPE EFFECT ON THE FLUORESCENCE CROSS SECTION FOR THE DISSOCIATIVE EXCITATION PROCESSES. II. CH_3OH AND ITS DEUTERATED COMPOUNDS.

Atsunari HIRAYA and Kosuke SHOBATAKE

Institute for Molecular Science, Myodaiji, Okazaki 444

In order to elucidate the conspicuous isotope effect on the quantum yield of $CN^*(A,B)$ formation in photodissociative excitation of CH_3CN and CD_3CN[1] by VUV light, fluorescence cross sections of CH_3OH and its deuterated compounds, in which CN group is replaced by OH or OD, have been investigated.

Figure 1 shows the absorption and fluorescence excitation spectra of CH_3OH and CD_3OD. The emission excitation spectrum was obtained by monitoring the total emission in the wavelength range 180 - 650 nm. Two emitting species are possible for the photodissociative excitation of CH_3OH, i.e. OH^* and CH_3O^*. The threshold wavelengths for the formation of OH^* and CH_3O^* are indicated by arrows in the fluorescence excitation spectra. The observed onsets of total emission for both compounds are in good agreement with the calculated threshold of 155 nm for $OH^*(OD^*)$ formation. Although the total emission excitation spectrum is a superposition of the excitation function of OH^* and CH_3O^*, the dispersed emission spectrum was found to be

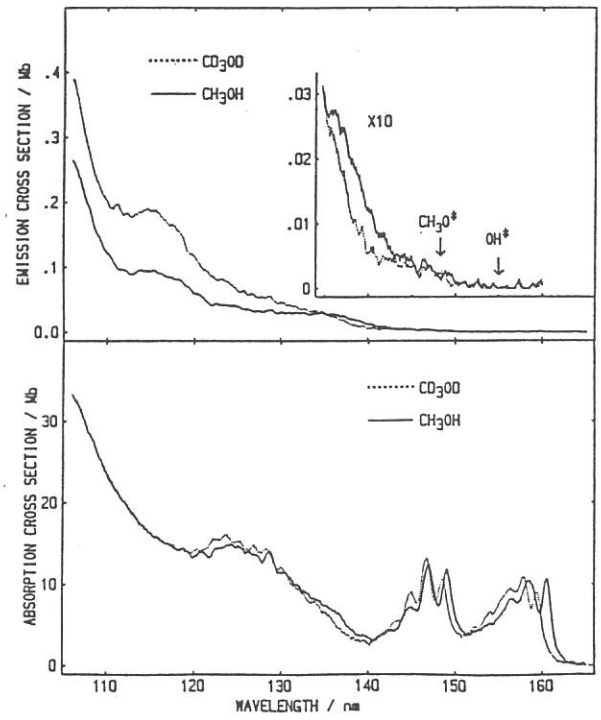

Figure 1. Absorption and total emission excitation spectra of CH_3OH (solid line) and CD_3OD (dotted line) in gas phase.

dominated by $OH^*(OD^*)$ emission band at 310nm. Therefore it can be said that the total emission excitation spectrum mainly represent the excitation function of OH^*.

The total emission cross section of CD_3OD is about a factor of two larger than that of CH_3OH in the shorter wavelength region than 134 nm. On the contrary, such a notable isotope effect was not found for CH_3OD within the experimental error. Therefore, it was concluded that the substitution of deuterium atoms for hydrogen atoms at methyl group enhances the formation of OH^*, as was already found for the formation of CN^* from CH_3CN and CD_3CN. The similar isotope effect observed for these two molecules, each having a different functional group OH or CN, strongly supports our previous model that such a conspicuous isotope effect on the emission cross section originates from the variation in the rates of other dissociation channels, which compete with OH^* or CN^* formation, and involve the motion of hydrogen (deuterium) atoms in the methyl group, i.e. C-H (C-D) rupture.

Because $CH_3O(^2A_1 - X^2E)$ emission extends from 280 to 450 nm, the excitation function of CH_3O^* can be obtained by monitoring emissions at wavelength longer than 350nm, as shown in Figure 2. These excitation functions of CH_3O^* are entirely different from both the absorption and the total emission excitation spectra. This implies that OH^* and CH_3O^* are formed via different electronic states. The observed isotope effect on the formation of CH_3O^* is quite different from that of OH^*. One can reasonably explain it in terms of the isotope effect on the competition between C-H bond and O-H bond ruptures.

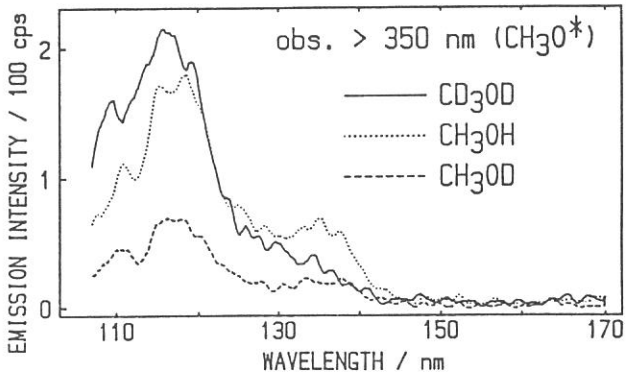

Figure 2. Emission excitation spectra obtained by monitoring longer wavelengths than 350nm

Reference

1) K. Shobatake et al., Ann. Rev. IMS 1984, p.96; UVSOR activity report 1984/85, p. 43.

ISOTOPE EFFECT ON THE FLUORESCENCE CROSS SECTION FOR THE DISSOCIATIVE EXCITATION PROCESSES. III. EVIDENCE OF CCl_2 FORMATION FROM $CHCl_3$ AND $CDCl_3$.

Atsunari HIRAYA, Toshio IBUKI*, and Kosuke SHOBATAKE

Institute for Molecular Science, Myodaiji, Okazaki 444
*Institute for Chemical Research, Kyoto Univ., Uji, Kyoto 611

As a part of a series of our investigations on the isotope effect upon the photodissociative excitation processes, relative emission cross sections of excited photofragment(s) formed by vacuum UV photolyses of $CHCl_3$ and $CDCl_3$ were determined. Figure 1(a) shows the emission excitation spectra of $CHCl_3$ and $CDCl_3$. The absorption spectrum of $CDCl_3$ is almost the same as that of $CHCl_3$ shown in Figure 1(b). The emission cross section for these two isotopic compounds are almost identical in the wavelength region above 122 nm, while below 120nm that for $CHCl_3$ is about a factor of 1.5 larger than that for $CDCl_3$. Two emitting species, CCl_2^* and $CHCl^*$, should be taken into account for the observed wavelength region. The observed isotope effect provides some more information about the emitting species. Below 120 nm, where isotope effect on emission cross section becomes apparent, CCl_2^* radical must be dominant because the CCl_2^* formation involves the C-H rupture whose rate is reduced by deuterium substitution. Above 120 nm where no isotope effect is observed, however, dominant emitting species must be $CHCl^*$ which is formed without C-H rupture. Consistently with this identification for emitting species, $CHCl^*$ radical is found to be dominant at 121.6 nm from lifetime measurements.

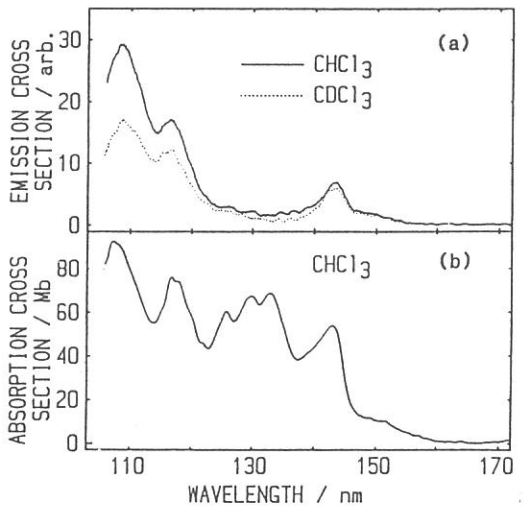

Figure 1. Emission excitation spectra of $CHCl_3$ and $CDCl_3$ (a), and absorption spectrum of $CHCl_3$ (b).

ABSORPTION AND FLUORESCENCE EXCITATION SPECTRA OF H_2O IN SUPERSONIC FREE JET

Atsunari HIRAYA and Kosuke SHOBATAKE

Institute for Molecular Science, Myodaiji, Okazaki, 444 Japan

Spectroscopic and photochemical investigations for the electronically excited molecules in the gas phase are often limited by thermal distrbutions of the vibrational and rotational levels. Such a limitation has been circumvented by using a supersonic free jet technique that provides rotationally and vibrationally cooled molecules in the gas phase. Furthermore, this technique has been known to be quite useful for producing many varieties of molecular clusters. However, for the jet-cooled molecules, only very few direct absorption spectra and emission excitation spectra have been observed in the VUV region. This is mainly due to some limitations, such as the wavelength region, tunability and stability of light soureces. These limitations can be overcome to a considerable extent by means of SOR as a light source, even though there are some disadvantages of SOR compared to lasers, i.e. wavelength resolution and intensity.

We report here preliminary results of the measurment of direct absorption and fluorescence excitation spectra of H_2O in a free jet. In the present measurement, the H_2O vapor at 250 torr was diluted with 1.5 atm He carrier gas and continuously expanded through an orifice (0.15 mm dia.) kept at 120°C into the main chamber pumped by a 10" difusion pump backed by a mechanical booster pump. Dispersed SOR light was focused on the

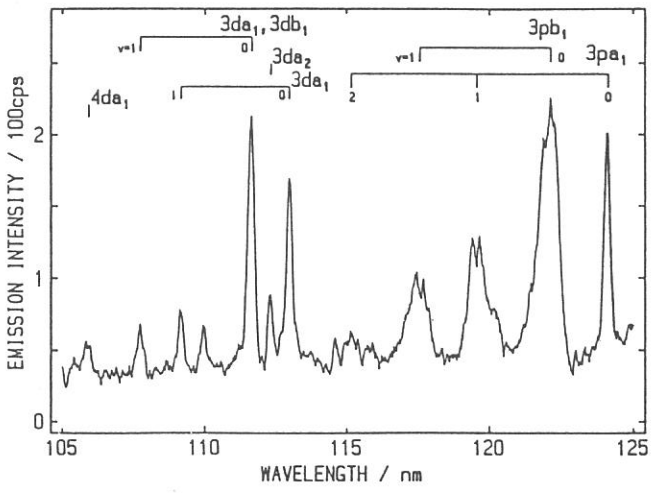

Figure 1. Emission excitation spectrum of H_2O cooled in free jet.

free jet and the emission from OH^* formed from the photo-dissociation of H_2O is recorded against excitation wavelength. An emission excitation spectrum of H_2O cooled in a continuously expanded free jet over 105 - 125 nm is shown in Figure 1. Almost all of the observed bands are Rydberg bands, already assigned as indicated in Figure 1. In order to examine the rotational cooling in the free jet, absorption and emission excitation spectra of room temperature vapor were also measured by filling low pressure H_2O vapor in the chamber without pumping. Figure 2 shows the absorption and emission excitation spectra obtained for room temperature vapor (upper) and for CW free jet (lower) conditions, where the wavelength resolution of light are 0.2 nm for both conditions. In the vapor, widths of 111.6 nm band in absorption and emission excitation spectra are 0.52 nm and 0.63nm, respectively, while those in the free jet is sharpened to 0.22 nm and 0.25 nm. It is quite evident that considerable cooling is attained by the CW free jet. It should be noted that the band widths and band shape of emission excitation spectra are different from those of absorption spectra for both conditions. This implies that the quantum yield for OH^* formation is strongly dependent on the rotational levels of the initially prepared Rydberg states.

It may be useful to give the detection limits for the absorption and emission band in a practical way as products $P \cdot \mu$ and $P \cdot \mu \cdot Q$, respectively, where P is sample pressure(torr) before expansion, μ is absorption coefficient given as absorption cross section σ(Mb = 10^{-18} cm^2) or molar extinction coefficient ε($dm^3 mol^{-1} cm^{-1}$) and Q(%) is emission quantum yield. For our present apparatus, these products should be

for absorption :

$$P \cdot \sigma > 10^4, \quad P \cdot \varepsilon > 3 \times 10^6$$

for emission :

$$P \cdot \sigma \cdot Q > 10^1, \quad P \cdot \varepsilon \cdot Q > 3 \times 10^3$$

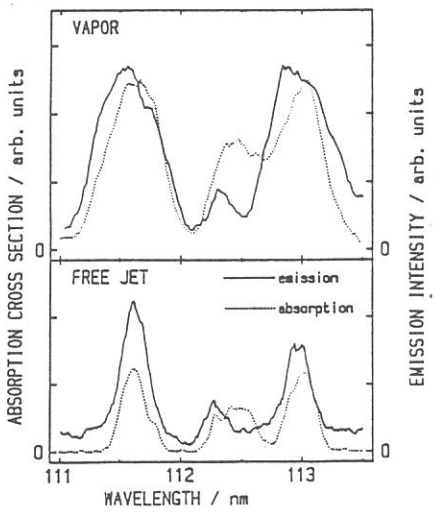

Figure 2. Absorption and emission excitation spectra of H_2O in room temperature vapor (upper) and in free jet (lower).

FLUORESCENCE LIFETIME MEASUREMENT FOR GAS PHASE MOLECULES EXCITED IN VUV REGION BY SYNCHROTRON RADIATION.

Atsunari HIRAYA and Kosuke SHOBATAKE

Institute for Molecular Science, Myodaiji, Okazaki, 444 Japan

The synchrotron radiation from UVSOR having pulse charactaristics of high repetition rate (90.1 or 5.63 MHz), short duration (ca. 400 ps) and stable intensity in the VUV - UV region, is a very useful light source for the studies of dynamics of highly excited states and photodissociative excitation processes. We reports the successfull installation of a time-resolved fluorescence measurement system in a gas phase fluorescence apparatus on a beam line BL2A. Figure 1 shows a block diagram for the time-resolved fluorescence measurement system.

As an example of the succcesful application of this system to the time-resolved measurements, the fluorescence decay curve of the CN^* radical formed by the photo-dissociation of CD_3CN vapor (50 mtorr) excited at 110 nm is shown in Figure 2. The time response of the scattered light is also shown for comparison. This measurement was performed when the machine was operated in a single bunch operation mode. Although the observed decay curve cannot be expressed exactly by a single exponential function, the lifetime of the fast decaying component is estimated to be about 80 ns. This value is in good agreement with the radiative lifetime (85 ns) of $CN^*(B-X)$.[1] It should be mentioned that a relatively high base-line (ca. 300counts) of the decay curve is mainly resulted from overlapping of successive slow decaying components whose lifetime is several times longer than the time interval of excitation light pulses. This slow decaying component should be due to the $CN^*(A)$ whose radiative lifetime to the ground state is known to be 4.2 μs.[1]

Reference

1) T. J. Cook and D. H. Levy, J. Chem. Phys., **57**, 5059 (1972); ibid. 57, 5050 (1972).

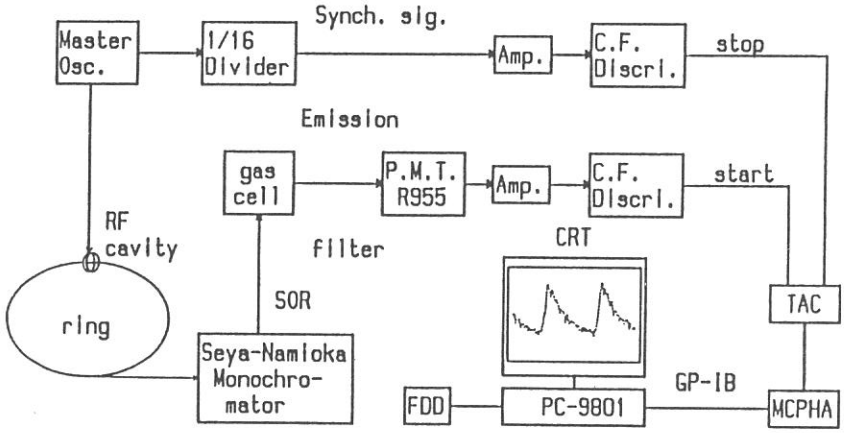

Figure 1. Block diagram for the time-resolved fluorescence measurement system installed in a beam line BL2A of UVSOR. TAC, time-to-amplitude converter; MCPHA, multichannel pulse-height analyzer.

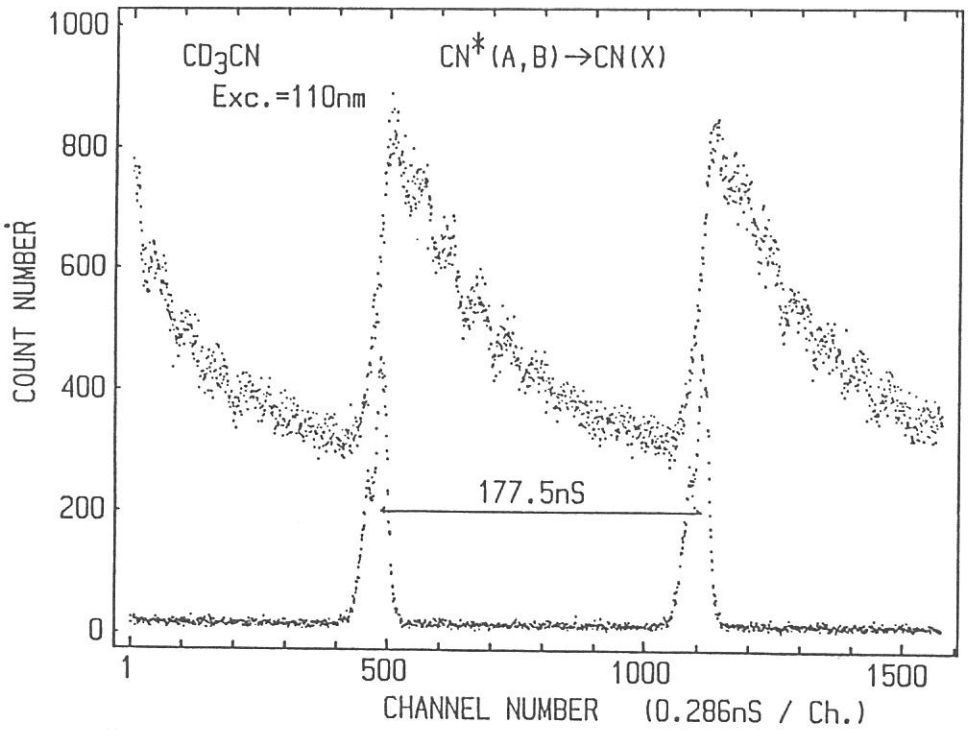

Figure 2. Decay curve of the emission observed from CD_3CN vapor (50 mtorr) after excitation at 110 nm (upper trace) and the time response for scattering light at 200 nm (lower trace).

Observation of the Threshold Energies of H^+ Formation Ethylene and Acetylene by Synchrotron Radiation. Determination of the C-H Bond Dissociation Energies.*

Haruo Shiromaru, Yohji Achiba**, Katsumi Kimura,
and Yuan T. Lee***
Institute for Molecular Science, Okazaki 444

The C-H bond dissociation energies of ethylene and acetylene, (D_0(R-H): R = C_2H_3, C_2H) are the important quantities to be accurately determined in chemistry. The D_0 values can be deduced from the relationship

$$D_0(R\text{-}H) = E_{th}(H^+) - I(H) \qquad (1)$$

where $E_{th}(H^+)$ is the threshold energy for the reaction

$$RH + h\nu = R + H^+ + e^- \qquad (2)$$

and I(H) is the ionization energy of the H atom (13.598 eV). In the present work, we have been able to determine D_0(R-H) values for the first time from the onset of photoionization efficiency curves.

Photoionization measurements were performed in the energy region 58 - 70 nm using the beam port BL2-B2 of UVSOR. Helium or argon gas was used as a filter to diminish the higher-order light. A sample gas was introduced as a molecular beam in order to avoid an ion molecular reaction. A Q-pole mass filter (ULVAC Model MSQ-400) was used for mass analysis and detection.

The H^+ efficiency curves obtained for ethylene and acetylene are shown in Figs. 1 and 2, respectively. The increasing backgrounds (indicated by solid lines) in Figs. 1 and 2 are due to the ionization by residual second-order radiation from the

* To be Published in J. Phys. Chem. (1987).

** Present address: Department of Chemistry, Tokyo Metropolitan Univ., Tokyo 158

*** On leave from Lawrence Berkeley Laboratory and the Department of Chemistry, University of California, CA 94720, as IMS visiting professor (March-June, 1986)

monochromator. The H^+ efficiency curves obtained at different pressures of the helium filter gas are compared in Fig. 1: (a) 0 Torr, (b) 0.050 Torr, (c) 0.098 Torr. The background signals seem not to affect the position of the onsets.

From the efficiency curves (Figs. 2 and 2), we have obtained

$E_{th}(H^+)$ = 18.66 eV, D_0 = 5.06 eV for ethylene

$E_{th}(H^+)$ = 19.35 eV, D_0 = 5.75 eV for acetylene

The D_0 values deduced here are in good agreement with these obtained from the analysis of the photofragment translational spectra but considerably higher than those derived from the onset of C_2H^+ or $C_2H_3^+$ using the relationship

$$D_0 = E_{th}(R^+) - I(R) \qquad (3)$$

The deviation may be due to the effect of ion pair formation.

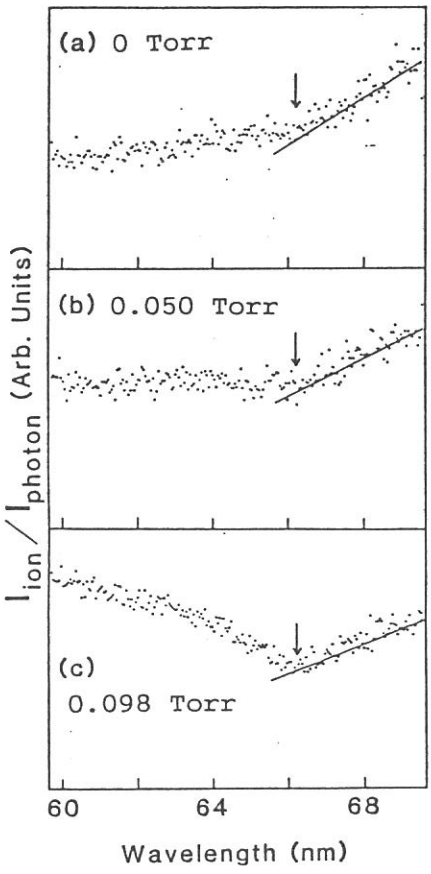

Fig. 1. The efficiency curves of H^+ for C_2H_4.

The synchrotron radiation is suitable for the determination of the C-H bond dissociation energies because of its high intensity and stability in the wavelength region relevant to the H^+ formation.

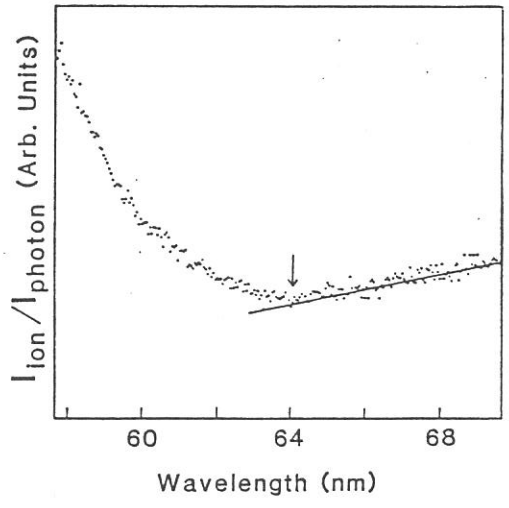

Fig. 2. The efficiency curves of H^+ for C_2H_2.

PHOTOIONIZATION MASS SPECTROMETRY OF DIMETHYLETHER AND CYCLOHEXANE

M. Ukai, S. Arai, T. Kamosaki, K. Hayashi, K. Shinsaka, and Y. Hatano.

Department of Chemistry, Tokyo Institute of Technology,
Meguro-ku, Tokyo 152.

H. Shiromaru and K. Kimura.

Institute for Molecular Science,
Myoudaiji, Okazaki-shi, Aichi 444.

Spectroscopy and dynamics of highly excited molecules produced by photon impact in extreme ultra violet region are of fundamental importance in understading the interaction of photons with molecules. Especially studies of chemically important molecules, such as hydrocarbons, alcohols, and ethers, are almost completely open field where importance of autoionization of highly excited molecules has been recognized.

The gross feature of the total photoabsorption cross sections and the ionization efficiencies near thresholds for C_3H_6, C_4H_8, C_6H_{12}, C_2H_6O, and C_3H_8O isomers have been determined by our previous works[1-3]. However, detailed information on the products has not been obtained extensively in a wide region of photon energy.

The present paper reports the photoionization mass spectra of dimethyl ether and cyclohexane obtained by using a quadrapole mass spectrometer in a wavelength region of 40-90nm of SR from BL-2B2 at UVSOR, IMS.

Mass fragment patterns of dimethyl ether are obtained at various photon energies. Intense peaks are observed at m/e=15, 29, 45, and 46 which, respectively, correspond to CH_3^+, CHO^+, $CH_3OCH_2^+$, and $CH_3OCH_3^+$. The peak of 45 is the most intense. The peak of 31 (CH_3O^+) is much weaker than that in the previous work[4]. Excitation spectra

for specific fragments are observed in which ionization onsets, peaks, and shoulders are observed (fig. 1). The gross maximum and the broad structures in the previous total absorption spectrum are explained by the respective structures in the present spectra. Characteristic vibrational structure which has been observed in the previous total absorption spectrum[2] are not observed in the present spectrum of 46.

Fragment patterns and excitation spectra are also obtained for cyclohexane.

References

1. H. Koizumi, T. Yoshimi, K. Shinsaka, M. Ukai, M. Morita, Y. Hatano, A. Yagishita, and K. Ito, J. Chem. Phys., 82, 4856 (1985).

2. H. Koizumi, K. Hironaka, K. Shinsaka, S. Arai, H. Nakazawa, A. Kimura, Y. Hatano, Y. Ito, Y. Zang, A. Yagishita, K. Ito, and K. Tanaka, J. Chem. Phys., 85, 4276 (1986).

3. H. Koizumi et al., J. Chem. Phys., (to be published).

4. R. Botter, J. M. Pechine, and H. M. Rosenstock, Int. J. Mass. Spectr. Ion. Phys., 25, 7 (1977).

Figure 1

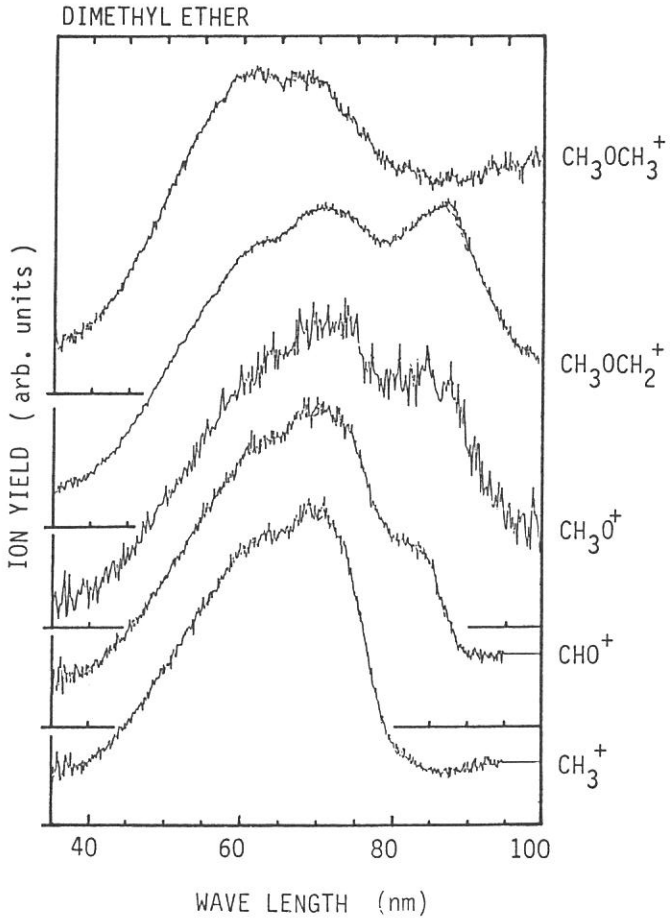

UVSOR STUDY OF CO_2-H_2O CLUSTERS

Hideyuki SUZUKI, Masahiro KAWASAKI, Hiroyasu SATO,
Haruo SHIROMARU* and Katsumi KIMURA*

Chemistry Department of Resources, Faculty of Engineering,
Mi'e University, Tsu 514
* Institute for Molecular Science, Myodaiji, Okazaki 444

CO_2-H_2O clusters formed under molecular-beam conditions by seeding H_2O in CO_2 gas were photo-ionized in the BL2B2 molecular beam photoionization spectrophotometer, and the resulting cluster ions were analysed by a quadrupole mass analyser. The diameter of the nozzle was 50 μm, that of the skimmer was 0.7 mm, and the distance of the nozzle and skimmer was set at 3 mm. The stagnation pressure was adjusted by mixing H_2O at the vapor pressure of the room temperature with CO_2 at various pressures. The sample gas was injected continuously through the nozzle.

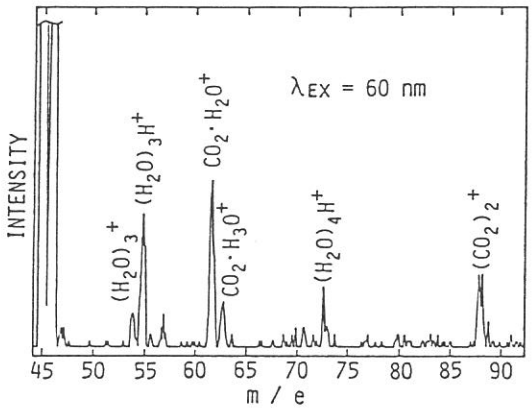

Fig. 1. Mass spectrum at a stagnation pressure of 3.9 atm.

The mass spectrum observed at the stagnation pressure of 3.9 atm. is shown in Fig. 1. The signals at the m/e values 54, 55, 62, 63, 73 and 88 can be asigned to $(H_2O)_3^+$, $(H_2O)_3H^+$, $CO_2 \cdot H_2O^+$, $CO_2 \cdot H_3O^+$, $(H_2O)_4H^+$, and $(CO_2)_2^+$, respectively.

The photoionization efficiency curve for m/e=62 ($CO_2 \cdot H_2O^+$) is given in Fig. 2. Broad humps at 76 nm and

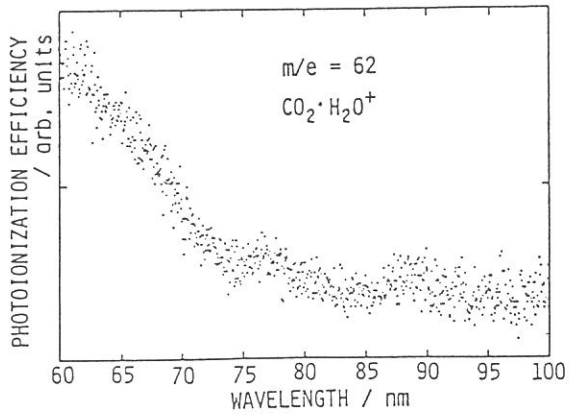

Fig. 2. Photoionization efficiency curve for m/e=62 ($CO_2 \cdot H_2O^+$).

88 nm may be due to the photoionization of the CO_2 moiety.

The photoionization efficiency curves for m/e=62 ($CO_2 H_2O^+$), 44 (CO_2^+), 18 (H_2O^+), and 19 (H_3O^+) are shown in Fig. 3. The curve of $CO_2.H_2O^+$ (Fig. 3a) differs in shape from CO_2^+ (Fig. 3b) or H_2O^+ (Fig. 3c); the photoionization efficiency increases fairly steeply to the shorter wavelength from ca. 74 nm. The appearance of $CO_2.H_2O^+$ (Fig. 3a) is close to that of H_3O^+ (Fig. 3d) which is considered to be formed from $(H_2O)_n$. The photoionization efficiency curve of m/e=63 ($CO_2.H_3O^+$) was also measured (not shown); its shape was similar to that of m/e=62 ($CO_2.H_2O^+$). These findings suggest that the observed intensity for m/e=62 ($CO_2.H_2O^+$) is due to the fragmentation of $Co_2.(H_2O)_n$, and this contribution causes the rise from ca. 74 nm. A similar situation occurs for the efficiency curve of H_3O^+.

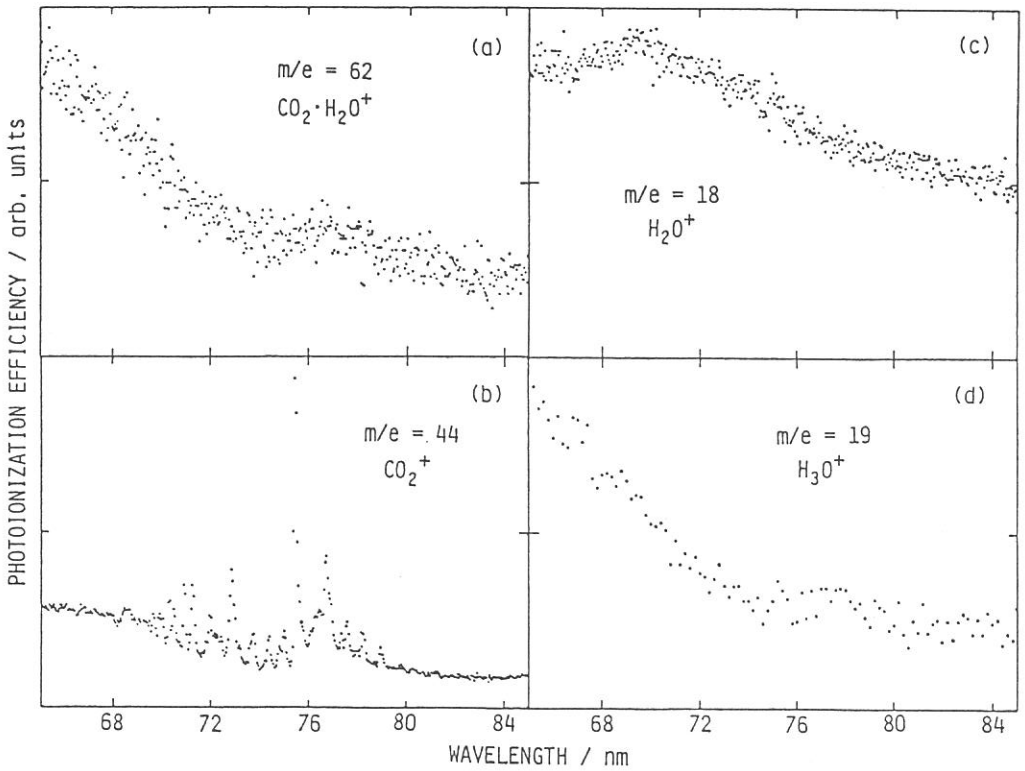

Fig. 3. Photoionization efficiency curve for (a) m/e=62 ($CO_2 \cdot H_2O^+$), (b) m/e=44 (CO_2^+), (c) m/e=18 (H_2O^+), (d) m/e=19 (H_3O^+).

THRESHOLD ELECTRON SPECTRA OF SOME DIATOMIC MOLECULES FOR THE STUDY OF STATE SELECTED ION-MOLECULE REACTIONS

Shinzo SUZUKI and Inosuke KOYANO

Institute for Molecular Science, Myodaiji, Okazaki 444

The TEPSICO-II apparatus[1] has been installed at BL3B for the study of state-selected unimolecular and bimolecular reactions of ions using synchrotron radiation. With this apparatus it is possible to utilize the TESICO (threshold electron-secondary ion coincidence) technique[2] to select internal states or internal energies of reactant ions. For the TESICO experiments, it is necessary to know threshold electron spectra (TES) of parent molecules for the reactant ions and see what electronic or vibrational states exist in the wavelength region of interest. Synchrotron radiation is a suitable continuum VUV light source for such experiments.

Fig. 1 shows the TES of O_2 in the wavelength range 63-83 nm taken with the TEPSICO-II apparatus. The gross features agree well with those of Guyon and Nenner.[3] A series of peaks appears in the so-called Franck-Condon gap (the region 95.3 - 77.5 nm) where there is no direct ionization probability. This demonstrates the advantage of the TESICO technique for the study of state-selected reactions.

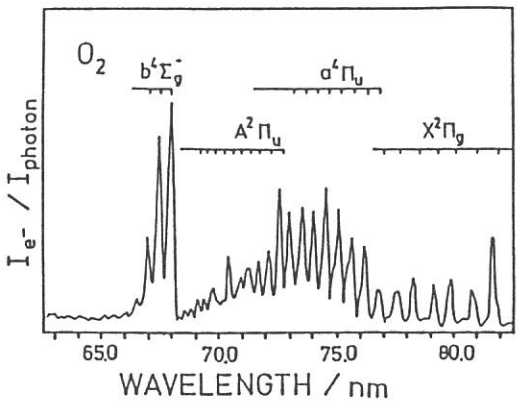

Fig. 1 Threshold electron spectrum of O_2

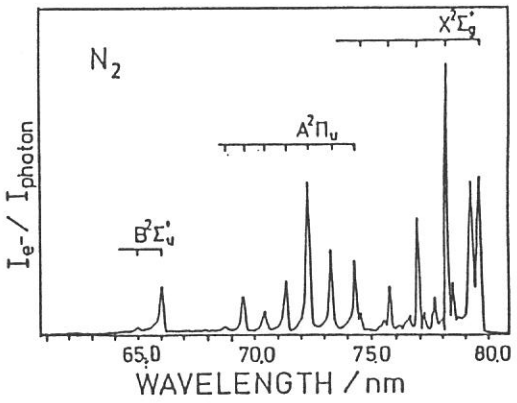

Fig. 2 Threshold electron spectrum of N_2

The TES of N_2 is shown in Fig. 2. It indicates that the reactions of $N_2^+(X)$ can be studied up to v = 4, while in the HeI photoelectron spectrum of N_2, $N_2^+(X)$ ions produced are dominated by v = 0, with small fraction of v = 1. The discrepancy between this and the Peatman et al.[4] spectrum concerning the peaks around the v = 0 and 1 thresholds is due to the difference in the resolution of the two electron energy analyzers.

Fig. 3 shows the TES of NO in the wavelength range 50.0 - 80.0 nm. The TES in the 50.0 - 60.0 nm range is reported here for the first time and shows a single peak at 57 nm, which is assigned in comparison with an ESCA spectrum [5] to $^3\Pi$ state resulting from removal of an 4σ electron. The occurrence of these threshold electrons suggests the possibility of studying processes following the inner valence excitation.

References

1. I. Koyano, K. Tanaka, T. Kato, S. Suzuki and E. Ishiguro, Nucl. Instr. Meth., A246 (1986) 507.
2. I. Koyano and K. Tanaka, J. Chem. Phys., 72 (1980) 4858.
3. P. M. Guyon and I. Nenner, Appl. Opt. 19 (1980) 4068.
4. W. B. Peatman, B. Gotchev, P. Gurtler, E. E. Koch and V. Saile, J. Chem. Phys. 69 (1978) 2089.
5. ESCA applied to free molecules. K. Siegbahn, C. Nordling, G. Johansson, J. Hedman, P. F. Heden, K. Hamrin, U. Gelius, T. Bergmark, L. O. Werme, R. Manne, Y. Baer (eds.), p.74. Amsterdam: North-Holland 1969.

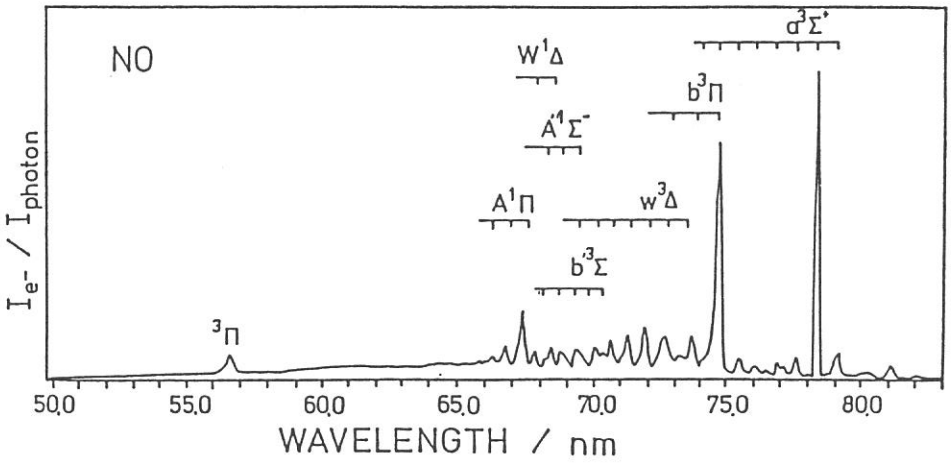

Fig. 3 Threshold electron spectrum of NO

Dissociation mechanism of state selected NO_2^+ ions

Kazuhiko SHIBUYA*, Shinzo SUZUKI, and Inosuke KOYANO

Institute for Molecular Science, Myodaiji, Okazaki 444
*Department of Chemistry, Tokyo Institute of Technology, Ohokayama, Tokyo 152

The equilibrium geometries of NO_2 molecules and NO_2^+ ions are quite different in their ground electronic states. This has long been baffle for the accurate determination of adiabatic ionization potential of NO_2. On the other hand, the ejection of an inner valence electron from NO_2 is Franck-Condon allowed due to their similar geometries. Therefore, one can prepare electronically excited and state selected NO_2^+ ions by a photoionization method in the spectral region shorter than 100 nm. For the purpose of elucidating the dissociation mechanism of state selected NO_2^+ ions, we have measured the threshold electron spectrum (TES) of NO_2, the photoionization efficiency (PIE) curves for its parent and fragment ions, and the threshold electron - ion TOF coincidence spectra in the range 40 - 80 nm using TEPSICO-II.

Fig.1 shows TES of NO_2, which accords well with the He I photoelectron spectrum of NO_2 [1]. In this region triplet states are mainly observed, $^3B_2(2b_2)^{-1}$ and $^1B_2(2b_2)^{-1}$ making a pair of $(2b_2)^{-1}$ ionization.

Fig.2 shows photoionization efficiency curves for the fragment (O^+,NO^+) and parent (NO_2^+) ions. The O^+ production was observed in the region shorter than 65 nm, which accords with the location of $^3B_2$. Fig.3 shows the TOF coincidence spectra obtained with excitation at 65.4 nm, corresponding to the onset of $^3B_2$ v_1=0. The O^+/NO^+ branching ratio was obtained to be 0.66. The vibrational dependence of the ratio was not observed within the $^3B_2$ state to an appreciable extent.

From similar measurements at 57.9 nm (formation of $^1B_2$ and/or $^3A_1$), the ratio of O^+/NO^+ was found to be 0.16, which is four times as small as the ratio derived for $^3B_2$. Possibly, the fragmentation pattern of excited NO_2^+ could be quite different depending on whether the relevant surface is singlet

or triplet.

Finally, we have observed NO_2^+ as a product with excitation around 71 nm, which prepares the parent ion in the $^3A_1$ and/or $^3B_1$ states lying approximately 5 eV above the dissociation limit. The $^3A_1$ and/or $^3B_1$ states are likely to be stabilized through radiative relaxation onto the $^3B_2$ and/or $^3A_2$ states.

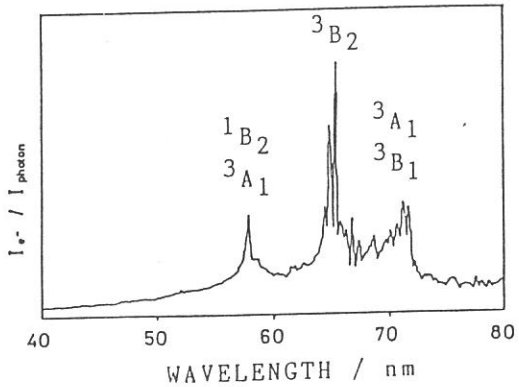

Fig. 1 TES of NO_2

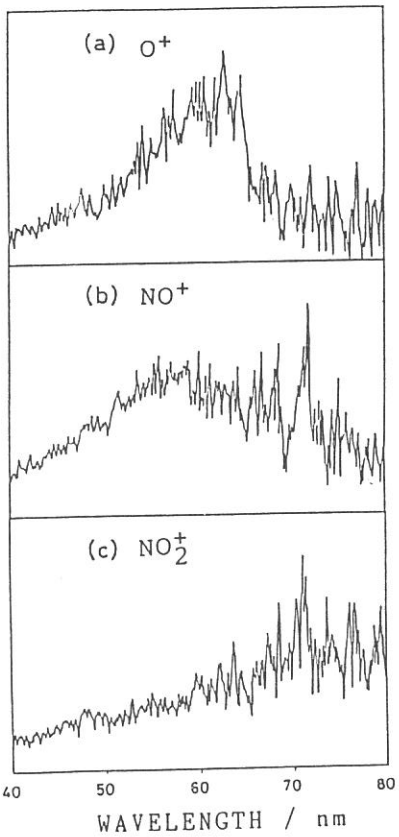

Fig. 2 PIE curves for parent and fragment ions

[1] C.R.Brundle et al.
J. Chem. Phys. 53, 705 (1970)

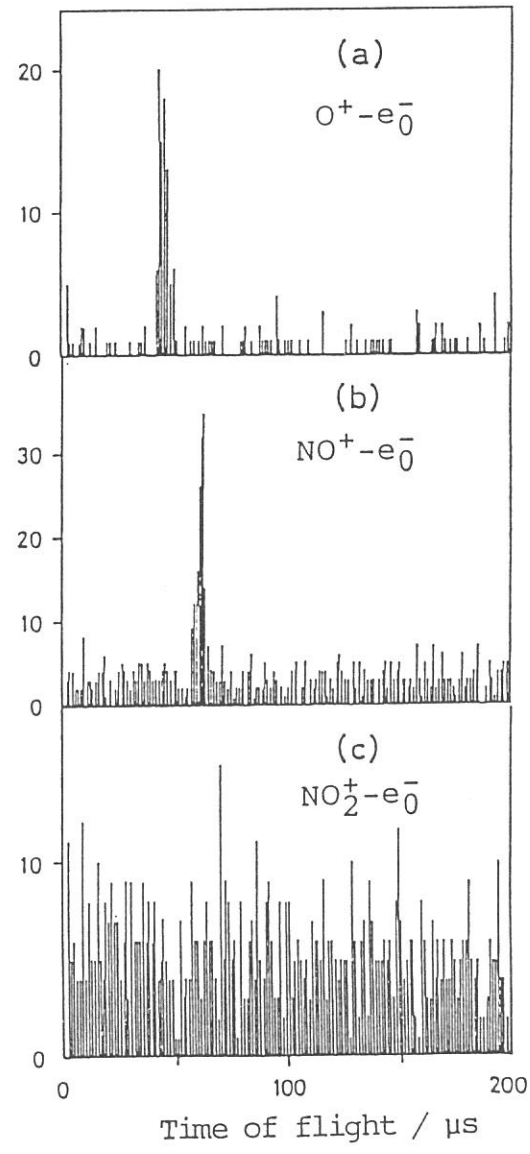

Fig. 3 TOF coincidence spectra obtained at 65.4 nm

INVESTIGATION OF FRAGMENTATION PROCESSES FOLLOWING CORE PHOTOIONIZATION OF ORGANOMETALIC MOLECULES IN THE VAPOR PHASE

Shin-ichi NAGAOKA, Shinzo SUZUKI and Inosuke KOYANO

Institute for Molecular Science, Myodaiji, Okazaki 444

Fragmentation processes following core photoionization of molecules are forming a research field of current interest. Volatile compounds with group II–V elements are particularly suitable for detailed investigations of these processes in the vapor phase, because the rather small binding energies of the (n-1)d core electrons allow the studies in the normal incidence region of the vacuum ultraviolet. Accordingly, we have attempted to study the core photoionization and subsequent fragmentation of such compounds ($Zn(CH_3)_2$, $Ga(CH_3)_3$, $Ge(CH_3)_4$, $Sn(CH_3)_4$, $Pb(CH_3)_4$, and $Bi(CH_3)_3$). Here, we report production of Pb^+ ion following Pb 5d core photoionization of tetramethyllead (TML) as revealed by using the threshold electron – photoion coincidence (TEPICO) method. The experiments were performed using the TEPSICO-II apparatus installed in BL3B beam line of UVSOR.

Figure 1 shows the threshold electron spectrum of TML. Several sharp bands seen in the region 44 – 75 nm are assigned to the photoionization from the Pb 5d core levels. Figure 2 shows the photoionization efficiency curves for fragment ions from TML. The photoionization efficiency curve for the Pb^+ ion has an appearance quite different from those for other fragments. Moreover, almost all peaks of the Pb^+ curve in the region 44 – 75 nm are found to coincide in position with those in the threshold electron spectrum of TML. Figure 3 shows an example of the time-of-flight coincidence spectrum. It is seen that sufficiently high signal-to-noise ratio is attained with reasonable data collecting time. Relative efficiency for the production of each fragment from various states of the TML parent ion were determined by use of TEPICO, and are given in Fig. 4. From these results, it is considered that the Pb^+ ion is predominantly produced following Pb 5d core photoionization.

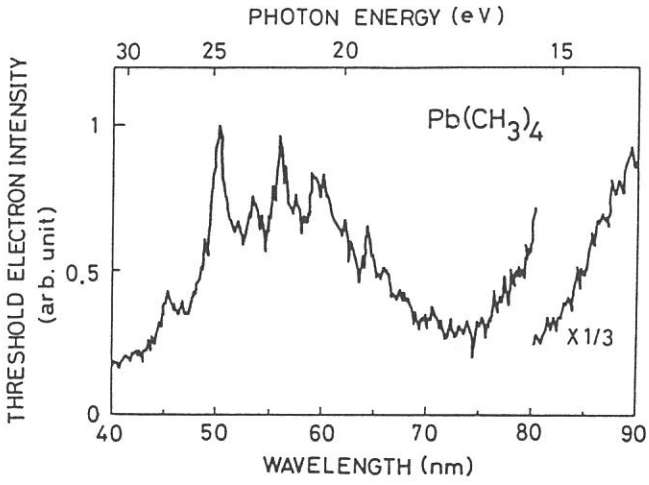

↑Fig. 1. Threshold electron spectrum of TML.

Fig. 2. Photoion efficiency curves for → fragment ions from TML.

↓Fig. 3. Time-of-flight TEPICO spectrum of the Pb^+ ion taken by excitation at 50.4 nm. Data collection time is 100 minutes.

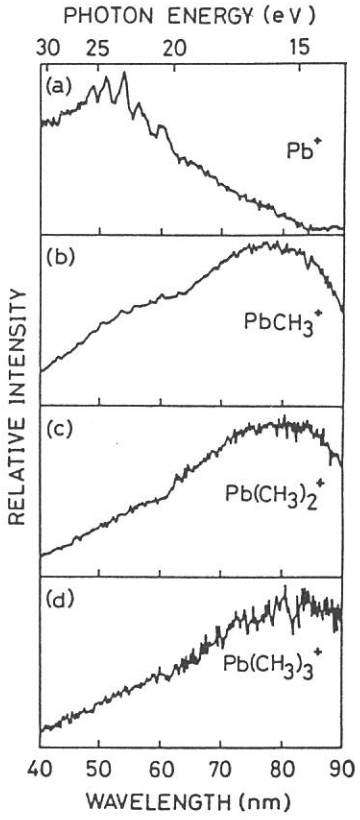

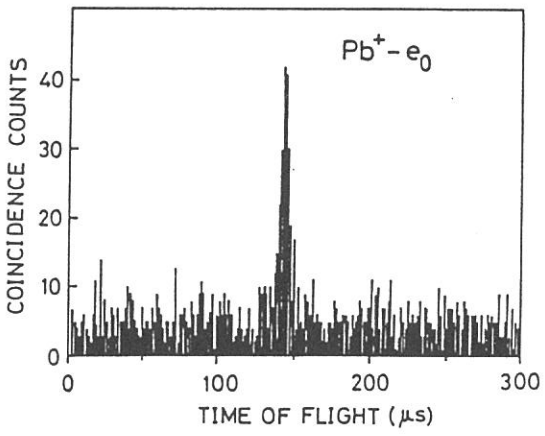

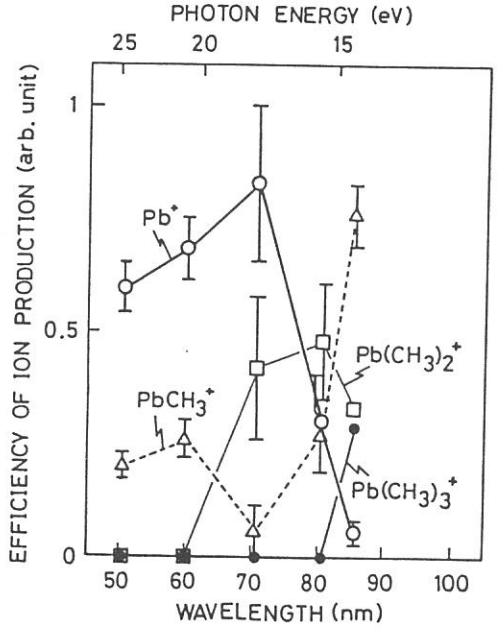

↑Fig. 4. State selected efficiency of ion production.

FORMATION OF H^- BY ELECTRON TRANSFER FROM Cs ATOMS TO H_2^+: DEPENDENCE ON THE VIBRATIONAL LEVEL OF H_2^+

Sigeo HAYAKAWA, Shinzo SUZUKI*, Masatugu KOGO, Toshio SUGIURA and Inosuke KOYANO*

The College of Integrated Arts and Sciences, University of Osaka Prefecture, Mozu-Umemachi 4-804, Sakai, Osaka 591
*Institute for Molecular Science, Myodaiji, Okazaki 444

This work is in progress, so that this report describe the development of the experiment and the interim results.

A large amount of work on the electron transfer for H^+ (or D^+) ions in metal vapour has been reported, from the viewpoint of neutral beam injection schemes in controlled thermonuclear fusion research. The study of the electron transfer processes with molecular ions, however, has not been published so far. Three of the present authors (Univ. Osaka Prefecture group) have obtained new information about the following successive electron transfer processes:

$$H_2^+ + Cs \longrightarrow H_2^* + Cs^+ \qquad (1)$$

$$H_2^* \longrightarrow 2H \qquad (2)$$

$$H + Cs \longrightarrow H^- + Cs^+ \qquad (3)$$

The formation cross section of H^- ions in these processes is over 2 times larger than that of H^- ion formation from H^+ ions. The H^- ions having various kinetic energies are formed, about a half of H^- ions formed having kinetic energy of 4.1 eV, and the other half having kinetic energies of 0.24 — 0.41 eV.

The purpose of the present experiment was to elucidate the dependence of process (1) on the vibrational level of the H_2^+ ions, using the coincidence measurements of product signals with threshold electrons. For this purpose, the photoionization chamber, reaction regions, and lens system of the TEPSICO-II apparatus[1] have been replaced with those shown in Fig. 1. An electron gun has been installed temporarily on the photo-ionization chamber, to examine the sensitivity of the detection system for the negative ions, using H^- ions formed in an ion pair process by electron impact.

A cylindrical Cs reservoir of 10 mm inner diameter and 50 mm long was made of stainless-steel. Chromel-alumel thermo-couples were attached to the target chamber, connecting tube, and Cs reservoir. These parts were heated separately by the nichrome wire insulated by glass sleeve. Cs vapour was fed to the target chamber by breaking in vacuum a glass ampule (containing 1g of Cs) put in the Cs reservoir. Cs density in the target chamber was estimated from available vapour pressure data.

Using this system, the following measurements have been made up to now: 1) photoionization efficiency curve and threshold electron spectrum of H_2, 2) time-of-flight coincidence spectrum of H_2^+ (v=0) ions as shown in Fig. 2, 3) the product spectrum of processes (1) to (3). The experiment 3) was performed under the condition that the impact energy of H_2^+ ions is 70 eV in the laboratory system and the Cs vapour density is 10^{14} atoms cm^{-3}. Under this condition, signals were obtained which were not affected by the potentials on the electrodes located downstream of the target chamber. These signals may be due to photons emitted from excited hydrogen atoms formed by dissociation process (2), or long-lived metastable excited hydrogen atoms. These signals would be distinguished by the measurement of the time of flight coincidence spectrum.

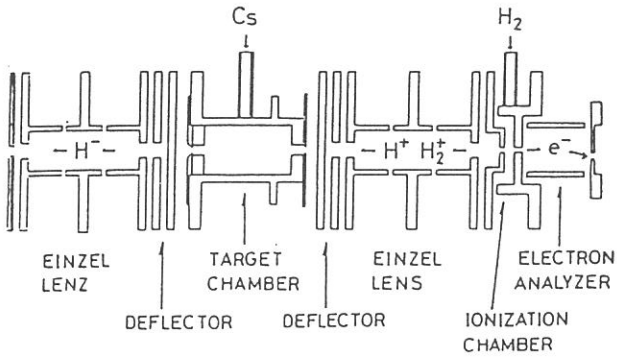

Fig.1 ionization and reaction region

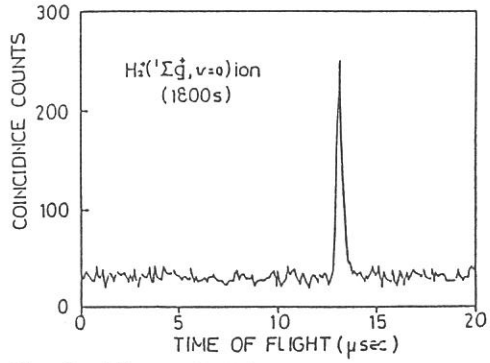

Fig.2. Time-of-flight coincidence spectrum of the H_2^+(v=0) ions

1) S. Suzuki et al., Z. Phys. D-Atoms, Molecules and Clusters 4, 111 (1986)

POLARIZED REFLECTION SPECTRA OF CADMIUM HALIDE CRYSTALS

Masami FUJITA, Hideyuki NAKAGAWA*, Yukio SHIMAMOTO*, Hiroaki MATSUMOTO*, Takeshi MIYANAGA**, Kazutoshi FUKUI*** and Makoto WATANABE***

Maritime Safety Academy, Wakaba, Kure 737
* Department of Electronics, Fukui University, Bunkyo, Fukui 910
** Department of Physics, Faculty of Education, Wakayama University, Sakaedani, Wakayama 640
*** Institute for Molecular Science, Myodaiji, Okazaki 444

Reflection spectra of single crystals of cadmium halides were measured by using synchrotron radiation of UVSOR. Light from strage ring was monochromatized with a plane grating monochromator at BL6A or a Seya-Namioka type monochromator at BL7B. Cleaved surfaces of single crystals were used for measurement.

In Fig. 1 are shown reflection spectra of $CdCl_2$, $CdBr_2$ and CdI_2 for polarization nearly perpendicular to the crystal c-axis ($E \perp c$) at liquid helium temperature. The spectra in the region below 10 eV agree with those measured with ordinary light sources.[1,2] Spectra obtained by Pollini et al. with SR[3] differ very much from present results.

The observed structures of three compounds can be classified into several groups. The peaks X, X_1 and X_2 around absorption edge are assigned to excitonic transitions from halogen p upper valence band to the lowest conduction band of Cd 5s character.[2] Sharp peaks A, B, B' and C are believed to be due to excitonic transitions in the deep interband energy region. A dip is observed at about 2 eV above the peak B. Beyond the dip appear peaks a – f. On going from chloride to iodide, the peaks a and b become distinct. Spin-orbit interaction of valence band may be responsible for the enhancement of the structure. Energy shift of the peaks d, e and f between chloride and iodide is somewhat smaller than that of a, b and c, which suggests that valence or conduction band relevant to the set of d, e and f is not the same as that of a, b and c.

The systematic variation in the spectral shape among three compounds suggests that the energy bands have the same ordering in each materials. From comparison of the spectra with band calculations,[3,4] set of peaks A, B, B' and C and that of a, b and c are assigned to transitions from upper valence band to Cd $5p_z$ and $5p_{x,y}$ conduction bands, respectively.

The peaks d, e and f are supposed to be associated with transitions from halogen p lower valence band.

In the region around 16 eV denoted by N are observed two (CdI_2 and $CdBr_2$) or three ($CdCl_2$) peaks. They are assigned to Cd 4d core excitons. The peaks are accompanied with several fine structures. Remarkable dichroic nature was revealed by preliminary measurement of the spectra for polarization parallel to the crystal c-axis (E // c). Crystal field at cadmium ion site is of D_{3d} symmetry. If optical excitation from $4d^{10}$ to $4d^9 5p$ of Cd^{2+} ion in the crystal field is assumed, 20 and 10 exciton states are allowed for E ⊥ c and E // c, respectively. Observed multiplicity and dichroism in the region N indicate that crystal field is essential to explain the Cd 4d core exciton states.

References

1) D. L. Greenaway and R. Nitsche: J. Phys. Chem. Solids 26 (1965) 1445.
2) S. Kondo and H. Matsumoto: J. Phys. Soc. Jpn. 51 (1982) 1441.
3) I. Pollini, J. Thomas, R. Coehoorn and C. Haas: Phys. Rev. B 33 (1986) 5747.
4) R. Coehoorn, G. A. Sawatzky, C. Haas and R. A. de Groot: Phys. Rev. B 31 (1985) 6739.

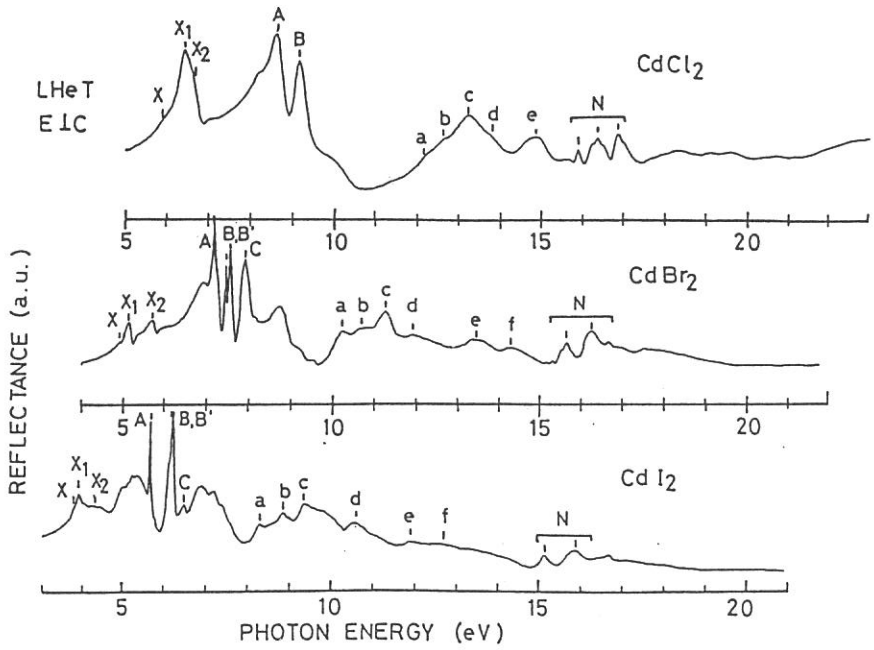

Fig. 1 Reflection spectra of cadmium halide single crystals at liquid helium temperature.

Polarized Reflection Spectra of Orthorhombic Indium Halides in 2 - 30 eV Region

Kaizo NAKAMURA, Yasuo SASAKI, Toru KISHIGAMI, Makoto WATANABE* and Masami FUJITA+

Department of Physics, Kyoto University, Kyoto 606
*Institute for Molecular Science, Okazaki 444
+Maritime Safety Academy, Kure 737

Polarized reflection spectra of orthorhombic indium halides (InBr and InI: space group D_{2h}^{17}) have been investigated at liquid helium temperature by using PGM spectrometer at BL6A2 in 2 - 30 eV region. Single crystals of InBr and InI were grown by Bridgman method. Results on InBr were reported previously.[1] In this report, results on InI are mainly described.

Figure 1 shows the spectra of InI for polarization parallel to the c-axis (E//c) and for E//a. The first exciton peak at 2.03 eV is due to the transition from the top valence band of iodine 5p, into which considerable amount of In 5s orbital admixes, to In 5p conduction band bottom. This transition is allowed for E//c. Many peaks are observed from 2 to 15 eV. They are attributed to the transition from the upper valence bands of I^- 5p and In^+ 5s to the lower conduction bands. At about 20 eV, In^+ 4d core exciton peaks are observed as in InBr.[1]

In Fig. 2, spectral features between 2 and 10 eV in both materials are compared with the energy shift of 0.85 eV. Many peaks coincide in energy suggesting that these transitions occur in In sublattice, that is, In 5s valence band (the second one) to In 5p conduction band.

Fig. 3 shows the spectra of In 4d core excitons in InI in an expanded energy scale. Spectra are very dichroic. Each of two main peaks, which have been observed in InBr with the separation of 0.8 eV, splits clearly in InI into two or more peaks. In the previous report, 4d exciton structure in InBr was explained by the atomic model without including the effect of crystal field.[1] To understand this dichroism and splitting, however, analysis

including crystal field as well as spin-orbit and exchange interactions has been attempted. It is found that the crystal field splitting amounts to 1 eV and is comparable to that of spin-orbit interaction.

1) K. Nakamura, Y. Sasaki, M. Watanabe, and M. Fujita: to be published in Physica Scripta 35 (1987).

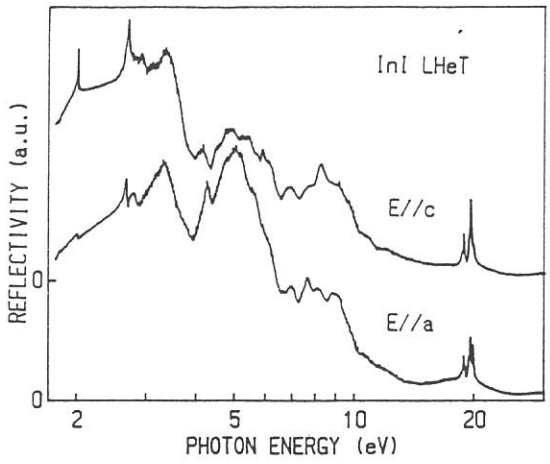

Fig. 1. Reflection spectra of InI at liquid helium temperature. (a) for E//c and (b) for E//a.

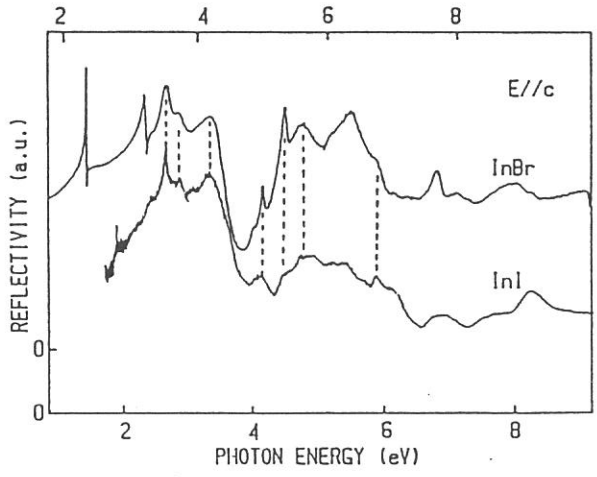

Fig. 2. Spectra of InBr and InI at LHeT for E//c from 2 to 10 eV. Energy for InI is shifted to higher energy by 0.85 eV.

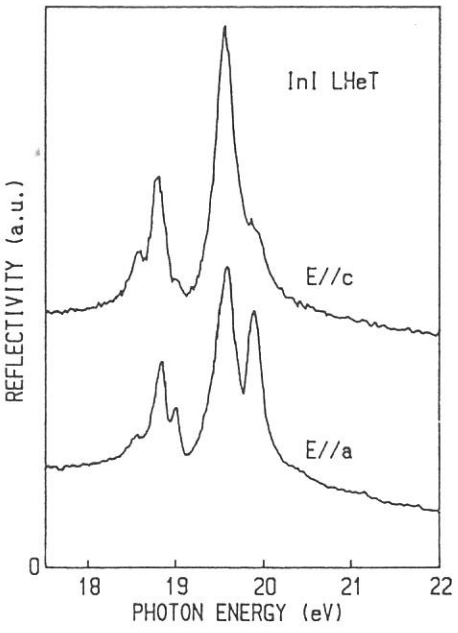

Fig. 3. Reflection spectra of 4d core excitons in InI at LHeT.

Absorption Spectra of SnTe Thin Films in 2-120 eV Region

Kazutoshi FUKUI, Jun-ichiro YAMAZAKI, Eiken NAKAMURA, Osamu MATSUDO,
Tadaaki SAITO*, Shin-ichi KONDO* and Makoto WATANABE

Institute for Molecular Science, Okazaki 444
*Department of Applied Physics, Fukui University, Fukui 910

SnTe films are known to be amorphous when evaporated onto substrates held at near liquid nitrogen temperature (LNT).[1] As the temperature goes up from LNT, irreversible amorphous-crystalline transformation occurs at the temperature T_c of about 200 K.[2] At T_c, the insulator-metal transition happens, that is, the resistivity shows an abrupt decrease from the order of 10^2 ohm.cm (amorphous phase) to 10^{-4} ohm.cm (crystalline phase). In this experiment, the effect of amorphous-crystalline transformation on optical spectra was investigated.

The substrates were thin collodion films. The in-situ measurements on SnTe films of both phases were carried out in 2 - 120 eV energy range by using a plane grating monochromator (PGM) at BL6A2. At the first time, SnTe film was evaporated on the substrate cooled to about 80 K under a vacuum of about 10^{-9}-10^{-10} Torr and the absorption measurement was carried out. Secondly, the film was annealed at room temperature and after that it was cooled to about 80 K, and the measurement was made again.

Figure 1 shows the absorption spectra of SnTe film of amorphous phase and crystalline phase at about 80 K. The structure below 26 eV is due to the transitions from valence band. Below 26 eV, a few broad peaks are observed in amorphous phase, and several peaks appear after crystallization. Below 6 eV, this result is consistent with the previous measurement.[3] The structure for crystallized SnTe below 20 eV is in good agreement with previous results.[4] The structure above 26 eV is due to the transition from core levels. Doublet structures around 26 eV are due to the transition from Sn 4d core level. They are likely to be due to the excitonic transition because the peaks are sharp. A structure around 44 eV is due to the transition from Te 4d core level. As the structure is broad, it does not seem to be due to the excitonic transition in contrast with the transition from Sn 4d core level. The electron-hole interaction for the transition from Sn 4d is larger than that from Te 4d. It may be related with the fact that the bottom of the conduction band consists

mainly of Sn 5p. (The top of the valence band consists mainly of Te 5p.) After crystallization, the peaks around 26 eV become sharper and several broad peaks appear above 50 eV.

In the MgBi alloy system, the insulator-metal transition occurs at the critical composition. In the core absorption spectra of this system, the excitonic shape of the first and the second peaks in the insulator phase (amorphous) became broad in the metal phase (crystalline).[5] This is attributed to the difference of screening effect, in which the difference of the conductivity is taken into account. In our system, however, we could not find such change in the line shape at the insulator-metal transition.

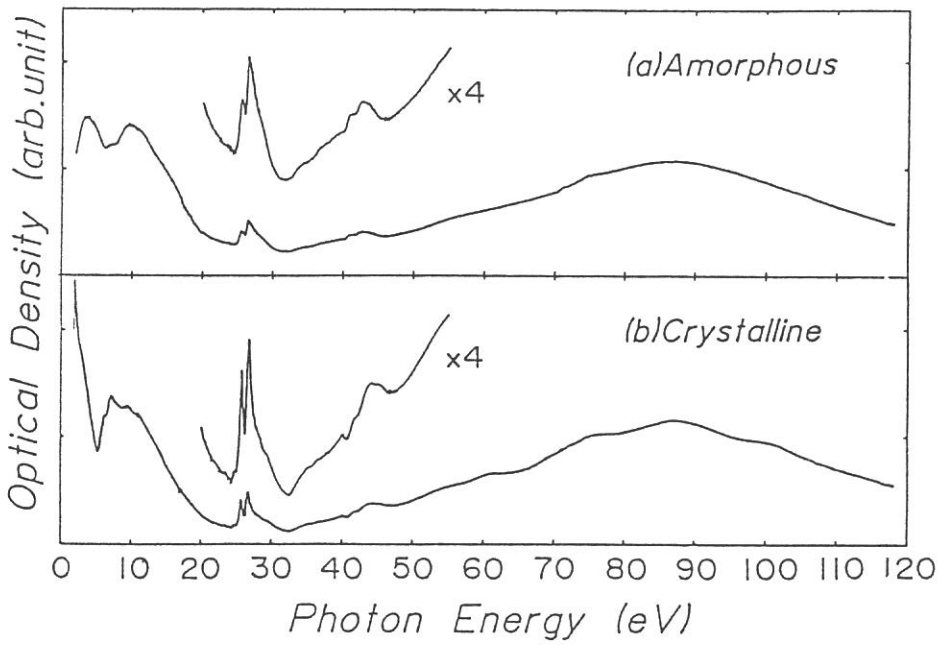

Figure.1. Absorption spectra of SnTe film at about 80 K.
(a) for amorpnous phase and (b) for crystalline phase.

REFERENCES

1) R.W.Brown,A.R.Millner and R.S.Allgaier:Thin Solid Films 5 (1970) 157.
2) K.Fukui,K.Inoguchi,S.Kondo and T.Tatsukawa:Jpn. J. Appl. Phys. 23 (1984) 1141.
3) M.Yoshikawa:Master Thesis (Fukui Univ. 1985)
4) M.Cardona and D.L.Greenaway:Phys. Rev. 133 (1964) A1685.
5) J.H.Slowik:Phys. Rev. B 10 (1974) 416.

K-Edge Absorption Spectra of Na and Mg Halides

Takatoshi MURATA, Tokuo MATSUKAWA*, Masaki OBASHI*, Shunichi NAO-E**, Hikaru TERAUCHI***, and Yasuo NISHIHATA***

Department of Physics, Kyoto University of Education, Fushimi-ku, Kyoto 612
*Department of Physics, College of General Education, Osaka University, Machikaneyama, Toyonaka 560
**Department of Physics, College of General Education, Kanazawa University, Kanazawa 920
***Department of Physics, Faculty of Science, Kwansei-Gakuin University, Nishinomiya 662

K-edge absorption specta of Na and Mg halides were measured at BL-7A soft x-ray beam line by using double crystal monochromator (DXM)[1]. Flat beryls were used as monochromator crystals.

Samples of NaF, NaCl, NaBr and MgF_2, $MgCl_2$, $MgBr_2$ were evaporated in situ onto collodion film deposited on Ni fine mesh. All the measurements were made at room temperature. We believe that this is the first measurement for the Mg K absorption in magnesium halides.

In Figs. 1 and 2 are shown the cation K-edge absorption spectra of NaCl and $MgCl_2$. In both spectra are observed a very sharp absorption bands at the lowest energy. Another intersting point is the appearance of a small hump at the lower edge of the sharp band in both spectra. This small hump is observed in all the spectra of other measured materials.

For the assingnment of the structure of the spectra, we classify the structure into two groups; above mentioned two peaks, and other structures beyond them. The first group may be attributed to the excitonic transition of the 1s core electron. The sharp band can be interpreted as core excitons arising from 1s-3p transitions in Na^+ or Mg^+ ions. The origin of the hump is not clear at the moment, but we tentatively assign the structure as a forbidden transition from 1s to 3s state in metal ions.

The structure at the higher energy side of the first peak is also very sharp in both materials, but the separation between the peaks are dependent upon the materials. Positions of peaks beyond them are also material depen-

dent. Therefore, these structure may be attributed to the transition to the final state due to multiple scattering of the excited electron.

Measurements at low temperature and detailed calculations along the multiple scattering formalism are now in progress.

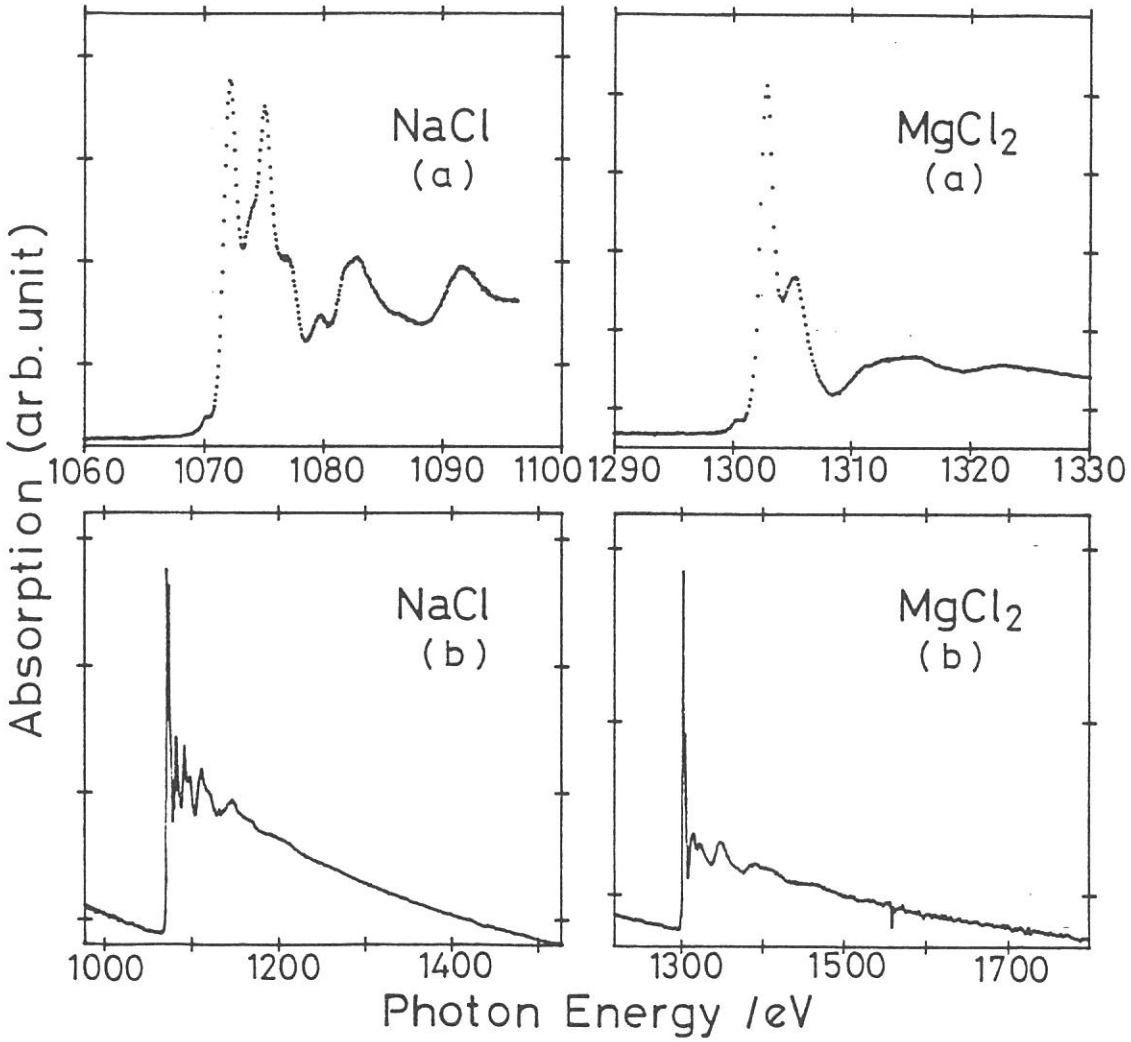

Fig. 1. K-edge spectrum of NaCl (a) XANES, (b) EXAFS.

Fig. 2. K-edge spectrum of $MgCl_2$ (a) XANES, (b) EXAFS.

Reference

1) T. Murata, T. Matsukawa, M. Mori, M. Obashi, S. Nao-e, H. Terauchi, Y. Nishihata, O. Matsudo, and J. Yamazaki, J. Physique Colloque C8 (1987) (in press).

XANES AND EXAFS STUDY ON DEHYDRATION PROCESS IN $Mg(OH)_2$

Yasuo NISHIHATA, Kazuya KAMON, Hirofumi SAKASHITA,
Hiromitu NAONO, Hikaru TERAUCHI, Takatoshi MURATA*,
Shun-ichi NAO-E**, Tokuo MATSUKAWA***, Masahiro MORI+,
Atsuo MATSUI++, and Ken-ichi MIZUNO++

Faculty of Science, Kwansei-Gakuin University, Nishinomiya 662
*Department of Physics, Kyoto University of Education, Kyoto 612
**College of General Education, Kanazawa University, Kanazawa 920
***College of General Education, Osaka University, Toyonaka 560
+College of General Education, Nagoya University, Nagoya 464
++Faculty of Science, Konan University, Kobe 658

Magnesium hydroxide $Mg(OH)_2$ is dehydrated to magnesium oxide MgO at high temperature. $Mg(OH)_2$ has a hexagonal layer lattice of CdI_2 type and MgO is of NaCl type. We feel so much interest in the $Mg(OH)_{2-2x}O_x$ system since the phase transition occurs by the dehydration. This system has been studied by x-ray diffraction technique[1] and it is found that the characteristic reflections of $Mg(OH)_2$ disappear at x_c=0.68 and the line broadings are observed near x_c. We are concerned with the local structure around the magnesium atoms and clarify the microscopic mechanisms of the dehydration in $Mg(OH)_2$.

The particles of $Mg(OH)_2$ (1000Å wide, 200Å thick) were dehydrated *in vacuo*. The degree of dehydration was determined from weight loss of $Mg(OH)_2$ by means of a vacuum electrobalance. Samples of $Mg(OH)_{2-2x}O_x$ with x=0.53, 0.71, 0.90, and 1.00 (MgO) were prepared by controlling temperature and heating time. The samples put in collodion which was dehydrated by molecular sieve. The top clean part of the solution was splashed on a nickel mesh.

X-ray absorption spectra near the Mg-K edge were taken by the use of the double crystal monochromator (DXM) constructed at BL-7A of UVSOR. Synchrotron energy was 750MeV. The intensity of the soft x-ray monochromatized by beryl crystals (2d= 15.97Å) was monitored with electron multiplier and the output current was lead into digital picoammeter.

Figure 1 shows the x-ray absorption spectra near the Mg-K edge of $Mg(OH)_{2-2x}O_x$ with x=0.00, 0.53, 0.71, 0.90, and 1.00. In the throuput transmission spectrum no structure appears near the Mg-K edge. On the other hand, there is a large anomalous dispersion near the Al-K edge since aluminium is one of the constituent elements in the monochromator crystals. Therefore, we can obtain the spectra up to about 250eV from the Mg-K edge when beryl crystals are used as monochromator. Apparently the spectra of $Mg(OH)_{2-2x}O_x$ with x=0.53, 0.71, 0.90, and 1.00 are almost the same. These spectra are distinct from that of $Mg(OH)_2$ concerning the spectrum just above the edge and the period of fluctuation. These results imply that the local structure around Mg atoms of the dehydrated samples is similar to that of MgO. The local structure of the sample with x=0.53 is also the MgO type though $Mg(OH)_{2-2x}O_x$ has a structure of $Mg(OH)_2$ below x_c=0.68 on an average. Detailed analysis is now in progress.

We are indebted to all the staffs of the UVSOR facility,

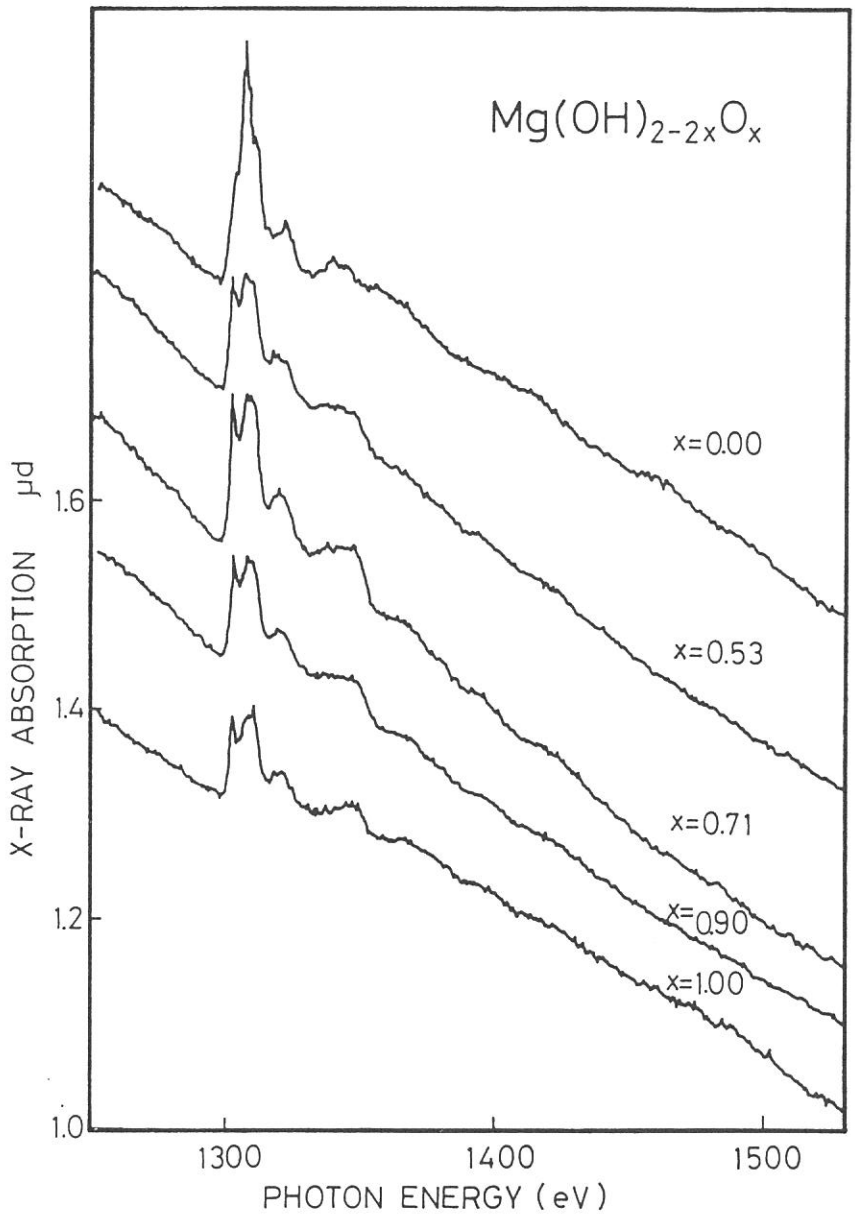

Fig. 1 X-ray absorption spectra near the Mg-K edge of $Mg(OH)_{2-2x}O_x$ with x=0.00, 0.53, 0.71, 0.90, and 1.00.

especially to Professor M. Watanabe, O. Matsudo, J. Yamazaki, and K. Fukui for their continuous support and encouragement through the work.

Reference

1) H. Terauchi, T. Ohga, and H. Naono, Solid State Commun. 35, 895 (1980).

INTRAMOLECULAR BAND MAPPING OF n-$CH_3(CH_2)_{34}CH_3$ AS A MODEL COMPOUND OF POLYETHYLENE

Hitoshi FUJIMOTO, Kazuhiko SEKI,* Nobuo UENO,**
Kazuyuki SUGITA,** and Hiroo INOKUCHI

Institute for Molecular Science, Myodaiji, Okazaki 444.
*Department of Materials Science, Faculty of Science,
Hiroshima University, Hiroshima 730.
**Department of Image Science and Technology,
Facuty of Engineering, Chiba University, Chiba 260.

The angle-resolved photoemission spectroscopy has an advantage in studying the electronic structures of oriented systems; the energy-band dispersion can be determined in addition to the density of states. We will report here on the preliminary angle-resolved UPS study of oriented films of hexatriacontane, n-$CH_3(CH_2)_{34}CH_3$, prepared by in situ vacuum evaporation using the synchrotron radiation of UVSOR as a tunable light source.

The oriented thin films of ~10 nm thickness were prepared in the preparation chamber (base pressre 10^{-9} Torr) and subsequently transferred to the main chamber. The detailed setup of the UPS system is reported in another article in this Report. Photoelectron spectra were measured for the normal emission from a sample surface with the incident angle of the light beam of 42°. The intramolecular energy-band dispersion was determined according to the method reported in Ref.1.

Figure 1 shows $h\nu$-dependent photoelectron spectra in the 30-65 eV photon energy region. Similar spectral changes at low photon energies ($\leq$54 eV) were already observed in the previous work,[1] but spectra at higher photon energies could not be measured. The experimental band structure obtained from these spectra is shown in Fig.2. As a guide for eyes, results of an ab initio calculation for a polyethylene chain by Karpfen,[2] which was 0.8 times contracted and shifted in an energy scale for a better fit, are also shown. The high-binding-energy bands of E_B=18 and 25 eV at k=0, which are assigned to C_{2s} bands, are smoothly connected at $k=\pi/a$, as expected theoretically.[2] This part could not be examined experimentally in the previous study.[1] It should be mentioned that these C_{2s}-originated bands become separated again at a higher photon energy of 74 eV (not shown in Fig.1).

In summary, we have presented a preliminary study of the angle-

resolved photoemission which covers the whole energy-band dispersion of oriented n-$CH_3(CH_2)_{34}CH_3$ films and demonstrated the powefulness of this technique for studying the intramolecular energy-band dispersion. Further detailed investigation is in progress on n-$CH_3(CH_2)_{34}CH_3$.

REFERENCES

1) K.Seki, N.Ueno, U.O.Karlsson, R.Engelhard, and E.-E.Koch, Chem. Phys., 105, 247(1986), and references therein.

2) A.Karpfen, J. Chem. Phys., 75, 238(1981).

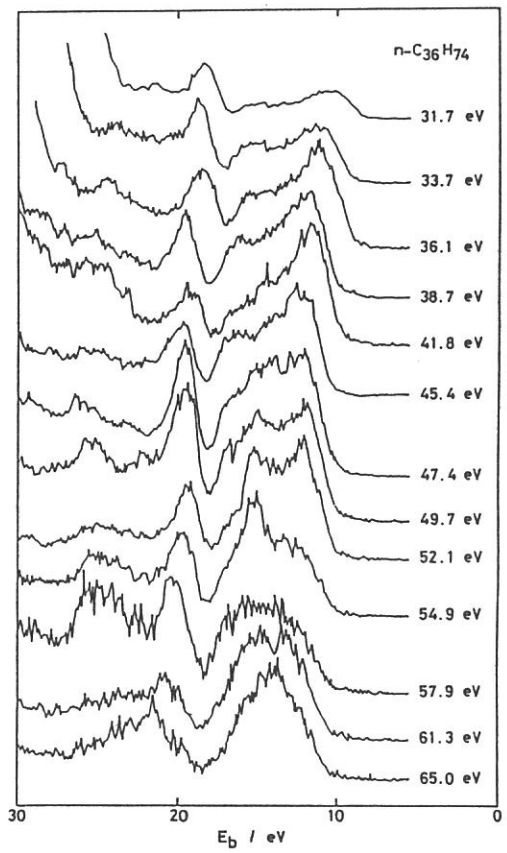

Fig.1 hν-dependent photoelectron spectra of n-$CH_3(CH_2)_{34}CH_3$.

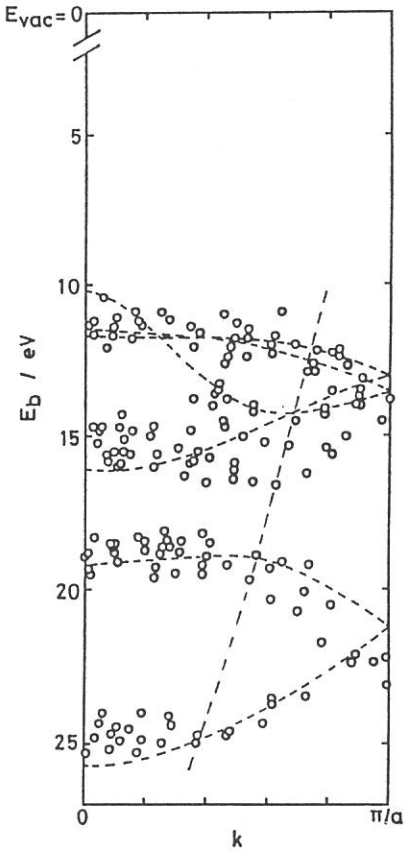

Fig.2 Energy-band dispersion of n-$CH_3(CH_2)_{34}CH_3$. The part at the right side of the broken line could not be accessed in the previous work.[1)]

PHOTON STIMULATED DESORPTION OF NEUTRAL SPECIES FROM LiF

Yoshitaka YAMADA, Tetsuji GOTOH*, Ayahiko ICHIMIYA, Yoichi KAWAGUCHI*, Masahiro KOTANI*, Shunsuke OHTANI*, Yahachi SAITO, Yukichi SHIGETA*, Shoji TAKAGI*, Yuji TAZAWA*, Goroh TOMINAGA* and Tsuneo YASUE

Department of Applied Physics, Nagoya University, Nagoya 464
*Institute of Plasma Physics, Nagoya University, Nagoya 464

In the previous work 1), we observed photon stimulated desorption (PSD) of positive ions from LiF. In the present work, we observed the desorption of neutral species from LiF and compared the energy dependence of PSD of neutral species with that of ions.

The experiments were carried out on BL6A2 of UVSOR. LiF (100) surface was cleaved in the air, and the specimen was mounted in a UHV chamber. The specimen temperature was held at 260 C during measurements in order to avoid electronic charging. The neutral species were ionized by electron impact with an energy of 30 eV and detected by a quadrupole mass spectrometer. The yields were normalized with the photon intensity.

Desorption yields of Li and HF were measured. The relative desorption yields of Li depended on the photon energy. The both yields of Li and HF gradually increased with the incident photon energy. Around the photon energy of 61 eV we reproducibly observed a sharp peak in the yield spectrum of Li as shown in fig. 1, while in the yield spectrum of HF no remarkable structures were observed in the same energy region.

For the desorption process of Li it is considered that the electronic processes are associated with the decay of the core-excitons. The sharp peak observed in the yield spectrum of neutral Li was located at the position of the strong peak in that of F^+ ions 1). Therefore the neutral Li desorption for the sharp peak is due to the interatomic Auger process such as

$$Li^{+*}+F^- \longrightarrow Li^*+F^++e^-, \qquad (1)$$

where asterisks indicate the core-excited states. Since the Li^* atoms interact weakly with the LiF crystal matrix, Li^* can easily desorb from the surface 2).

The broad background of the spectra showed quite different profiles from the yield spectra of the ions obtained previously 1). It is

considered that the desorption is due to migration of defects induced by photons as pointed out by Taglauer et al. 3) and Loubriel et al. 4).

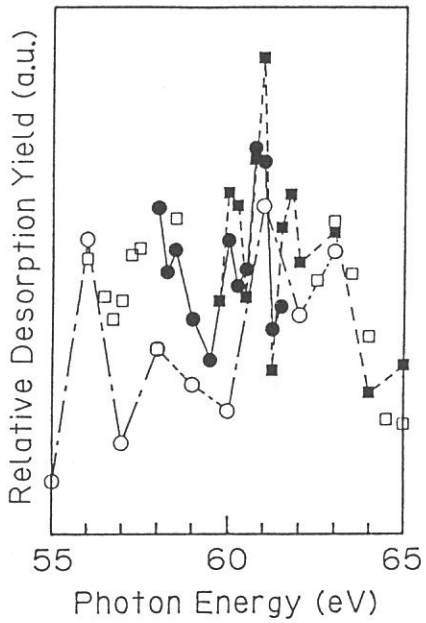

Fig.1. The relative Li yield spectra taken in several series of measurements around 61 eV, as shown with the different kind of plots and lines.

References

1) T. Yasue et al., Jpn. J. Appl. Phys. 25 (1986) L363.
2) N.H. Tolk et al., Phys. Rev. Lett. 49 (1982) 812.
3) E. Taglauer et al., Surf. Sci. 169 (1986) 267.
4) G.M. Loubriel et al., Phys. Rev. Lett. 57 (1986) 1781.

RADIATION-INDUCED DEGRADATION OF AMORPHOUS SILICON SOLAR CELLS

Akira YOSHIDA, Hiroyuki SUEZUGU, Tetsuya HIRANO,
Hiroshi OGAWA*, Hidehiko ITO*,and Takashi HIRAO**

Toyohashi University of Technology, Toyohashi, 440
*Saga University, Saga, 840, **Matsushita Electrical
Industrial Co.,Ltd., Osaka, 570

There is now considerable interest in the use of hydrogenated amorphous silicon(a-SiH) as one of the most promising materials for low cost solar cells, when prepared by decomposition of silane in a glow discharge. However, Staebler and Wronski (1) found that dark conductivity and photoconductivity are reduced significantly by prolonged illumination with intense visible light. These induced changes are found to be reversible and the original values are restored by annealing at temperature above 150°C. These metastable changes degrade the device characteristics. An understanding of the observed changes is crucial for the future applications. In this report, we show very rapid degradation of amorphous silicon solar cells exposed to synchrotron radiation beam.

Samples(p-i-n diodes) were prepared by glow discharge decomposition of SiH_4 gas on ITO-coated glass(Fig.1). Thicknesses of the p,i,and n layers were 10,400 and 40 nm, respectively. Another metal electrode of Al(70nm) or Ti(50nm) was deposited on the n layer, and used as a filter to synchrotron radiation beam. The short-circuit current of the sample exposed through the metal electrode was measured, showing very rapid decrease only in several seconds (Fig.2). Under illumination of the visible light in the SR beam (through a glass filter), no change in the I-V characteristics was observed (the curve at t=0 in Fig.3). But the degraded cell exposed to the beam with shorter wavelength has smaller output current and voltage, shown in Fig.3. Figs.4(a) and (b) represent a typical evolution after irradiation of the dark I-V characteristics. In Fig.4(a), the forward-bias current in the low bias range increases rapidly, and the diode quality factor becomes from 1.17 to 1.49. Large increase in the reverse-bias current was induced (Fig.4(b)). Fig.5 shows the I-V characteristics under illumination of white light of 5.4 mW/cm^2. Degraded characteristics recovered gradually even when kept in air at room temperature after exposure. Annealing at 75°C made them restored nearly to the original values. The degradation of p-i-n diodes is due to the increase in density of states caused by the beam.

(1) D.L.Staebler and C.R.Wronski, Appl. Phys. Lett. 31 292 (1977)

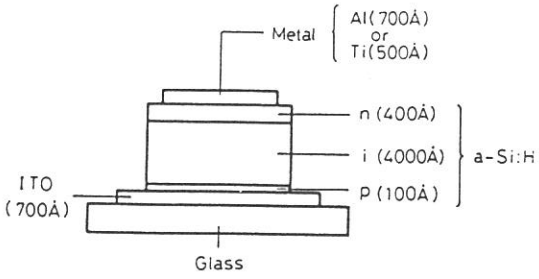

Fig.1 Sample(p-i-n diode)

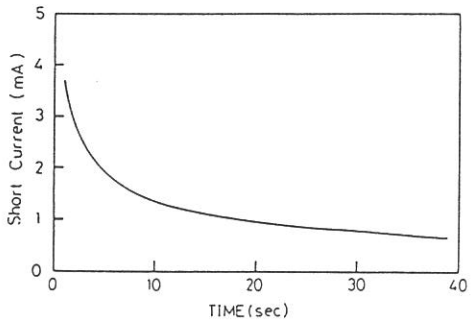

Fig.2 Time dependence of short-circuit current

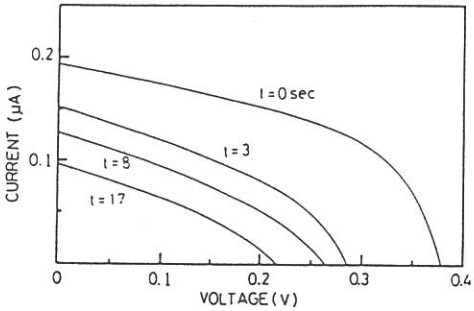

Fig.3 I-V characteristics under illumination of visible light in the SR beam

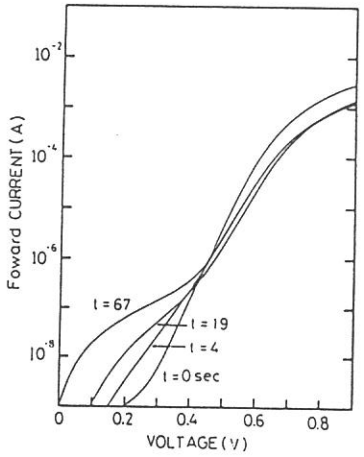

Fig.4(a) Dark forward-bias current

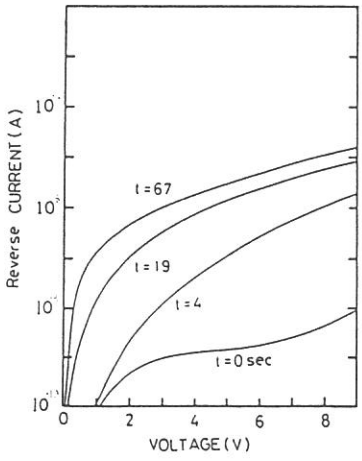

Fig.4(b) Dark reverse-bias current

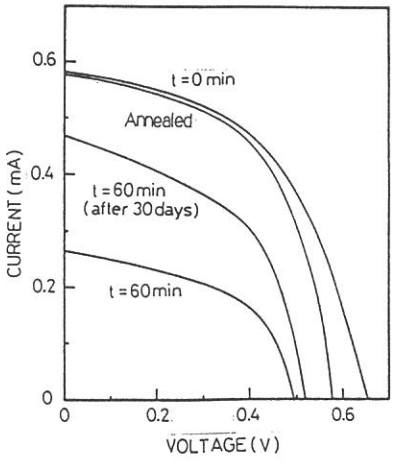

Fig. 5 Illuminated I-V characteristics ($5.4\ mW/cm^2$)

X-RAY VACUUM LITHOGRAPHY

Hitomi YAMADA, Takao SATO, Satoshi ITOH, Shinzo MORITA and Shuzo HATTORI
Department of Electronics, Nagoya University, Chikusaku Nagoya 464

X-ray lithography is one of the most promising technology to fabricate microelectronis circuit fabrication. Several efforts have been made to confirm the effectiveness of X-ray lithography. Synchrotron Radiation (SR) is supposed to be usefull, because the flux of usable X-ray from SR is large compared with other X-ray sources and SR is also highly collimated. Therefore, SR was used in this work.

The resists were decomposed randomly by SR exposure resulting in reduction of film thickness, which is known as self development. Dependence of self development characteristics of resists on SR wavelength was investigated in this experiment. SR exposure to resists was performed under the condition of 600 MeV and a current of 30 mA. For division of SR wavelength, polyimide and Be film were used as X-ray filters. The typical radiation is shown in Fig.1.

As the resists, plasma polymerized resists and conventional resists for comparision were used. Plasma polymerized resists were formed in an inductively coupled gas flow type reactor using methyl methacrylate (MMA) amd MMA with tetramethyl tin (TMT), SF_6, or styrene as monomers. The polymer structure of resists were investigated by IR and ESCA. ESCA results showd a smsll amount of Sn, S and F were incorporated into the polymer.

Self development characteristics are shown in Fig.2 for PMMA and in Fig.3 for PPMMA as a function of exposure dose. It was found that the removed thickness was increased linearly at low doses region, while it was saturated completely at high doses region for direct exposure. For exposure through X-ray filters, the removed thickness was linearly increased without saturation and exceeded the saturated region. Self development characteristics in a soft X-ray region are shown in Fig.4 for plasma polymerized resists. The self development was enhanced significantly by doping Sn, S and F as sentizers. The self development of PBS was more effectively developed than that of PMMA, which is considered to be attributed to be high G value of PBS.

In ordre to investigate the mechanism of self developmen, IR and ESCA measurement were performed before and after exposure. Also, the decomposed products released from film were detected by mass spectroscopy.

From these results, it was found that the change of molecular structure was varied by SR wavelength region. Therefore, the self development characteristics were changed under both exposure conditins. Recombination reaction was actively induced by direct exposure and the molecular structure which was hard enough to withstand to SR exposure was formed. By using X-ray filters, decomposition connecting with self development was more effectively advanced than that for direct exposure.

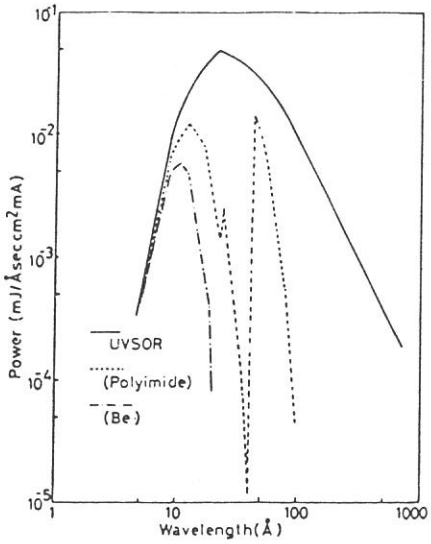

Fig.1 Sr wavelength distribution

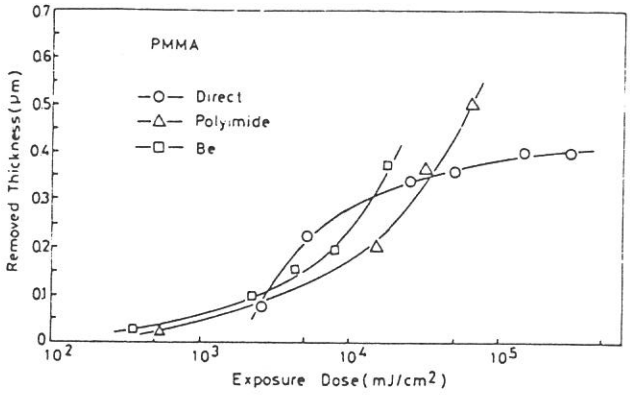

Fig.2 Self development characteristics of PMMA

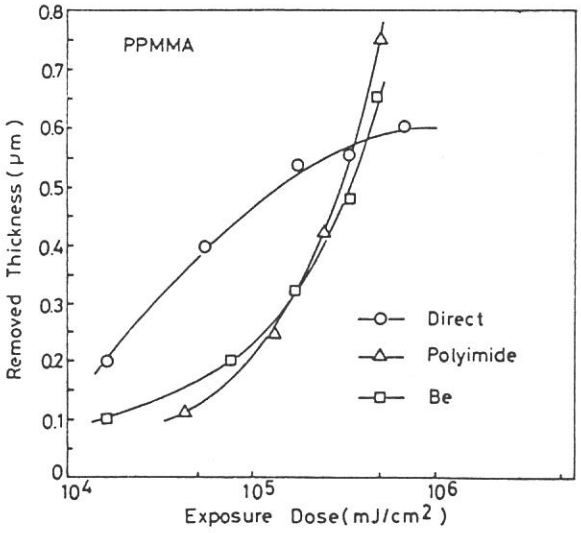

Fig.3 Self development characteristics of PPMMA

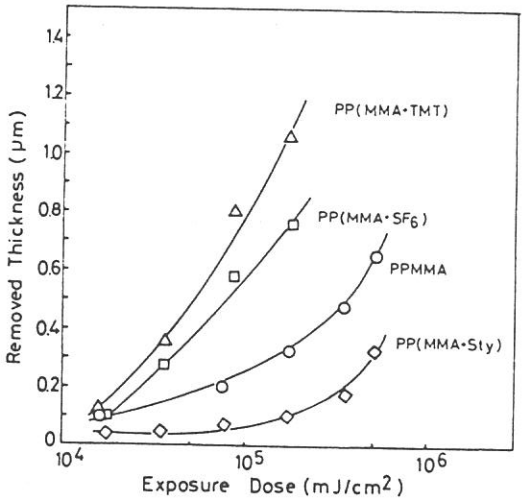

Fig.4 self development characteristics of plasma polymerized resists in a soft X-ray region

CHARACTERISTICS OF MULTILAYER REFLECTORS IN 80-300A REGION

Koujun YAMASHITA, Hiroshi TSUNEMI, Akira MIYAKE,
Yoshiaki KATO*, Hiroyuki SHIRAGA*, Takuma ENDO*,
and Katsuya KAMEI*

Department of Physics, Osaka University, Toyonaka 560
*Institute of Laser Engineering, Osaka University, Suita 565

The development of multilayer reflectors makes it possible to fabricate the normal incidence x-ray telescope and the x-ray laser mirror in the wavelength region 40-300A. The multilayer reflector is the most promising optical element to get the high reflectivity for the normal incidence, although the sensitive wavelength band is limited to $\lambda/10$. It is also possible to apply it for the x-ray spectrometer and polarizer.

The measurement of reflectivities of multilayer reflectors was carried out with the monochromatized synchrotron radiation in 80-300A region on BL-6A2. The incident beam is monochromatized with the plane grating monochrometer and introduced to the reflectometer. The multilayer is mounted on the rotation axis and the detector(sodium salicylate sprayed photomultiplier) on the rotation arm. The incidence angle is changed from 10° to 85° by 5° step, which is measured from the the normal of the reflecting surface. The rotation axis of the reflectometer is perpendicular to that of the grating, so that we can mostly measure the reflectivity of p-polarized beam. However the reflectivity for the normal and grazing incidence does not much depend on the degree of polarization. Multilayer reflectors, such as Mo/Si, W/C, Ni/C and Ru/Si with 2d=112-250A and 5-60 layer pairs, were evaluated with this system by measuring the peak reflectivity, the wavelength resolution and Bragg angle. The peak reflectivity of Mo/Si(2d=226A, N=60) was obtained to be 37% at 212.6A for the first order and 5% at 113.7A for the second order at the incidence angle 10°, as shown in Fig.1. That for the incidence angle is shown in Fig.2, which shows minimum reflectivity at 45° and sharp decrease at Si-L edge (123A). Open circles are values corrected for the contribution of the second order caused by the grating. In the wavelength range 80-150A, the incident beam is purely first order, whereas that in the longer wavelength range than 150A is contaminated with the second order beam. This contribution is evaluated with

the wavelength scan at the fixed incidence angle. If the second order is dominant, we can observe the second peak at the wavelength just as twice as the fist order, which is longer than 2d value.

The observed peak reflectivities are compared with values calculated with optical constants. Barbee et al.[1] reported that the peak reflectivity of Mo/Si was 50% at 170A in the near normal incidence and was higher than the theoretical value. We have to investigate the quality of multilayer reflectors, taking into account the opical constant, the surface roughness of substrate and the interfacial roughness of each layer.

Reference

1) T.W. Barbee,Jr, S. Mrowka, and M.C. Hettrick, Appl. Opt. 24 (1985) 883.

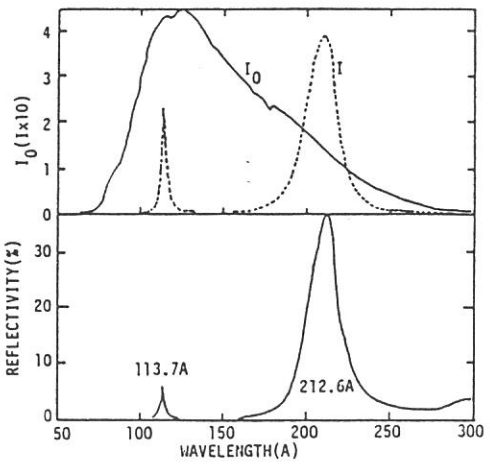

Fig.1 Reflectivities of Mo/Si (2d=226A, N=60) at the incidence angle 10°. I_0: incident beam I: reflected beam.

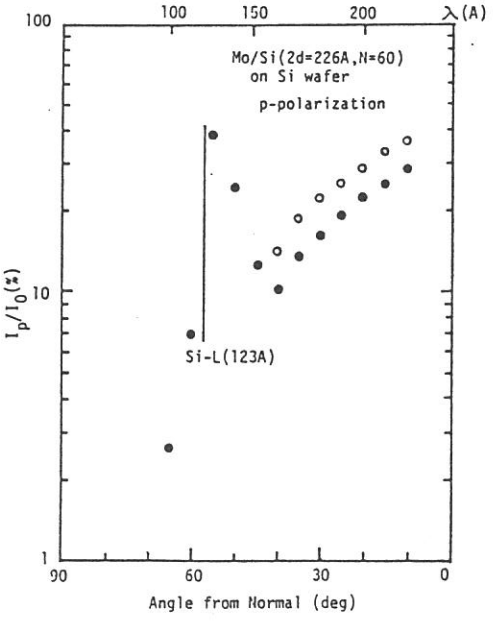

Fig.2 Peak reflectivities vs. the incidence angle. Open circle: corrected for the second order.

Focusing Test of Free Standing Zone Plate in VUV Wavelength Region

Yutaka Watanabe[1),4)], Shigetaro Ogura[1)], Yoshinori Nagai[2),4)], Yasushi Nakajima[3)], and Hiroshi Kihara[4)]

1)Electronic Material Division, Research Department 34, Canon INC., Atsugi 243-01, 2)Laboratory of Molecular Biology, School of Veterinary Medicine, Azabu University, Sagamihara 229, 3)Department of Physics, Waseda University, Shinjuku-ku, Tokyo 160, 4)Department of Physics, Jichi Medical School, Minamikawachi - machi, Tochigi 329-04

A free standing zone plate was fabricated as an optical element of X-ray microscope, and was tested at UVSOR beam line BL6A2 at Institute for Molecular Science. The zone plate was designed for observing biomolecules in VUV wavelength region [1] with features of 150 mm in focal length at 80 Å, about 1000 μm in diameter, 1.2 μm in outermost zone width, and 104 in the number of transparent zones. Optical arrangement of the test system is shown in Fig.1, where an electron multiplier (for one-dimensional intensity distribution) or photographic films (for two-dimensional intensity distribution) is used.

After X-ray passed through the pinhole and the zone plate, the intensity at the slit plane was measured by the electron multiplier (Hamamatsu PhotonicsR595) and by sliding the slit across the X-ray beam. In Fig.2 the intensity distribution of X-ray at 145.7 Å is shown with a hole of 1mm ϕ instead of the zone plate in Fig.1. Figure 3 shows the intensity distribution of X-ray at 145.7 Å with the zone plate, whereas Figure 4 shows the intensity distribution at 145.7 Å, sliding the zone plate by 0.4 mm toward y-axis. The central part of Fig.3 is contributed by mainly the zeroth order diffraction from the zone plate, and by sharp peaks probably due to the other order diffractions by the zone plate.

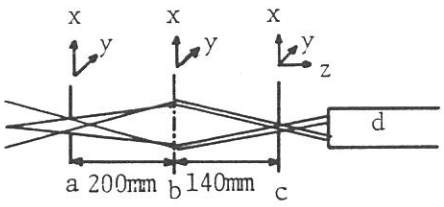

Fig.1 Test system a:pinhole b:zone plate c:slit or photographic film (in film's case $\overline{ab}$=264.4mm, $\overline{bc}$=235.9mm) d:electron multiplier

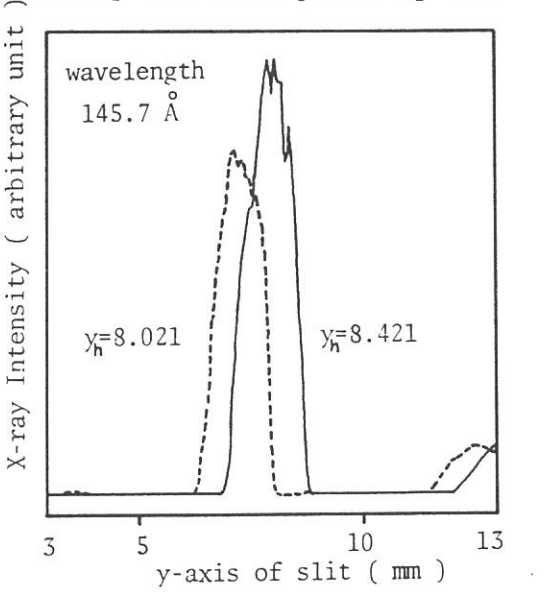

Fig.2 Intensity distribution with a hole of 1 mm ϕ
y_h: y-axis of a hole

At the same time, the two-dimensional distribution of 96.2 Å X-ray through the zone plate was taken with a photographic film (minicopy ASA 32),shown in Fig.5. X-ray intensity of the film was measured densitometrically (Fig.6). High intensity at the center of the film may indicate the focusing of the first order diffraction.

[1] Y.Nagai,Y.Nakajima,Y.Watanabe,S.Ogura,K.Uyeda,Y.Shimanuki,and H.Kihara,Proceedings of X-ray Microscopy '86,Springer-Verlag, (1986) in press.

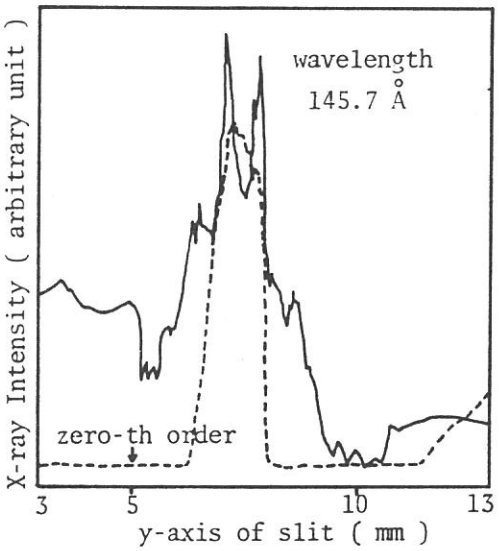

Fig.3 Intensity distribution with the zone plate (zone plate y=8.021 mm)

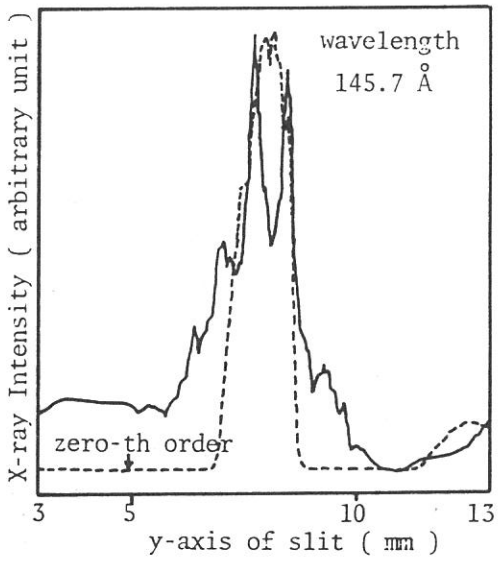

Fig.4 Intensity distribution with the zone plate (zone plate y=8.421 mm)

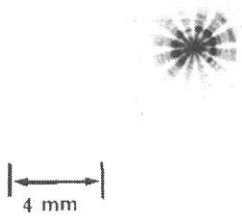

Fig.5 Two-dimensional distribution

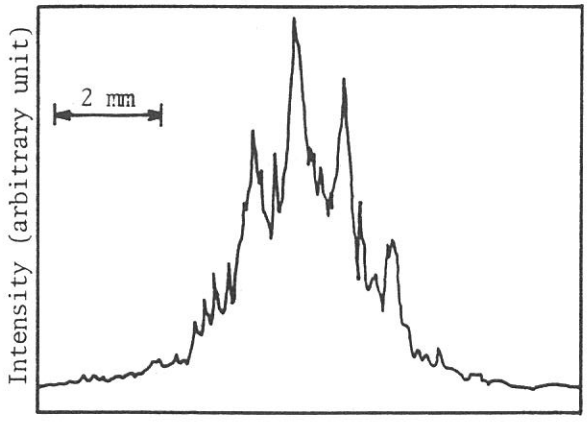

Fig.6 densitometrically scanned intensity distribution

Measurement of a far infrared pulse width by Fourier transform spectroscopy

Tetsuhiko OHBA and Shun-ichi IKAWA

Department of Chemistry, Faculty of Science,
Hokkaido University, Sapporo 060, Japan

The pulse width of the far-infrared radiation from UVSOR has been estimated to be about 0.5 nsec at least from a measurement of interference fringes due to a hyperpure silicon plate of 0.3 cm thickness by use of a Martin-Puplett interferometer installed at BL6A.

Because of a spatially finite length of the pulsed radiation, the interference efficiency will decrease with increasing optical path difference between two arms of the interferometer. The shape of the radiation pulse from UVSOR can be approximated by a Gaussian funtion, so that the relative interference efficiency at a path difference, x, is given by $\exp[-(\ln 2/a^2)x^2]$, where a is the length of the pulse. Consequently, the observed interferogram can be expressed as,

$$I_p(x) = I(x)\ \exp[-(\ln 2/a^2)x^2], \qquad (1)$$

where I(x) is the interferogram to be observed at $a=\infty$. Therefore, the effect of the finite pulse width on the interferogram is similar to the apodization and the related instrument line shape function is given by,

$$B_i(\nu) = \int_{-L}^{L} \exp[-(\ln 2/a^2)x^2]\ \mathrm{COS}2\pi\nu x\ dx, \qquad (2)$$

where L is the maximum optical path difference. The shapes of $B_i(\nu)$ for several pulse widths are shown in Fig.1. It is easily seen that the spectral resolution lowers as the pulse width becomes comparable to or less than the maximum path difference.

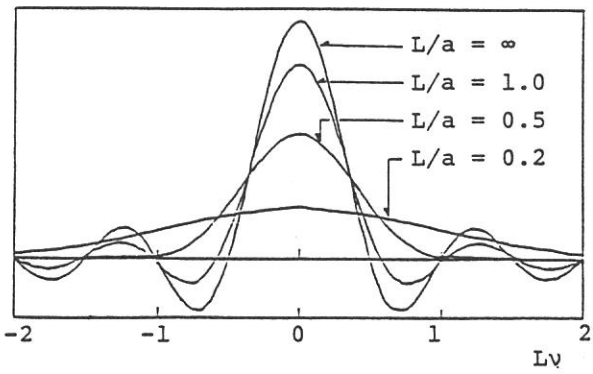

Fig.1 Instrument line shape functions for gaussian pulsed source.

The observed spectrum is given by the Fourier transform of Eq.(1) and

can be written as,

$$B_p(\nu) = \int_{-\infty}^{\infty} B(\nu') \, B_i(\nu-\nu') \, d\nu', \qquad (3)$$

where $B(\nu') = \int_{-\infty}^{\infty} I(x) \, \cos 2\pi\nu' x \, dx$

is the true spectrum.

Fig.2 shows the observed interference fringes due to the silicon 0.3 cm window in the 25-40 cm^{-1} range measured at L=5.12 cm. The average amplitude of the observed fringes is estimated to be 64.6%. A theoretical calculation of the spectrum, $B_p(\nu)$, was carried out for several pulse widths using the optical constants of hyperpure silicon, and are listed in Table 1. Uncertainty or spread of the incident angle of the radiation on the window and imperfectness in the flatness and the parallelism of the window surfaces were not taken into the calculations. Though these effects should be small in the present measurement, they will always reduce the amplitude of the fringes to a certain extent. Thus we conclude from Table 1 that the pulse width of the far-infrared radiation is about 0.5 nsec at least.

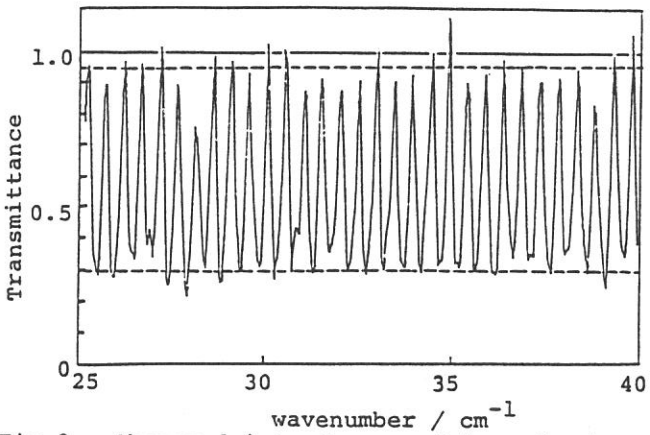

Fig.2 Observed interference fringe due to silicon 0.3cm window measured at L=5.12cm. The broken lines indicate the average amplitude.

Table 1 Calculated amplitudes of the interference fringes due to silicon 0.3cm window for several pulse widths.

Width/cm	Duration/nsec	Amplitude/%
∞	∞	65.3
25.6	0.85	64.9
20.48	0.68	64.7
15.36	0.51	64.3
10.24	0.34	63.0
5.12	0.17	57.7
2.56	0.08	41.5
observed		64.6

Measurement of the far infrared optical constants of liquid acetonitrile

Tetsuhiko OHBA and Shun-ichi IKAWA

Department of Chemistry, Faculty of Science,
Hokkaido University, Sapporo 060, Japan

The far-infrared optical constants of liquid acetonitrile were determined from a transmission spectrum measured by use of a far-infrared interferometer at BL6A.

For normal incidence, a transmittance of a liquid cell as shown in Fig.1, is given by,

n_1	Air	
$\hat{n}_2$	Window	d_2
$\hat{n}_3$	Sample	d_3
$\hat{n}_4=\hat{n}_2$	Window	d_4
$n_5=n_1$	Air	

Fig.1 A liquid cell.

$$T_5(\nu) = \left| \frac{(1-\hat{r}_{12}^2)(1-\hat{r}_{23}^2)e^{i(\hat{\beta}_2+\hat{\beta}_3+\hat{\beta}_4)}}{1+\hat{Q}} \right|^2 , \qquad (1)$$

where $1 + \hat{Q} = 1 + \hat{r}_{12}\hat{r}_{23}(e^{2i\hat{\beta}_2}+e^{2i\hat{\beta}_4}-e^{2i\hat{\beta}_2+2i\hat{\beta}_3}-e^{2i\hat{\beta}_3+2i\hat{\beta}_4})$

$$- \hat{r}_{23}^2 e^{2i\hat{\beta}_3} - \hat{r}_{12}^2 e^{2i\hat{\beta}_2+2i\hat{\beta}_3+2i\hat{\beta}_4} + \hat{r}_{12}^2\hat{r}_{23}^2 e^{2i\hat{\beta}_2+2i\hat{\beta}_4} ,$$

$$\hat{r}_{ij} = \frac{\hat{n}_i - \hat{n}_j}{\hat{n}_i + \hat{n}_j} , \qquad \hat{\beta}_i = 2\pi\hat{n}_i\nu d_i , \qquad \hat{n}_i = n_i + ik_i .$$

The observed transmittance is given by the convolution of Eq.(1) with the instrument line shape function, $f(\nu)$, as,

$$T_{obs}(\nu) = \int_0^\infty T_5(\nu') f(\nu-\nu') d\nu' . \qquad (2)$$

In Eq.(2), unknown parameters are the complex refractive indices of the sample, $\hat{n}_3(\nu) = n_3(\nu) + ik_3(\nu)$, because all the other variables could be measured separately. In addition, $n_3(\nu)$ is related with $k_3(\nu)$ by the Kramers-Kronig relation,

$$n(\nu) = n(\nu_r) + \frac{1}{2\pi^2} P\int_0^\infty \frac{\alpha(x)}{x^2-\nu^2} dx - \frac{1}{2\pi^2} P\int_0^\infty \frac{\alpha(x)}{x^2-\nu_r^2} dx , \qquad (3)$$

where $\alpha = 4\pi\nu k$ and $n(\nu_r)$ is the refractive index at the anchor point. We assumed for the absorption coefficient the following analytical form,

$$\alpha(\nu) = \frac{\nu^2}{P_0 + P_1\nu^2 + P_2\nu^4 + P_3\nu^6 + \cdots\cdots + P_N\nu^{2N}} \qquad (4)$$

This expression is identical with the spectral density of the continued-fraction representation by Mori, which gives quantum statistically exact result at the limit of $N=\infty$.

Using Eqs.(1)-(4), we performed the simulation of the observed transmittance. N was taken to be 6, and the adjustable parameters were P_0-P_6, d_3, and the difference in thickness between two silicon windows, Δd_{24}. The best fit obtained for neat CH_3CN is shown by a solid curved line in Fig.2. The agreement between the observed and calculated values is excellent. Two types of interference fringes are seen in Fig.2; one ($\Delta\nu$=30cm^{-1}) is explained by Δd_{24} (=0.05mm) and the other ($\Delta\nu$=130cm^{-1}) by d_3 (=0.03mm). This is the first observation of the former kind of fringes as far as we know. This fact and the successful simulation without any other effect, such as a spread of a incident angle of the radiation, are owing to a good coherency of the radiation from UVSOR. In Fig.3, the absorption coefficient of neat CH_3CN determined in the present work is compared with several literature data recently reported. The present result agrees very well with the laser ATR result from Ref.1.

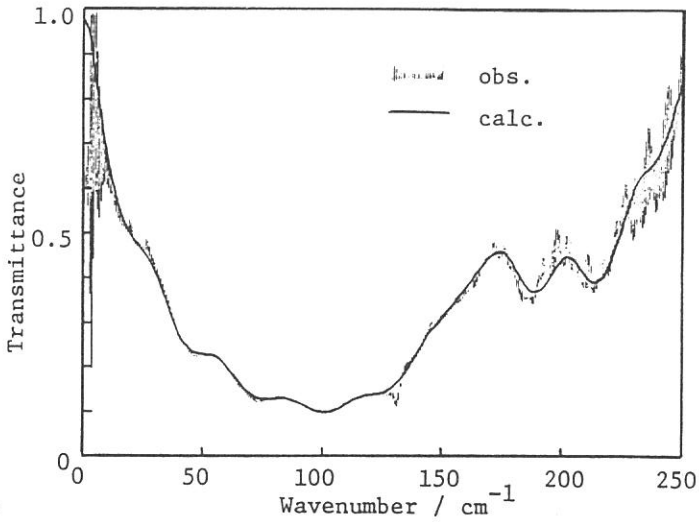

Fig.2 Transmittance of acetonitrile.

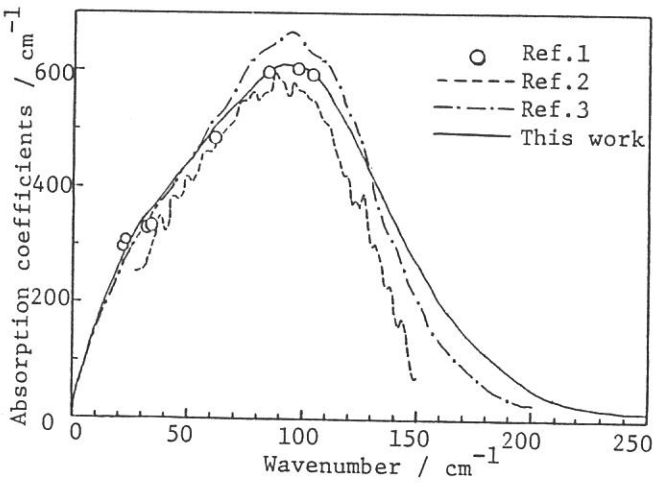

Fig.3 Absorption coefficients of acetonitrile.

References

1. S.Ikawa et al. Intern.J.Infrared Millimeter Waves, 6, 287(1985)
2. J.R.Birch et al. Chem.Phys.Lett., 117, 197(1985)
3. K.E.Arnold et al. Molec.Phys., 48, 451(1983)

FAR-INFRARED SPECTROSCOPY OF SMALL SOLID STATE SPECIMENS

Takao NANBA, Yasuhito URASHIMA, Mikihiko IKEZAWA,
Makoto WATANABE* and Hiroo INOKUCHI*

Department of Physics, Tohoku University, Sendai 980
*Institute for Molecular Science, Myodaiji, Okazaki 444

One of the most useful characteristics of the system of far-infared spectroscopy by synchrotron radiation at the beam line BL6A1 is that the size of the light beam for measurement is very small. The cross sectional diameter of the light beam is as small as 3 mm at the position of the specimen.[1] Therefore, one can observe the reflectivity or transmission spectrum using a small specimen. Moreover, the light is linearly polarized and the spectroscopic system is convenient for the observation of anisotropic materials.

(I) Alkali silver halide crystals

The alkali silver halide crystal has the orthorhombic structure.[2] Reflectivity spectra of Rb_2AgI_3 and K_2AgI_3 crystals were measured with the normal incidence configuration at 300, 80 and 15 K. Examples of spectra of Rb_2AgI_3 are shown in Fig.1. The diameter of the measuring light beam was 2 mm. The light was polarized along the three directions of the crystal. A number of lines were resolved and the reflectivity spectra were analyzed to obtain the dielectric constants by the Kramers-Kronig analysis.

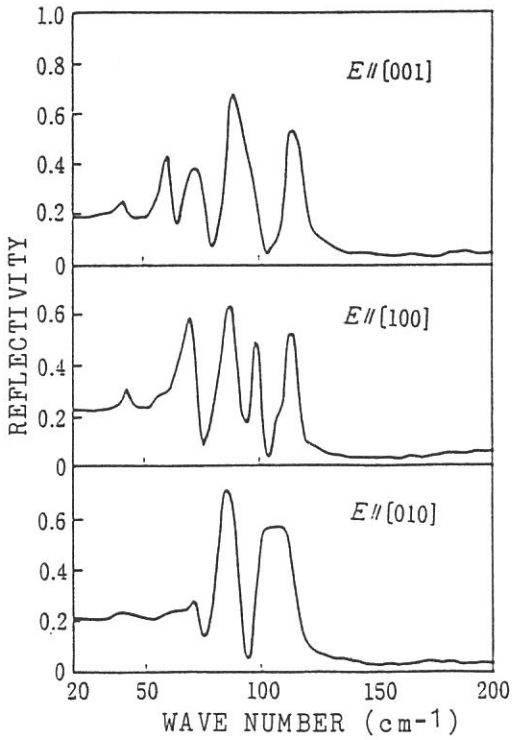

Fig.1 Reflectivity spectra of Rb_2AgI_3 crystal at 80 K. The diameter of measuring light beam is 2 mm and the electric vector is parallel to the crystal axes.

(II) Black phosphorus crystal

The black phosphorus crystal has two infrared active modes of the lattice vibration.[3] We have observed the B_{1u} mode in the far-infrared region with a high resolution of $\Delta\nu=0.3$ cm^{-1}. In Fig.2 reflectivity spectra at 300 and 15 K are shown. The light for measurement was polarized along the x-axis[3] of the crystal.

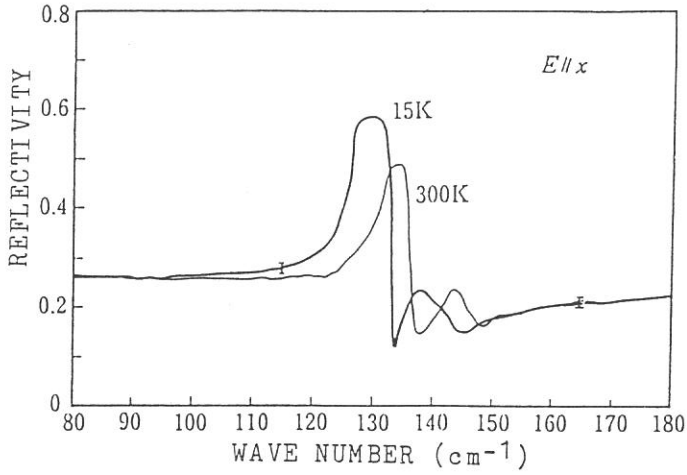

Fig.2 Reflectivity spectra of black phosphorus crystal. The diameter of the measuring light beam was 4 mm and the spectral resolution $\Delta\nu=0.3$ cm^{-1}.

By Kramers-Kronig analysis of the spectra dielectric constants were obtained. From a peak of the spectrum of ε_2 the TO phonon energy was determined as 134.0 and 128.3 cm^{-1} at 300 and 15 K, respectively. The TO mode was found to shift to the low energy side at low temperature. The temperature dependence explains a discrepancy between reported values[4,5] of the TO phonon energy. From the peak of the loss function, the energy of the LO mode at 15 K was determined as 133.6 cm^{-1}. Then the TO-LO splitting energy is 5.3 cm^{-1}. This value is about three times larger than a previously reported value[5] but is in good agreement with the theoretically calculated value[6] of 6 cm^{-1}.

References

1) T.Nanba, Y.Urashima, M.Ikezawa, M.Watanabe, E.Nakamura, K. Fukui and H.Inokuchi: Int. J. Infrared and Millimeter Waves 7(1986)1769.
2) K.Edamatsu, M.Ikezawa, H.Tokailin, T.Takahashi and T.Sagawa: J. Phys. Soc. Jpn. 55(1986)2880.
3) C.Kaneta, H.K.Yoshida and A.Morita: Solid State Comm. 44 (1982)613, J.Phys. Soc. Jpn. 55(1986)1213.
4) M. Ikezawa, Y.Kondo and I.Shirotani: J. Phys. Soc. Jpn. 52 (1983) 1518.
5) S.Sugai and I.Shirotani: Solid State Comm. 53(1985)753.
6) C.Kaneta and A.Morita: J. Phys. Soc. Jpn. 55(1985)1224.


UV
50R
T.O
E.N
H.Y
K.F
J.Y
O.H
M.H
K.S
T.K
T.K
H.L
M.W

OKAZAKI CONFERENCE

The 28th Okazaki Conference* on Solid State Chemistry with VUV Synchrotron Radiation

H. Inokuchi, M. Watanabe and K. Seki#
UVSOR Facility, Institute for Molecular Science
#Department of Material Science, Hiroshima University

During this Conference on "Solid State Chemistry with VUV Synchrotron Radiation" the principal topic for discussion was the interaction of VUV photons with bulk materials as an approach to the production of new materials with VUV photons.

Much of the oscillator strength of materials lies in VUV, resulting in a major interaction between photons and materials in the VUV range. That is, many photochemical, photophysical and even photobiological changes can be produced in that region and there is therefore the possibility to produce quite new materials using VUV photons. For example, this includes the action of VUV photons as a trigger mechanism as exploited during the exposure of film. The programme was arranged to incorporate all these topics and included contributions on fundamental processes in spectroscopy and photoelectron spectroscopy, basic photochemical reactions in solids and molecules, dynamical processes in liquids and proposals for making new materials such as photo-assisted etching, photo-chemical vapor deposition and so on.

Although solid state chemistry is a rather new field in association with synchrotron radiation research, the full and intensive discussions made us feel sure that the Conference has been a milestone in considering the production of new materials with VUV photons. A total number of 25 talks were presented, including 6 invited lectures. The programme, the collected abstracts and the list of participants are presented below.

---

* Okazaki Conferences are the principal symposia at the Institute for Molecular Science. They are held twice or three times per year, with a total number of participants of about 50, including several invited foreign speakers.

The 28th Okazaki Conference on
Solid State Chemistry with VUV Synchrotron Radiation
5-7, February 1987, Room 101

February 5

12:30-13:30 Registration

13:30-13:40 Opening Address S.Nagakura (IMS)

Spectroscopy T. Murata (Kyoto Univ. Educa.) Presiding

13:40-14:10 K. Nakamura (Kyoto Univ.), "Core Excitons in Orthorhombic Indium Halides"

14:10-14:40 M. Taniguchi (Univ. of Tokyo), "Electron-Core-Hole Interaction in Layered Semiconductors"

14:40-15:10 N. Kosugi (Univ. of Tokyo), "Near Edge Structure of Coordination Compounds"

15:10-15:40 T. Fujikawa (Yokohama National Univ.), "Theory and Applications of Multiple Scattering in Solids"

15:40-16:10 Group Photograph
Coffee Break

Photoelectron Spectroscopy T. Ishii(Univ. of Tokyo) Presiding

16:10-16:40 T. Takahashi (Tohoku Univ.), "Angle-Resolved Ultraviolet Photoelectron Spectroscopy of Alkali-Metal Graphite Intercalation Compounds"

16:40-17:10 K. Seki (Hiroshima Univ.), "Photoelectron Spectroscopy of Organic Materials"

17:10-18:10 V. Saile (HASYLAB), "Two - Photon Photoemission from Molecular Crystals Combining Synchrotron Radiation with a Laser"

18:30-20:00 Reception, Cafeteria 2F

February 6

Time Resolved Spectroscopy (I) T. Okada (Osaka Univ.) Presiding

9:00-10:00 I. Munro (Daresbury Lab.), "Time Resolved Flourescence Anisotropy of Biochemical Systems"

10:00-10:30 Y. Hatano (Tokyo Inst. Tech.), "Time Resolved Fluorescence Spectroscopy of Liquid Alkanes"

10:30-11:00 Coffee Break

Time Resolved Spectroscopy (II) T. Kobayashi (Univ. of Tokyo) Presiding

11:00-12:00 J. Klein (Strasbourg Univ.), "Relaxation of Highly Excited States in Molecular Solids and Liquids

12:00-12:30 T. Mitani (IMS),"Time Resolved Fluorescence and Modulation Spectroscopies of Molecular Crystals"

12:30-13:30 Lunch

Self-Trapped Exciton, Defect Formation
H. Nakagawa (Fukui Univ.) Presiding

13:30-14:00 K. Nasu (IMS), "Dynamics of Tunneling and Relaxation from Free State to Self-Localized State of Exciton"

14:00-15:00 F. C. Brown (Illinois Univ.), "Defect Formation in Solids by Vacuum Ultraviolet Synchrotron Radiation"

15:00-15:30 Coffee Break

Photodesorption S.Ohtani(Nagoya Univ.) Presiding

15:30-16:30 R. Stockbauer (NBS), "Ion Desorption from Surfaces"

16:30-17:00 A. Ichimiya (Nagoya Univ.), "Photon Stimulated Desorption from LiF Surface"

17:00-17:30 H. Kanzaki (Fuji Photo Film Co.), "Photon-Stimulated Desorption of Neutrals from Silver and Alkali Halides"

Introduction to UVSOR Facility I. Koyano (IMS) Presiding

17:30-18:00 M. Watanabe (IMS), "Introduction to UVSOR Facility"

18:00-18:30 UVSOR Tour

February 7

Photofragmentation J.R.Grover (IMS & BNL) Presiding

9:00- 9:20 S. Nagaoka (IMS),"Investigation of Fragmentation Processes Following Core Photoionization of Organometallic Molecules in the Vapor Phase"

9:20- 9:30 H. Shiromaru (IMS),"Measurements of H^+ formation for Hydrocarbons"

9:30-10:30 T.K.Sham (BNL),"Site-Selective Photofragmentation of Molecules and Its Implication to VUV Induced Solid State and Surface Chemical Processes"

10:30-11:00 Coffee Break

Photochemistry in Solids Y.Maruyama (IMS) Presiding

11:00-11:30 H. Masuhara (Kyoto Inst. Tech.), "Photochemistry and Morphological Changes of Polymer and Deposited Organic Films"

11:30-12:00 S.Morita, H.Yamada and S.Hattori (Nagoya Univ.) "Wavelength Dependence of Chemical Process in X-Ray Resist"

12:00-12:30 T. Ito (Univ. of Tokyo), "VUV Photodegradation of Biomolecules --- DNA, ATP and Oligonucleotide"

12:30-13:30 Lunch

Prospective Projects K. Kimura (IMS) Presiding

13:30-14:00 K. Shobatake (IMS), "Photo-Excited Etching Reactions of Silicon Crystals"

14:00-14:30 A. Yoshida (Toyohashi Univ. Tech.), "Thin Film Deposition by VUV Synchrotron Radiation"

14:30-15:00 H. Inokuchi (IMS), "Concluding Remark -Application of VUV Photons to Organic Chemistry-"

Core Excitons in Orthorhombic Indium Halides

Kaizo NAKAMURA, Yasuo SASAKI, Toru KISHIGAMI, Makoto WATANABE* and Masami FUJITA+

Department of Physics, Kyoto University, Kyoto 606
*Institute for Molecular Science, Okazaki 444
+Maritime Safety Academy, Kure 737

Polarized reflection spectra of orthorhombic InBr and InI (space group D_{2h}^{17}) have been investigated at LHeT by using synchrotron radiation in the energy region 2 - 30 eV. Results on InBr were reported previously.[1)]

Figure 1 shows the spectra of InBr for E//c and for E//a. The first exciton peak at 2.33 eV is due to the transition from the top valence band of bromine 4p, into which considerable amount of In 5s orbital admixes, to In 5p conduction band bottom. This transition is forbidden for E//a. At about 20eV, In 4d core exciton peaks are observed.

Structure between 2 and 7 eV in both materials are compared with the appropriate energy shift. Many peaks coincide in energy suggesting that these transitions occur in In sublattice, that is, In 5s valence band to In 5p conduction band.

Fig. 2 shows the spectra of In 4d core excitons in InI in an expanded energy scale. Spectra of InI are very dichroic. Two main peaks in InBr are separated by 0.8 eV (see Fig. 1). This structure is explained approximately by free ion model. On the other hand, in InI each peak splits into two or more peaks. To understand this dichroism and splitting, analysis including crystal field as well as spin-orbit and exchange interactions is attempted. It is found that the crystal field splitting amounts to 1 eV and is comparable to that of spin-orbit interaction.

1) K. Nakamura, Y. Sasaki, M. Watanabe, and M. Fujita: to be published in Physica Scripta 37 (1987).

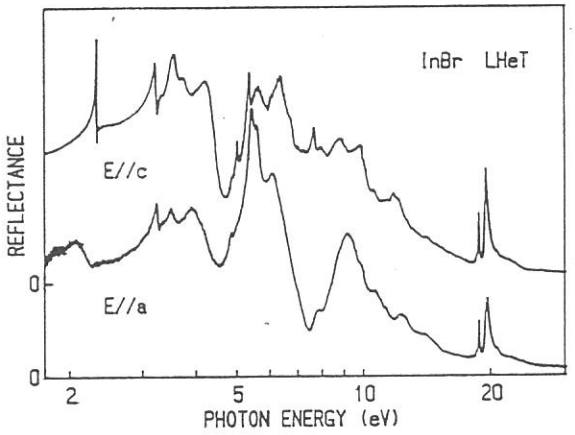

Fig. 1. Reflection spectra of InBr at liquid helium temperature. (a) for E//c and (b) for E//a.

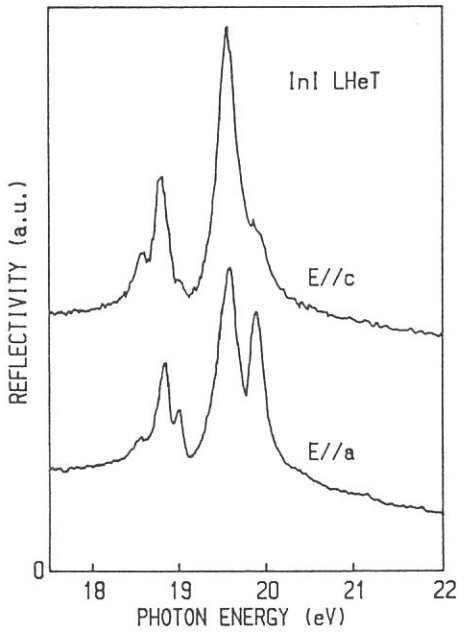

Fig. 2. Reflection spectra of 4d core excitons in InI at LHeT.

Electron-Core-Hole Interaction in Layered Semiconductors

M. Taniguchi

Synchrotron Radiation Laboratory, Institute for Solid State Physics,
The University of Tokyo, Tanashi, Tokyo 188, Japan

Core level absorption spectra in semiconductors exhibit quite different behaviour depending on the degree of electron-core-hole (e-c.h.) interaction. For weak e-c.h. interaction, the spectra reflect the density of states (DOS) of empty conduction bands, whereas strong e-c.h. coupling leads to an excitonic enhancement of the absorption near the core absorption thresholds. In an attempt to investigate the conditions that lead to the different behaviour, a comprehensive study of core excitations in GeS, GeSe, SnS and SnSe layered single crystals with black phosphorus (P) have been performed using synchrotron radiation[1]. The core absorption spectra were measured by partial yield spectroscopy at Flipper II beam line of HASYLAB.

We find consistently that the anion core (S 2p and Se 3d) absorption spectra reflect the DOS of conduction bands, whereas the cation core (Ge 3d and Sn 4d) spectra show intense and sharp spin-orbit doublets at thresholds. The excitonic nature of the latter is exemplified by a strong e-c.h. exchange interaction which leads to a reversal of the intensities of the two components compared to their statistical weight (6:4 for $d_{5/2}$ and $d_{3/2}$ components). The localized nature of the excitations favours their direct recombination decay channel which is observed as a pronounced Fano-type resonance in the valence band photoemission cross section near the core absorption thresholds.

The data are analyzed in terms of band structure, wavefunction and e-c.h. exchange interaction in the compounds. The difference between excitonic and non-excitonic core transition rests on the cationic origin of the states near the bottom of conduction bands as well as the anionic origin of the high DOS features at the top region of valence bands.

By the same line of argument, characteristic features of the 2p core-exciton absorption[2] in black P single crystal can be also interpreted.

References

1) M. Taniguchi, J. Ghijsen, R. L. Johnson and L. Ley, in Proceedings of the 17th International Conference on the Physics of Semiconductors, Stockholm (1986).
2) M. Taniguchi, J. Ghijsen, R. L. Johnson, S. Suga, Y. Akahama and S. Endo, Annual Report of HASYLAB (1986).

NEAR EDGE STRUCTURE OF COORDINATE COMPOUNDS

Nobuhiro KOSUGI

Department of Chemistry, Faculty of Science,
The University of Tokyo

The author reviewed metal K-edge XANES (X-ray Absorption Near Edge Structure) spectra of 3d transition metal complexes, which were all measured by him and coworkers at Beam Line 10B of Photon Factory. It is well known that in the compounds containing the first-row elements there are $1s \rightarrow 2p\pi^*$ and $1s \rightarrow$ Rydberg transitions below the ionization threshold and $1s \rightarrow 2p\sigma^*$ (so-called shape resonance) above or near the threshold; however, it is little appreciated whether we can observe $1s \rightarrow$ Rydberg and $4p^*$ transitions in XANES of 3d transition metal compounds. The author found that weak pre-edge structures are $1s \rightarrow$ Rydberg transitions in Fe K-edge XANES of $Fe(CO)_5$ by comparing gas phase with liquid phase, and that $1s \rightarrow 3d$ transitions show d-d splitting ($1s \rightarrow 3dt_{2g}, e_g$) distinctly in XANES of octahedral $Fe^{III}(CN)_6^{3-}$ [$^2T_{2g}$: $(3dt_{2g})^5 (3de_g)^0$] but no d-d splitting ($1s \rightarrow d_{x^2-y^2}$, d_{z^2}) in XANES of square-planar Fe^{II}-phthalocyanine complex [^3E_g : $(d_{x^2-y^2})^0 (d_{z^2})^1 (d_{xz}d_{yz})^3 (d_{xy})^2$], due to anisotropic stabilization of each d level upon core-hole creation. He successfully observed $1s \rightarrow 4p\pi^*$ transitions below the threshold in polarized XANES of square-planar $Ni(CN)_4^{2-}$ and Ni-phthalocyanine complexes, and proposed that $1s \rightarrow 4p\pi^*$ and $4p\sigma^*$ transitions split to two peaks through the orbital interaction with occupied and unoccupied orbitals of the covalent ligands. He also found shake-down and shake-up transitions in polarized XANES of square planar $Cu^{II}Cl_4^{2-}$ (completely ionic ligand) and Cu^{II} (trimethylimidazole)$_4^{2+}$ (less ionic), respectively, and no satellite structure in Cu^I complexes, and interpreted the appearance of satellite structures based on a three-electrons-in-two-orbitals model (configuration mixing between $(d_{x^2-y^2})^1$ (ligand σ)^2 and $(d_{x^2-y^2})^2$ (ligand σ)^1; the former corresponds to d^9 and the latter to d^{10}).

REFERENCES : Chemical Physics, 91 (1984) pp.249-256 ; 103 (1986) pp.101-109 ; 104 (1986) pp.449-453 ; See also Activity Reports from Photon Factory (Annual).

Theory and Applications of Multiple Scattering in Solids

Takashi Fujikawa
Faculty of Engineering,Yokohama National University
Hodogaya,Yokohama 240, JAPAN

For solid X-ray absorption and X-ray photoelectron spectroscopy, multiple scattering is usually important to describe the dynamics of outgoing photoelectrons especially in the low energy scattering. However,"multiple scattering" is frequently used in the two different meanings. One is used to construct the one electron wave function of an ejected electron to include the potential effect. For example, XANES(X-ray absorption near edge structure) theory has been developed by use of this multiple scattering function[1,2]. As an example, we will talk about the results of XANES analyses based on our short-range order full multiple scattering calculation for halogen doped polyacetylene[3]. Linearly polarized X-ray gives us some useful information;E//c(parallel to chain axis) polarization gives us the information on the X-C correlation(X=Br,I).The nearest X-C distance is longer than the sum of the van der Waals radii of X and C. This result can explain the increase of the anisotropy of electric conductivity with halogen doping. Our XANES analyses also confirm the charge distribution on polyanion I_3^- and I_5^- determined by Mössbauer spectroscopy[4]. In the bromine low doping region it is proved that mono-anions exist. We also obtained the information about the charge distribution on carbon chains around the mono-anions. The maximal amplitude of the charge density is larger than 0.4, which supports the result of Sasai et al.[5].

In another case we use "multiple scattering" to describe the inelastic,resonance and exchange scattering during the travel in the solid sample. As an example of this physical process, the interference effects between intrinsic and extrinsic excitation processes[6,7,8]. Especially, a somewhat detailed discussion will be given for plasmon loss process[7].

[1]P.J.Durham,J.B.Pendry and C.H.Hodges:Comput.Phys.Commun.25 (1982)193.
[2]T.Fujikawa,T.Matsuura and H.Kuroda:J.Phys.Soc.Jpn.52(1983)905
[3]T.Fujikawa,H.Oizumi,H.Oyanagi,M.Tokumoto and H.Kuroda:J.Phys. Soc.Jpn.55(1986)4074,4090.
[4]T.Matsuyama,H.Sakai,H.Yamada,Y.Maeda and H.Shirakawa:J.Phys. Soc.Jpn.52(1983)2238.
[5]M.Sasai and H.Fukutome:Solid State Commun.51(1984)609.
[6]T.Fujikawa:Z.Phys.B54(1984)215.
[7]T.Fujikawa:J.Phys.Soc.Jpn.55(1986)3241.
[8]T.Fujikawa:Z.Phys.B(1987) in press.

Angle-Resolved Ultraviolet Photoelectron Spectroscopy of Alkali-Metal Graphite Intercalation Compounds

Takashi Takahashi
Department of Physics, Tohoku University, Sendai 980, Japan

It is well known that the charge transfer plays an essential role in characterizing the novel properties of graphite intercalation compounds (GICs). Yet at present there is a great theoretical and experimental confusion in the first-stage alkali-metal GICs. The controversial point is the charge balance between the π^* band at the $\tilde{K}$ point and the interlayer band at the Γ point; the electron occupancy of the π^* band in the calculation by Ohno, Nakao, and Kamimura (ONK)[1] is about 0.6 while all the s electron is transferred to the π^* band in the calculation by DiVincenzo and Rabii (DR)[2]. In this report, we present the first angle-resolved ultraviolet photoelectron spectroscopy (ARUPS) on the first-stage alkali-metal GICs single crystals (C_8M, M = K, Rb, Cs).

Figure 1 shows the experimental two-dimensional band structure of C_8K determined in this study [3]. The band calculation by ONK is shown for comparison together with the theoretical π^* band at $\tilde{K}$ point calculated by DR. The agreement in the overall feature between the experiment and the ONK's calculation is very good. The electron occupancy of the experimental π^* band estimated from the dispersive feature is about 0.5 unit electronic charge. This strongly suggests that a K 4s electron in C_8K is shared by the π^* band and the interlayer band with almost equal weight, supporting the ONK band calculation rather than the DR model.

1) T. Ohno, K. Nakao, and H. Kamimura, J. Phys. Soc. Jpn. 47, 1125 (1979).
2) D.P. DiVincenzo and S. Rabii, Phys. Rev. B 25, 4110 (1982).
3) T. Takahashi, N. Gunasekara, T. Sagawa, and H. Suematsu, J. Phys. Soc. Jpn. 55, 3498 (1986).

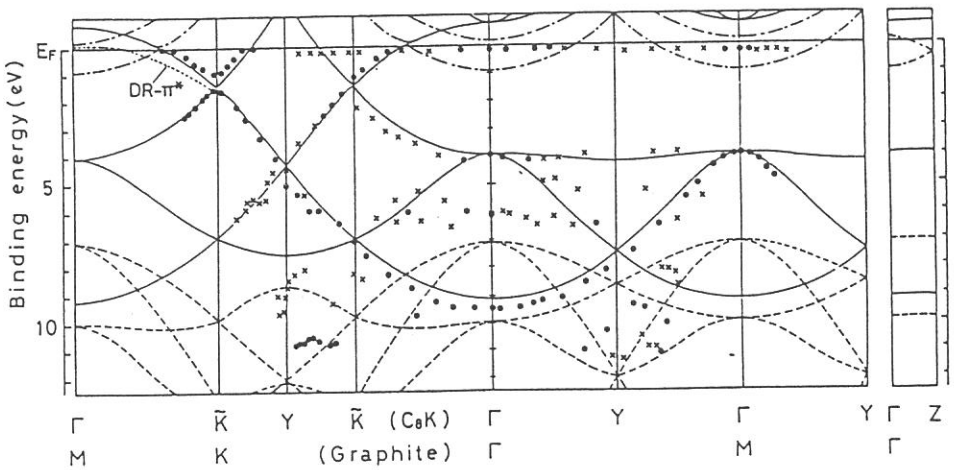

Fig.1 Comparison of experimental and theoretical (ONK) band structure of C_8K

PHOTOELECTRON SPECTROSCOPY OF ORGANIC MATERIALS

Kazuhiko SEKI

Department of Materials Science, Faculty of Science,
Hiroshima University, Hiroshima 730, Japan

Organic materials have several unique points in photoemission experiments such as (i) generally small intermolecular interaction, (ii) rather inactive surface, (iii) insulating electric property, and (iv) feasibility of radiation damages. The first point makes the observed spectra similar to the gas-phase spectrum, and also makes the observation of intermolecular energy-band dispersion difficult. The latter three factors make the experimental conditions different from those of inorganics. After a brief summary of these aspects, we will concentrate on the studies of organic polymers with extended electronic states. (For a more complete survey, see Ref. [1]). The topics included are: (i) extension of pi states at the photopolymerization of diacetylene Langmuir-Blodgett films [2], (ii) formation of intramolecular pi-delocalized states in phenyl-containing polymers [3], and (iii) intramolecular energy-band mapping of polyethylene using model compounds and angle-resolved photoemission with synchrotron radiation [4].

References

[1] H. Inokuchi, K. Seki, and N. Sato, Proc. 8th VUV Conference (Lund, 1986)(Physica Scripta, in press).
[2] H. Nakahara, K. Fukuda, K. Seki, and H. Inokuchi, to be published.
[3] K. Seki, S. Asada, T. Mori, H. Inokuchi, I. Murase, U. O. Karlsson, R. Engelhardt, and E.-E. Koch, Synth. Metals, 17 (1987) 629 and references therein.
[4] K. Seki, N. Ueno, U. O. Karlsson, R. Engelhardt, and E.-E. Koch, Chem. Phys. 105 (1986) 247 and references therein; H. Fujimoto, K. Seki, H. Inokuchi, N. Ueno, and K. Sugita, to be published.

Two - Photon Photoemission from Molecular Crystals Combining Synchrotron Radiation with a Laser

V. Saile
Hamburger Synchrotronstrahlungslabor HASYLAB at DESY,
Notkestr. 85, D-2000 Hamburg 52, Germany

During the past decade photoelectron spectroscopy has proven to be an excellent experimental technique for the investigation of occupied states in solids and with the advent of inverse photoemission also the conduction bands including their dispersion in k-space became accessible. Bound states, however, like excitons in semiconductors and insulators can usually be studied by neither of these powerful techniques.

In order to apply photoemission also on excited states we have combined VUV-radiation (HeI source or synchrotron radiation) with a laser (1). Until now, two systems, i.e. metal-phthalocyanines and rare gas solids, have been studied successfully.

For the phthalocyanine films (2) it could be demonstrated that the laser prevents or reduces charging of the samples due to holes created in the photoemission process. At low temperatures electrons originating from triplet states and defects populated by the laser have been observed in electron energy distribution curves.

In the case of rare gas solids, excitons or transitions to the bottom of the conduction bands were excited by synchrotron radiation. A dye laser served for ionizing the excitons or for ejecting electrons from the conduction bands into vacuum. The latter process could be exploited for an accurate band gap determination for all rare gas solids (3). From fluorescence and transient absorption spectroscopy (4) it is well accepted that excitons in rare gas solids relax to self-trapped states. By monitoring the number of electrons emitted from excitons upon laser irradiation as a function of the laser-wavelength (5), we have been able to determine the relaxation energies of the excitons. However, a much more precise method for this purpose is to measure directly the kinetic energies of the outgoing electrons. This has been accomplished very recently and a typical result is shown in Fig. 1. While the relaxation energies determined from photoemission are compatible with calculated ones (6), the lifetimes disagree grossly with

luminescence data. On the basis of these results we postulate a new type of long living centers created by excitons in rare gas solids.

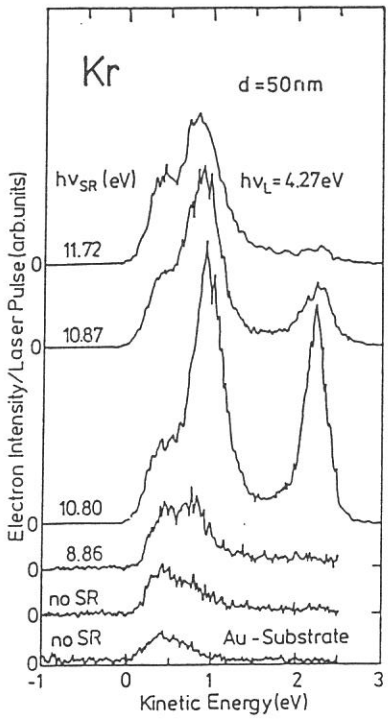

Fig. 1: Photoelectrons from a 50 nm thick Kr film on Au. Only electrons ejected by the laser ($h\nu_L$=4.27 eV) have been detected. The two lowest curves correspond to the signal without synchrotron radiation for the substrate and the Kr/Au sample. At $h\nu$=8.86 eV Kr is still transparent. For $h\nu$=10.80 eV the n'=1 - excitons are excited leading to a pronounced emission at E_{KIN} = 0.9 eV and 2.2 eV. At 10.87 eV there is still exciton absorption and at 11.72 eV interband transitions take place.

References:

(1) V. Saile, D. Rieger, W. Steinmann and T. Wegehaupt, Phys. Lett. A75, 221 (1980);
V. Saile, Applied Optics 19, 4115 (1980)

(2) W. Gädeke, V. Saile and E.E. Koch, XIth Molecular Crystal Symposium, Sept. 30-Oct.4, 1985, Lugano, Switzerland, Ext. Abstracts, p. 87

(3) S. Bernstorff and V. Saile, Opt. Comm. 58, 181 (1986)

(4) For a compilation of data see: N. Schwentner, E.E. Koch and J. Jortner, Electronic Excitations in Condensed Rare Gases (Springer-Verlag, Berlin, 1985)

(5) S. Bernstorff and V. Saile, Annals of the Israel Physical Society 6, 188 (1983);
S. Bernstorff, Thesis University of Hamburg, 1984

(6) I.Ya. Fugol, Advances in Physics 27, 1 (1978)

Time Resolved Fluorescence Anisotropy of Biochemical Systems

I. H. Munro

Daresbury Laboratory, Warrington WA4 4AD, UK
Institute for Molecular Science, Okazaki 444, Japan

The pulsed properties of storage ring sources have been applied to several research fields for nanosecond and subnanosecond timing studies across an extensive wavelength range from the visible to the x-ray region (1) (2) (3). The source characteristics include a subnanosecond pulse width, a high degree of linear polarisation, identical time registration for all wavelengths and exceptional long term stability in pulse shape and timing. These properties are ideal for studies of time resolved fluorescence anisotropy,in particular, where instrumental pulse shifts (sometimes introduced in the analysis of fluorescence lifetime data) are difficult to justify. So far, fluorescence anisotropy data has been reported from the storage rings at Daresbury, UK, (SRS), Orsay, France, (ACO), Stanford, USA, (SSRL), Hamburg, FRG, (HASYLAB).

At the SRS, the source has a F.W.H.M. of about 200 ps and the pulse repetition frequency is 500 MHz in the multi-bunch mode and 3.125 MHz in the single-bunch made. In single bunch mode, the inter-bunch period is 320 ns and the circulating current is typically between 10 mA and 20 mA at 2 GeV giving up to 10^7 photons per pulse at the sample, depending on the band width selected for excitation. Data is accumulated at rates of about 30 kHz.

At Daresbury, a programme is underway to study the time dependent anisotropy of a variety of intrinsic and extrinsic probes bound in well characterised sites within large molecules such as proteins and within membrane structures (4). Following a rather complex data analysis, it is possible to deduce information about conformational changes and molecular flexibilty, such as segmental rotation, close to the probe site. When the probe is tightly bound then the overall size and shape of the intact protein (including its hydration envelope) can be established (5). Interpretation of the data requires knowledge of the photophysical properties of the probe and of the absence (or otherwise) of competing decay processes such as energy transfer.

An interesting example of the effect of excited state selection on the behaviour of anisotropy decay has been shown for the case of lumazine protein where a negative anisotropy is introduced when high electronic state transitions are selected. Analysis of the time dependent anisotropy both for the amino acid and the prosthetic group yields an estimate of the time dependence of the energy transfer process (6).

A programme has also been established to develope and test effective probes to study membrane fluidity. A range of "quasi-intrinsic" probes have been studied which are usually

linear polyenes such as diphenyl hexatriene and its many derivatives (e.g. DPHPC) and also probes containing the triazinylaniline chromophore (7). Using unilamellar lipid vesicles a study has been made of the effect of temperature, pressure, the inclusion of a membrane "stiffener" such as cholesterol and on the fluidising effects of an anaesthetic (e.g. ethanol) on probe mobility within the membrane (4) (8).

An independent study of molecular order and reorientational dynamics of fluorescent probe molecules has been carried out using macroscopically oriented membrane systems such as POPC. Using a range of incident angles for excitation onto the membrane and a range of angles for collection of probe fluorescence, it is possible to describe the order and dynamics of the probe using a Strong Collision model (9). First results reveal that the ordering of the probes (DPH and TMA DPH) included within bilayers of the phospholipid POPC is enhanced and their rates of motion are increased by the addition of cholesterol (10) - a surprising result.

The range of activities in this field, making use both of laser and synchrotron radiation sources and of the techniques of photon counting and phase and modulation spectroscopy (11) is likely to increase and be extended to cover a wide range of materials (e.g. synthetic polymers, nucleic acids etc) in the near future.

References

1. I. H. Munro and N. Schwentner : Nucl. Instr. Meths., 208, (1983), 819.
2. T. Moller and G. Zimmerer : Proc. 8th Int. Conf. VUV Radiation Physics, Lund, Sweden, Aug. 1986, Physica Scripta 1987 (in press).
3. D. M. Mills : Physics Today, April 1984, 1.
4. I. H. Munro, D. Shaw, G. R. Jones and M. M. Martin : Anal. Instrum. 14, (1985), 465.
5. I. H. Munro, I Pecht and L. Stryer : Proc. Nat. Acad. Sci. USA. 76 , (1979), 56.
6. A. J. Visser and I. A. v. Hoek : Private communication.
7. D. J. Cowley : Private communication.
8. C. G. Morgan , E. W. Thomas, Y. P. Yianni and I. H. Munro : Daresbury Laboratory, Synchrotron Radiation Annual Report, 1985/86.
9. G. v. Ginkel, L. J. Korstanji, H. v. Langen and Y. K. Levine, Far. Disc. Chem. Sci. 81, (1986), 1.
10. H. v. Langen, M. v. Gurp, G. v. Ginkel, Y. K. Levine, D. A. Shaw and I. H. Munro : Daresbury Laboratory, Synchrotron Radiation Annual Report,1985/86.
11. I. H. Munro in "Spectroscopy and the Dynamics of Molecular Biological Systems" Acadamic Press (1985), 307, ISBN 0-12-083240.

Time-Resolved Fluorescence Spectroscopy of Liquid Alkanes

Yoshihiko HATANO, Department of Chemistry,
Tokyo Institute of Technology, Meguro-ku, Tokyo 152, JAPAN

Fluorescence from liquid alkanes has been one of the important subjects of research in physical chemistry since an early experiment by Hirayama and Lipsky,[1] and extensively studied by many groups using different kinds of excitation sources, i.e., α, β, γ and X-rays, accelerated electron beams, UV-photons from discharge lamps, and laser photons. Fluorescence lifetimes as well as excitation spectra have been measured for a variety of liquid alkanes.

Our group[2] has measured recently fluorescence lifetimes and excitation spectra of liquid alkanes by means of synchrotron radiation as combined with a delayed coincidence single photon counting technique and compared the obtained results with previous ones. This is an extention of our previous experiment[3] in which a superior advantage of the use of SR pulse character in reaction dynamics studies is clearly demonstrated.

Each of excitation spectra of liquid alkanes, i.e., cyclohexane, bicyclohexyl, cis- and trans-decalin, n-decane and n-dodecane, shows a single broad peak at the excitation wavelengths between 163 and 185 nm. The lifetimes show no dependence on the excitation wavelength examined in this experiment and agree well with those obtained using the pulse character of ionizing radiation and laser two photons.

1) F. Hirayama and S. Lipsky, J.Chem.Phys., 51, 3616 (1969).
2) K. Shinsaka, H. Koizumi, T. Yoshimi, N. Kouchi, Y. Nakamura, M. Toriumi, M. Morita, Y. Hatano, S. Asaoka, and H. Nishimura, ibid., 83, 4405 (1985).
3) Y. Hatano, M. Ohno, N. Kouchi, H. Koizumi, A. Yokoyama, G. Isoyama, H. Kitamura, and T. Sasaki, Chem.Phys.Letters, 84, 454 (1981).

RELAXATION OF HIGHLY EXCITED STATES IN MOLECULAR SOLIDS AND LIQUIDS

J. Klein
Centre de Recherches Nucléaires & Université Louis Pasteur
STRASBOURG (France)

Frame

- Highly excited states are the states beyond the first excited triplet and singlet (excitation energy in the UV and VUV domain)
- Molecular solids and liquids are characterized by small intermolecular interactions compared to the intramolecular ones.

Main Features

- Due to the weak coupling the isolated molecular characteristics prevail in the dense phase
- However, the intermolecular interactions promote :

(i) perturbative changes

+ the energy levels are broadened (in small excitonic bands)

+ the level diagram undergoes typical "red shift"

+ internal conversion, intersystem crossing, autoionization which are the main decay processes of an excited isolated molecule are conserved

(ii) new specific relaxation modes (see decay scheme)

+ vibrational relaxation leading to an energy dissipation via the bulk

+ transitions to charge transfer (CT) states where the hole (positive ion) and the electron occupy different molecular sites (c)

+ transitions to biexcitonic configurations of two excited triplet (T^*) (b) or two singlet (S^*) (a)

- In the dense phase the slowing down of a "hot" electron produced in an autoionization or a direct ionizing process may promote the concomittant

creation of a S^* (or T^*) exciton **and** a CT or free charge state(c).

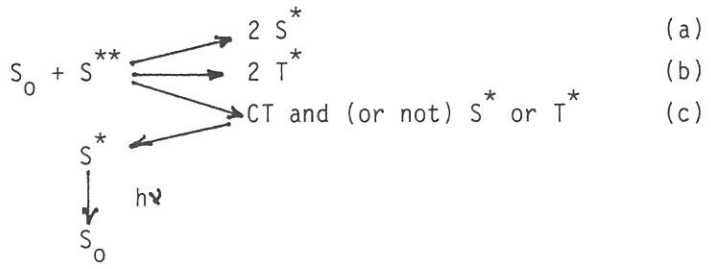

Experimental Evidence

- single photon excited (S^{**}) photon-photon coincidence revealing the desexcitation of the two correlated S^* in channel (a) (1)

- magnetic field modulated fluorescence decay (1,3) due to

· fine structure interactions decoupling in channel (b)

· hyperfine interaction decoupling in the CT or charge carrier recombination process (channel (c))

- electrical field modulated fluorescence decay (4) due to perturbed CT or charge carrier recombination (channel (c))

- single photon excited (S^{**}) fluorescence photon-emitted photoelectron coincidence (channel c) (2).

References

1. G. Klein, "Electronic Excitations and Interaction Processes", in Organic Molecular Aggregates (Eds. P. Reineker, H. Haken and H.C. Wolf, Springer, Berlin 1983, p.149 ; Chem. Phys. Lett. 97, 114 (1983)
2. G. Klein, Chem. Phys. Lett. 95, 305 (1983)
3. J. Klein, P. Martin, R. Voltz, Chem. Phys. Lett. 94, 10 (1983)
   J. Klein, J. Chim. Phys. 80, 627 (1983)
   P. Martin, G. Klein, J. Klein, R. Voltz ; XIth Molecular Crystal Symposium, Lugano 1985, p.190
4. G. Klein, Chem. Phys. Lett., 124, 147 (1986)

Time Resolved Fluorescence and Modulation Spectroscopies of Molecular Crystals.

Tadaoki Mitani

Institute for Molecular Science, Myodaiji, Okazaki 444

The highly excited states in anthracene crystals have been investigated by time-resolved fluorescence spectroscopy based on single-photon counting technique and by electric and magnetic field-modulation spectroscopies in the energy range of 4-20 ev using a synchrotron radiation source. By the former technique, the dynamical behaviors of the highly excited states in a short time period less than several nanoseconds have been elucidated in details: The time-resolved fluorescence spectrum from the lowest exciton is significantly dependent on time and exciting photon energy in an initial stage of decay of about 100 ps after the pulse excitation. Its excitation spectrum show a remarkable dependence on the exciting photon energy and exhibit a high quantum efficiency at the exciton bands. To the contrary, for the delayed fluorescence component by about 1 nsec obeying a purely single-exponential decay, the excitation spectra are almost independent of the exciting photon energy. The close correlation between exciting and emitted photon energies in the initial stage of the decay curves indicates that the fast component of fluorescence emitted immediately after pulsed excitation is predominantly due to the annihilation of excitonic polaritons at the crystal surface before the radiative recombination of excitons takes place within the bulk crystal.

The time-decay contains a long tail being continued to sub-nanosecond, which may be concerned with geminate recombination between the excitons and electron-hole pairs. From the modulated excitation spectra by applying alternative electric- and magnetic-field, it was found that such a relaxation process is quite sensitive to the magnitudes of both modulation fields; the fluorescence is quenched in a low field regime but strongly enhanced by applying the high fields. Their efficiensies have characteristic thresolds for the excitation energy, T_1+T_1 and E_g+T_1 for magnetic field and E_g+S_1, E_g+2S_1 and E_g+3S_1 for electric fields, where E_g, S_1 and T_1 present a band gap energy, the lowest singlet and triplet exciton energy, respectively. These characteristic features provide a qualitative understanding of complicated relaxation processes in anthracene crystals.

Dynamics of Tunneling and Relaxation from Free State to Self-Localized State of Exciton
— Theory for Intermediate Coupling Case —

Keiichiro Nasu
Institute for Molecular Science

The rates of tunneling and relaxation of an exciton from its free (F) state to its self-localized (S) state are worked out, so as to clarify the non-adiabatic effects of the exciton-phonon coupling on these rates, as well as the adiabatic ones. The Frenkel exciton coupling with the longitudinal acoustic phonon is taken as a typical example. The localization is assumed to occur successively through a series of exciton states with different localization raduii, and also through a one-dimensional configuration coordinate space of phonon, called "tunnel-mode". The manifold of vibronic states in the exciton tunnel-mode coupled system is numerically calculated, and the vibronic relaxation within this system is brought about through the coupling between the tunnel-mode and other phonon modes, which acts as a resovior. The rates are calculated within the generalized master equation method, and the results[1] are compared with the recent experiment in pyrene[2], in a quite good agreement.

1) K. Nasu: "Solid State Optics, Electron-Phonon Coupling" Special Volume of Solid State Physics ed. by K. Nasu (1987, Agune-Technical Center, Tokyo) in Japanese.
2) A. Matsui, K. Mizuno, N. Tamai and I. Yamazaki: to be published in Chemical Physics 1987.

Abstract of talk at 28th Okazaki Conference on Solid State Chemistry with VUV Synchrotron Radiation. Institute of Molecular Science, Okazaki, Japan, February 6, 1987.

Defect Formation In Ionic Solids By Vacuum Ultraviolet Synchrotron Radiation*

Frederick C. Brown

Department Of Physics, University Of Illinois
1110 West Green Street
Urbana, IL 61801, USA

In this talk recent results will be presented on the efficiency of production of F-centers in the alkali halides by both strongly absorbed vacuum ultraviolet radiation (photon energies 5 to 1500 eV) as well as by monochromatic x-ray radiation near the bromine K-edge (13.4 keV). The main part of the work was carried out at the low emittance 1 GeV electron storage ring at the Synchrotron Radiation Center, Stoughton, Wisconsin. This facility is now fully operational with circulating beam currents at either 800 MeV or 1 GeV in excess of 100 ma. One of the unique features of the machine is low energy electron injection from a 100 MeV microtron. The storage ring contains four long straight sections one of which is now occupied by a variable gap 64 pole undulator. Part of the work on the defect production in ionic crystals was carried out using an intense monochromatic photon beam (50 to 1500 eV) from the extended range grasshopper monochromator[1] on the University of Illinois beam line. Other parts of the spectrum were covered by laboratory sources including a rotating anode x-ray tube with a bent silicon crystal monochromator.

In order to observe F-centers over a wide dynamic range, a sensitive laser-induced luminescence technique was developed[2,3] which could detect a very small number of point defects (10^{10} cm^{-3}) during the early stages of growth as well as high concentrations (10^{18} cm^{-3}) as the coloration approached saturation. This technique makes use of the large separation between F-center absorption and emission (Stokes shift), and it requires that the alkali halide crystal be cooled to 77K. F-center production efficiences of the order of one

KeV/F-center were obtained during early stages of growth for KBr and KCl throughout the spectral range studied. The efficiency was observed to drop sharply in regions of very strong absorption such as in the exciton bands (6-8eV)and in the near vacuum ultraviolet below 60eV. These effects are probably due to proximity of the surface resulting in secondary electron emission and photo desorption which, in regions of very small x-ray absorption depth, can compete with F-center formation by electron-hole recombination. The results overall are consistent with a model in which the absorbed vacuum untraviolet photon initiates a sequence of electron scattering events resulting in approximately $h\nu/2E_g$ electron-hole pairs (E_g is the band gap). F-centers and H-centers are then generated by the well known self trapped exciton recombination mechanism.[4] At 6.7 eV, just below the exciton peak in KBr, a self trapped exciton is found to recombine with an efficiency of about 0.007 to form an F-center. At low temperature in KBr the maximum efficiency of luminescence[5] is found to be only about 0.03, therefore other inelastic phonon processes and back reactions compete favorably with F-center generation and luminescence. A definite increase in early stage F-center formation efficiency was observed at the K-edge of Br in KBr(13.4 keV). This is probably because the energy distribution of secondary photoelectrons changes appreciably above the edge, as pointed out many years ago by Itoh, Sharma and Smoluchowski.[6]

---

* Supported in part by the National Science Foundation under Grant No. NSF DMR84-15396.

1. S. L. Hulbert, J. P. Stott, F. C. Brown and N. Lien, Nucl. Instrum. Methods Phys. Res. 208, 43 (1983).
2. B. R. Sever, N. Kristianpoller and F. C. Brown, Phys. Rev. 34, 1257 (1986).
3. F. C. Brown, B. R. Sever and J. P. Stott; Phy. Rev. Lett. 57, 2279 (1986); see also Physica Scripta, to be published.
4. Y. Toyozawa, J. Phys. Soc. Japan, 44 482 (1978).
5. M. Yanagihara, Y. Kondo and H. Kanzaki, J. Phys. Soc. Japan, 52, 4397 (1983).
6. N. Itoh, J. Sharma and R. Smoluchowski, Proc. of International Symposium on Color Centers in Alkali Halides (Urbana, 1965).

Ion Desorption from Surfaces

Roger Stockbauer
Surface Science Division
National Bureau of Standards
Gaithersburg, MD 20899

Electron and photon stimulated desorption (ESD and PSD) are the surface analogues of radiation induced gas phase ionization and radiation damage in solids[1]. In stimulated desorption, beams of incident electrons or photons incident on a surface containing bulk atoms or adsorbed monolayers of atoms or molecules will cause electronic excitation in the surface species. These excitations can lead to desorption of ions, neutrals or metastable species from the surface. A major difference between surface and gas phase dissociative ionization processes is that the surface provides pathways for electronic deexcitation which are not available in the gas phase.

Ion desorption has unique properties which make it a useful surface probe. Ions are desorbed only from the outermost surface layer making ion desorption highly surface sensitive. Mass analysis of the desorbing ion can be used to identify the surface species. Since ion desorption is, in general, a fast process ($\sim 10^{-14}$s) the surface species moves little between the time of excitement and desorption. Hence, by measuring the angular distribution of the ions information is gained about the bonding configuration of the neutral species. Lastly, the photon energy dependence of the ion emission can be used, in some cases, to identify the species or site to which the ion was attached on the surface.

Since there is much theoretical and experimental interest in the physics and application of ion desorption, it is necessary to know something about the desorption mechanism. A picture of the mechanism has evolved which views ion desorption as a three step process. The first step is the formation of a core hole by photon, electron or even ion impact, the second is the decay of the core hole leaving 2 holes localized on a single bond resulting in a long-lined repulsive state, the third is the expulsion of the ion from the surface.

In general, the most common type of core hole decay which leads to two localized holes is Auger decay. Hence, the term Auger Stimulated Desorption (ASO) has been used to describe the ion desorption mechanism. A specific case of ASD was developed by Knotek and Feibelman[2] for maximal valency compounds in which the valence electrons are depleted from the metal cation and reside on the anion. TiO_2 in which the titanium is configured as Ti^{4+} and oxygen as O^{2-} was used as a model maximum valency compound. As in the general ASD process they viewed the initial step of ion desorption as the formation of the core hole in the metal cation Ti^{4+}. However, the decay of this core hole cannot proceed by the normal Auger decay mechanism since the valence electrons on the Ti are depleted. Instead, they postulated an interatomic Auger decay where an electron from the O anion fills the core hole with the subsequent emission of 1 or 2 electrons. If 2 electrons are emitted, the oxygen has lost 3 electrons and is configured as an O^+ surrounded by Ti^{4+} ions and the resulting coulomb repulsion expels the O^+ from the surface.

The Knotek - Feibelman as well as the more general ASD models predict that the ion desorption cross section should have the same energy dependence as the core hole production. This, in fact, has been demonstrated in a large number of both maximal valency as well as covalent systems. The original Knotek - Feibelman (K-F) model, however, predicted that ion desorption should be strong for maximal valency but greatly reduced for non-maximal valency compounds. While this appears to be true for a number of systems studied, an exception is MgO.

In recent experiments[3] on MgO(100) and (111) done at HASYLAB, we detected little or no ion desorption at any of the Mg core levels. Since MgO is a highly ionic compound, according to the model it should be a very strong ion emitter. The fact that it is not, is probably due to reneutralization, to bonding geometry, or to lattice-dynamics.

We did observed, however, O^+ and H^+ desorption from the O1s level in MgO(100) and (111). The desorption cross section above the O 1s edge follows the absorption cross section of the core hole as given by high energy electron energy loss spectra. Two additional features are observed below the O1s onset which we ascribed to O1s surface core excitons. The decay mode of the exciton in which the excitonic electron remains a spectator results in the loss of 3 electrons from the O^{2-} which then desorbes as an O^+.

The requirement of maximal valency has been investigated further by observing the effects of electronic and lattice defects on desorption from two crystal faces of TiO_2, the (100) and (110).[4] Since these surfaces are identical electronically as can be seen from their photoelectron spectra, any difference in their relative ion yield must be due to their different geometry. The valency of the surfaces can be reduced by ion sputtering and then restored by annealing. As the surfaces are annealed, the ion yield from both decreases and then increases as one would expect from the K-F model. Above 600K, however, the ion yield from the (110) surface decreases drastically while that from the (100) saturates at a level ~6 times that of (110). The difference is due to the fact that the (100) surface facets, that is, it forms pyramidal structures with {011} planes. Measurement of the angular distribution of the ions from this surface shows that they are emitted from the edges of the facets rather than from the planar faces. This study as well as the MgO study shows that while the formation of a core hole is a necessary condition for ion desorption, it is not always sufficient. Geometry of the surface plays a significant role in the ion desorption.

Lastly, one must consider the effect of secondary electrons in the ion desorption process. If the secondary electrons produced by the primary photon or electron beam have sufficient energy as they pass through the surface layer into the vacuum, they can produce excitations which lead to ion desorption. To evaluate this effect, an overlayer experiment was performed at HASYLAB in which ion desorption was measured from a YbO_x overlayer on Sm bulk.[5] The Sm and Yb excitations are clearly distinguishable in the Constant Final State (CFS) spectra. The Sm spectrum has a broad structure with many peaks between 125 and 165eV while the YbO_x has only 1 narrow peak at 181eV. The ion yield from the overlayer shows both structures. The Sm structure in the ion yield can arise only if the secondary electrons from the Sm bulk excite the Yb core level which then Auger decays to initiate the desorption. An evaluation of these data and those of other groups proposing to show secondary electron stimulated desorption (SESD) shows this to be one of the few clear cases of SESD.[6] The effect is dominant here due to the fact that the direct ASD process is weak since the dominant decay made of the Yb core hole is a direct recombination which does not lead to desorption. In general the SESD is always present as a background and should become more dominate at higher X-ray energies. SESD affects only the ability to detect the bonding partner of the desorbed ion; it has no effect on the mass or angular distribution determination.

In summary, the basic mechanism of ion desorption has been well establish over the past few years. The future holds many challenges and much excitement.

This work was supported in part by the U.S. Office of Naval Research.

1) "Desorption Induced by Electronic Transitions: DIET I," edited by N.H. Tolk, M.M. Traum, J.C. Tully, T.E. Madey, Springer-Verlag, New York (1983); "...DIET II," edited by W. Brenig and D. Menzel, Springer-Verlag, New York (1985); T.E. Madey, D.E. Ramaker, R. Stockbauer, Ann. Rev. Phys. Chem 35, 215 (1984).
2) M.L. Knotek and P.J. Feibelman, Phys. Rev. Lett. 40, 964 (1979); Surf. Sci. 90, 78 (1979).
3) R.L. Kurtz, R.L. Stockbauer, R. Nyholm, S.A. Flodström and F. Senf, V. Vac. Sci. Technol., to be published; Phys. Rev. B. (submitted).
4) R.L. Kurtz, Surf. Sci. 177, 526 (1986).
5) J. Schmidt-May, F. Senf, J. Voss, C. Kunz, A. Flodström, R. Nyholm and R. Stockbauer, DIET II (Ref. 1 above), pg. 94.
6) D.E. Ramaker, T.E. Madey and R.L. Kurtz, to be submitted.

Photon Stimulated Desorption from LiF Surface

Ayahiko Ichimiya, Yoshitaka Yamada and Tsuneo Yasue
Department of Applied Physics, Nagoya University, Nagoya 464, Japan
Tetsuji Gotoh, Yoichi Kawaguchi, Masahiro Kotani, Shunsuke Ohtani,
Yukichi Shigeta, Shoji Takagi and Yuji Tazawa
Institute of Plasma Physics, Nagoya University, Nagoya 464, Japan

Photon stimulated desorption (PSD) from LiF (100) surface is observed in the photon energy region between 30 and 70 eV. The experiments were carried out using the UVSOR. The relative yields, which were normalized with the relative photon intensity, were measured as a function of the incident photon energy (the desorption yield spectrum).

In both yield spectra of Li^+ and F^+ ions there are a rapid rise of ion yields at about 56 eV, and a structure at about 58 eV. However the considerable difference in the yield spectra of Li^+ and F^+ ions is observed above 60 eV. The Li^+ yields are almost constant between 61 and 67 eV, while there are a sharp peak at 60.2 eV and a deep valley at 63.5 eV in the F^+ yield spectrum. A threshold of PSD of Li^+ ions was not observed down to 27 eV. That of F^+ ions was observed to be about 30 eV.

Desorption of neutral Li and HF species was observed, while that of F species could not observed because of rather abundant atomospheric F gas. In the Li yield spectrum there is a sharp peak at about 61 eV reproduciblly. Relative intense background yields were observed over all the photon energies. The HF yield spectrum, however, does not show the strong energy dependence.

In order to consider the mechanism of PSD of positive ions, we compare the ion yield spectra with the photoabsorption spectrum. The structures at 56 and 58 eV are also seen in the photoabsorption spectrum. The structures in the photoabsorption spectrum are ascribed due to the creation of the Li^+ core exciton in the crystal. Therefore the initial step of PSD of positive ions is the core excitation of the Li^+ 1s state. The valence band should well localize on F^- ions in the complete ionic crystal of LiF. Then following two different decays of the core exciton are considered;

$$Li^{+*}+F^- \rightarrow Li^*+F^++e^- \qquad (1)$$

and

$$Li^{+*}+F^- \rightarrow Li^++F+e^-, \qquad (2)$$

where asterisks indicate the core-excited state. Since the sharp peak in the Li yield spectrum locates at nearly the same energy as that in the F^+ yield spectrum, it is considered that the desorption of Li^* and F^+ takes place simultaneously. Therefore the process of eq. (1) is dominant in the desorption processes. The background yields are due to the thermal process which is attributed by the photoinduced defects as already observed.

Photon-stimulated desorption of neutrals from silver and alkali halides

H. Kanzaki, Ashigara Research Laboratories, Fuji Photo Film

PSD studies are reviewed for silver and alkali halides under valence excitation. In addition to those on bulk crystals[1,2], recent results on microcrystals of silver halide will be included.

For PSD from bulk surface, there is a distinct difference of desorption species between silver and alkali halides; halogen molecules and alkali and halogen atoms, respectively. In AgBr, photo-holes diffuse as a neutral hole-vacancy complex, which is transformed to bromine molecule at the surface. On the other hand, the self-trapped hole (STH) is stable in alkali halide. Halogen atom desorption due to STH is followed by the alkali desorption due to F-center near the surface. Thus, the origin of molecule vs. atom difference can be understood as due to the different nature of stable photo-excited states.

On the other hand, however, there are evidences suggesting the importance of surface-residence time of desorption precursors. In bulk AgBrI mixed crystals, for example, iodine desorption which corresponds to stable species turned out far less efficient than bromine. The situation changes completely for microcrystals, in which idodine desorption is the strongest. Apparently, the desorption efficiency has changed by the existence of thin gelatin layer in contact with microcrystals.

The gelatin layer covering silver halide surface is also responsible for the strong PSD of CO_2, through either of the following two mechanisms. One is the reaction of gelatin with bromine from excited silver halide. The other is due to the excitation of interface-state at the surface of silver halide, the nature of which becomes evident from the desorption yield spectra at the lower energy side of silver halide absorption threshold.

1) H. Kanzaki and T. Mori, Semicond. Insulators 5, 401 (1983)
2) H. Kanzaki and T. Mori, Phys. Rev. B29, 3573 (1984)

INVESTIGATION OF FRAGMENTATION PROCESSES FOLLOWING CORE PHOTOIONIZATION OF ORGANOMETALIC MOLECULES IN THE VAPOR PHASE

Shin-ichi NAGAOKA

Institute for Molecular Science, Myodaiji, Okazaki 444

We have studied the fragmentation following Pb 5d core photoionization of tetramethyllead (TML). In the threshold electron spectrum of TML, several sharp bands are seen in the region 44 – 75 nm, and are assigned to the photoionization from the Pb 5d core levels. The photoionization efficiency curve for the Pb^+ ion has an appearance quite different from those for other fragments. Moreover, almost all peaks of the Pb^+ curve in the region 44 – 75 nm are found to coincide in position with the peaks in the threshold electron spectrum. Branching ratio of each fragment in various states of the TML parent ion were determined by use of the threshold electron – photoion coincidence method, and are given in Figure 1. From these results, it is concluded that the Pb^+ ion is predominantly produced following Pb 5d core photoionization.

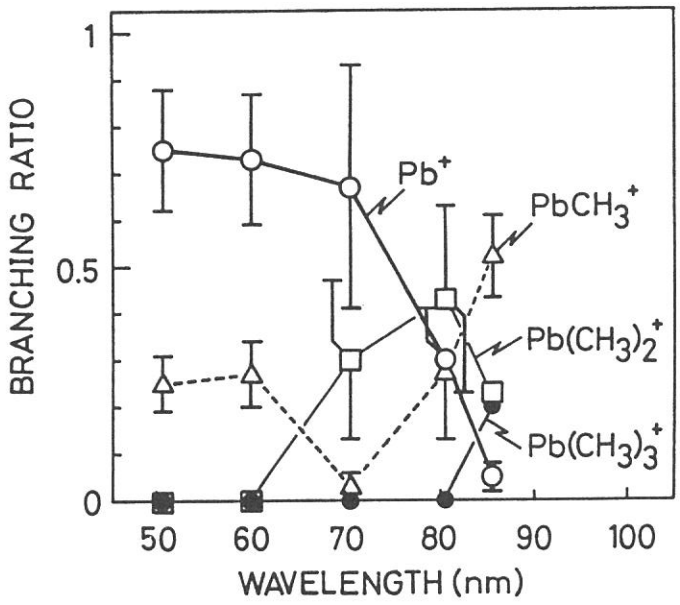

Figure 1. Braiching ratio.

Measurements of H^+ Formation from Hydrocarbons

Haruo Shiromaru, Institute for Molecular Science

The C-H bond dissociation energies of ethylene and acetylene, $D_0(R-H)$, where R = C_2H_3, C_2H, are important quantities to be accurately determined. The D_0 values have often been obtained with the relationship $D_0 = E_{th}(R^+) - I(R)$, where $E_{th}(R^+)$ is the threshold energy for $RH + h\nu = R^+ + H + e^-$, and I(R) is the adiabatic ionization energy of the R radical. The disadvantage of this method is that there are some uncertainties in the I(R) value affecting the result of D_0. A new method recently proposed for determining the D_0 values from the H^+ threshold energy is briefly explained here.[1]

The H^+ threshold energies for ethylene and acetylene have been measured with a Q-pole mass filter by scanning in the wavelength region 58 - 70 nm on the beam port BL2-B2 in the UVSOR facility of this Institute.[1] Then the $D_0(R-H)$ values have been deduced from the relationship $D_0(R-H) = E_{th}(H^+) - I(H)$, where $E_{th}(H^+)$ is the threshold energy for $RH + h\nu = R + H^+ + e^-$, and I(H) is the ionization energy of H atom (13.598 eV).

From the onsets of the efficiency curves, the following values have been obtained[1]

$E_{th}(H^+)$ = 18.66 eV, D_0 = 5.06 eV for ethylene

$E_{th}(H^+)$ = 19.35 eV, D_0 = 5.75 eV for acetylene

The D_0 values deduced here are in good agreement with those obtained from the analysis of the photofragment translational spectra but considerably higher than those derived from $E_{th}(R^+)$.

Synchrotron radiation is suitable for determining the C-H bond dissociation energies from the H^+ formation because of its high intensity and stability in the wavelength region used.

[1] H. Shiromaru, Y. Achiba, K. Kimura, and Y. T. Lee, J. Phys. Chem., **91**, 17 (1987).

Site-Selective Photofragmentation of Molecules and Its Implication to VUV Induced Solid State and Surface Chemical Processes

T. K. Sham, Chemistry Department
Brookhaven National Laboratory, Upton, NY 11973 USA

Photofragmentation of molecules following the excitation and ionization of core electrons was for sometime a relatively unknown phenomenon in comparison with similar processes involving valence electrons. In recent years, the availability of intense and tunable VUV and soft X-rays from electron storage rings has greatly facilitated the experimental investigation of the photofragmentation of molecules following the creation of a core hole.[1,2]

This presentation will deal with some general considerations of the phenomenon, the experimental situations, the interpretation of the results and its implications. Major developments in the last five years in this area will also be reviewed.

One unique feature of the core electron excitation and ionization process is that the core hole created in the process decays predominantly via the Auger channel for low z (atomic number) elements such as carbon, nitrogen and oxygen. These processes are Franck-Condon like and often resulted in various two-hole state in the molecular orbitals.[3] These two-hole states (or the Coulomb repulsion U between the core holes) play a determined rule in the fragmentation pattern of the molecules.[4] For site selectivity, it is important to consider the core levels that are closest to the valence levels. The K hole in carbon for example interacts directly with the chemically sensitive electrons in the molecular orbitals. Fig. 1 illustrates the site selectivity when the photon is tuned to the 1s → π* absorption of the carbonyl carbon of acetone. It can be seen from Fig. 1 that C^+ and O^+ are produced with large abundance at the resonance involving the carbonyl carbon.

The partial ion yield absorption spectra shown in Fig. 1 were recorded with a set-up in which the synchrotron light passed through a glass capillary array (50% transmission) into the ionization area of a UTI 100 C mass spectrometer. With differential pumping, a pressure differential of 10^{-5} was achieved across the channel plane and the partial pressure of the gas in the ionization region was ~ 10^{-4} torr.

Photofragmentation patterns of CH_3COOH, C_6H_6, C_6H_5Cl and $C_2H_3Cl_3$ are also discussed. These molecules all exhibit an intense C 1s → π* transition which correlates with the breaking of all the bonds at the absorbing carbon site.

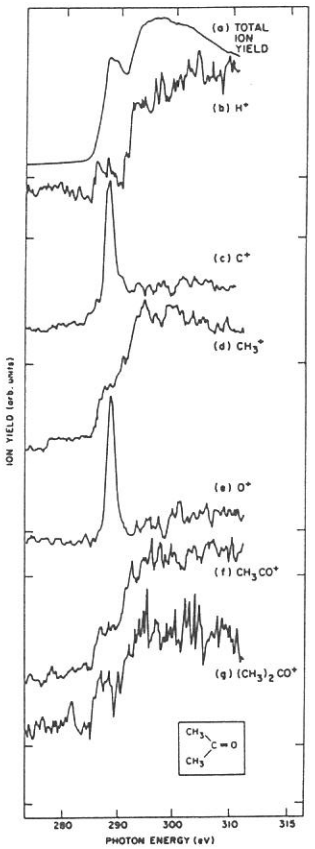

Fig. 1. C K edge absorption spectra of acetone recorded in the ion yield mode.

Recently developed techniques such as threshold photoelectron-photoion coincidence,[5] photoion-photoion coincidence[6] and Augerelectron-photoion coincidence[7,8] have enabled more detailed studies of the process. Some of these results will be discussed.

Acknowledgment. This research was carried out at Brookhaven National Laboratory under contract DE-AC02-76CH00016 with the U. S. Department of Energy and supported by its Division of Chemical Sciences, Office of Basic Energy Sciences.

References

1. W. Eberhardt, T. K. Sham. R. Carr, S. Krummacher, M. Strongin, S. L. Weng, and D. Wesner, Phys. Rev. Lett. 50, 1038 (1983).

2. W. Eberhardt, J. Stöhr, J. Feldhaus, E. W. Plummer and F. Sette, Phys. Rev. Lett. 51, 2370 (1983).

3. W. E. Moddeman, T. A. Carlson, M. O. Krause, B. P. Pullen, W. E. Bull and G. K. Schweitzer, J. Chem. Phys. 55, 2317 (1971).

4. See for example D. Ramaker, J. Chem. Phys. 78, 2998 (1983).

5. K. Müller-Dethlefs, M. Sander, L. A. Chewter and E. W. Schlag, J. Phys. Chem. 88, 6098 (1984).

6. P. Morris, G. G. B. de Souza, I. Nenner and P. Lablanquie, Phys. Rev. Lett. 56, 131 (1986).

7. J. Murakami, M. C. Nelson, S. L. Anderson and D. M. Hanson, J. Chem. Phys. 85, 5755 (1986).

8. W. Eberhardt, E. W. Plummer, I. W. Lyo, R. Carr and W. K. Ford, Phys. Rev. Lett. 58, 207 (1987).

PHOTOCHEMISTRY AND MORPHOLOGICAL CHANGES OF POLYMER AND DEPOSITED FILMS

Hiroshi MASUHARA

Department of Polymer Science and Engineering
Kyoto Institute of Technology, Matsugasaki, Kyoto 606

Since photophysical and photochemical processes of π-electronic molecules have been studied in detail, photo-induced morphological changes such as annealing and ablation of organic solid containing these molecules can be correlated with their photoprocesses. Major spectroscopic and photochemical data, however, are limited to UV and visible wavelength regions, so that studies on laser photochemistry of organic solid are fruitful at present. Here, annealing and ablation phenomena of organic films containing representative π-electronic chromophores are described.

Vacuum-deposited films of ω-(1-pyrenyl)alkanoic acids gave two kinds of new fluorescence which were ascribed to some minor aggregates of pyrenyl chromophores. Most of these chromophores were in another aggregate which is nonfluorescent or transfers excitation energy rapidly to a neighbouring isolated pyrene. Upon irradiation with a 308 nm excimer laser and a Xe-lamp, these films showed characteristic fluorescence spectral change, indicating interconversions between these aggregates. Since annealing phenomena were observed with an optical microscope, the present structural change of aggregates is considered to give a molecular viewpoint for laser annealing.(1)

Increasing laser irradiation intensity lead to ablation of organic films. This process of poly(methyl methacrylate) films doped with pyrene and benzophenone and poly(N-vinylcarbazole) films was investigated, using the 308 nm and 248 nm excimer lasers, respectively. The presence of absorbing chromophores resulted in efficient etching. Scanning electron micrographs revealed that the surface condition of etched areas depends on spectroscopic as well as chemical characters of the chromophore, its concentration, laser irradiation intensity.(2,3)

In both studies we examined effects of irradiation intensity and repetition rate of excimer lasers and came to the conclusion that some nonlinear laser processes such as interactions between excited states and successive two-photon absorption are involved. This means an important role of the higher excited state in photo-induced morphological changes.

References

(1) A. Itaya, T.Kawamura, H. Masuhara, Y. Taniguchi, and M. Mitsuya, Chem. Phys. Lett., in press (1987).
(2) H. Masuhara, H. Hiraoka, and K. Domen, Macromolecules, in press (1987).
(3) H. Masuhara, H. Hiraoka,and E. E. Marinero, Chem. Phys. Lett., in press (1987).

WAVELENGTH DEPENDENCE OF CHEMICAL PROCESS IN X-RAY RESIST

S. Morita, H. Yamada and S. Hattori
Nagoya University, Department of Electro Mechanical Engineering
Furo-cyo, Chikusa-ku, Nagoya 464, JAPAN

Introduction

Conventional poly-methyl-methacrylate(PMMA) film spin coated revealed positive pattern without any additional developing treatments, when it was exposed to syncrotron radiation(SR) through an X-ray mask[1]. The phenomenon is known as a self development. However, the self developed pattern depth was saturated at the high X-ray dose. In this study, phenomena of self development were investigated experimentally and it was observed that the self development was enhanced significantly by using a short wave length region of SR and elevating a substrate temperature of resist in a vacuum up to 160 ℃[2-4]. Effects of X-ray wavelength on chemical process in organic resists were discussed with using IR, ESCA and mass spectra.

Experimentals

Ultra violet syncrotron orbital radiation(UVSOR) from the electron storage ring at Institute for Molecular Science, Okazaki was used as an X-ray source, which were operated usually at 600MeV and 30mA with an orbital radius of 2.2m. Two types of resists used were fromed by a wet and a dry process which are conventional poly-methyl-methacrylate(PMMA) and plasma polymerized methyl-methacrylate(PPMMA). In order to limit the wavelength range of SR exposure, polyimide, berillium and aluminum film were selected as a filter.

Results and Discussions

When the resist films were exposed to an X-ray through any filters, the self development did not show any tendency to saturate in this experimental conditions and was enhanced significantly by heating the substrate at higher temperature than the melting point. IR spectra showed that polyer was decomposed by scissoring the chain. However the decomposition of polymer was accompanied by side chain dissociation significantly on the surface for the direct exposure without the filter.

References

1) M.Hori, S.Hattori, T.Yoneda and S.Morita; J.Vac.Sci.Technol. B4(2)(1986)500.
2) H.Yamada, S.Morita and S.Hattori; Submitted to J.Electrochemical Soc.
3) H.Yamada, T.Sato, S.Ito, M.Nakamura, S.Morita and S.Hattori; ACS, Sym. on Plasma Polymerization and Plasma Treatment of Polymer, Denver, Apr 6-10(1987).
4) Preparing submission to appropriate journal.

VUV Photodegradation of Biomolecule--DNA, ATP and Oligonucleotide

Takashi Ito

Institute of Physics, College of Arts and Sciences, University of Tokyo, Meguroku, Komaba 3-8-1, Tokyo 153

Our recent concerns on the effects of VUV radiation have been focused on such important biomolecules as DNA and related compounds. The work using SR shows that a long thread-like DNA molecule is fragmented effectively in VUV region by induced nicks on the backbone.[1] But to analyse detailed processes occurring in this complex molecules is facing some difficulties. On the other hand, with ATP molecule, a building block of such a polynucleotide, the release of adenine is observed upon VUV radiation above 7 eV.[2] Detailed processes are not understood either, but pentose sugar is a likely candidate first destructed. A oligonucleotide dApdA, two deoxyadenosine(dA) linked by phosphodiester bond (p), is thought to be a good model substance to investigate further; complete photoproducts analysis maybe possible. Densitometric analysis of thin-layer chromatogram of VUV-irradiated dApdA in the range from 7.3 to 22.5 eV showed that adenine and 5'-dAMP are the two major photoproducts independent of photon energy employed, indicating a specific site is selectively destructed in this molecule regardless of the primary excited states. The site-selective degradation from the highly excited state seems a remarkable characteristic of the VUV radiation action.

References

1) Hieda, K. et al., Photochem. Photobiol., 44, 379-383 (1986).

2) Ito, T. et al., Photochem. Photobiol., 44, 273-277 (1986).

Synchrotron Radiation-Assisted Etching of Silicon Surface

Nobuo HAYASAKA, Atsunari HIRAYA, and Kosuke SHOBATAKE

Institute for Molecular Science, Myodaiji, Okazaki 444 Japan
* Sponsorial Research Fellow from VLSI Research Center, Toshiba Corporation, Komukai Toshiba-cho, Saiwai-ku, Kawasaki 210 Japan

The photo-assisted etching of heavily phosphorous-doped polycrystalline silicon (n^+ poly-silicon) by chlorine was studied using synchrotron radiation from UVSOR as a vacuum UV light source. The apparatus used for the present study is described in 1986 UVSOR Activity Report. Formation of electronically excited Cl^+ ions upon VUV irradiation was confirmed from the emission spectra observed from a glow in the light path. The quantum yield for the removal of the Si atoms at a chlorine pressure of 0.3 Torr was found to be about 0.5 % photon^{-1} using the Ti-filtered light, which is mostly in the soft x-ray region, 1-20 nm.

Negative bias applied to the Si crystal was found to increase the etch rate. A micrograph of the silicon surface photo-etched for 230 mA hr irradiation at a 75 volt bias voltage and 0.3 Torr Cl_2 gas pressure is illustrated in Figure 1, the etch depth of which was measured to be 900 ± 100 Å, corresponding to the quantum yield =1.0%.

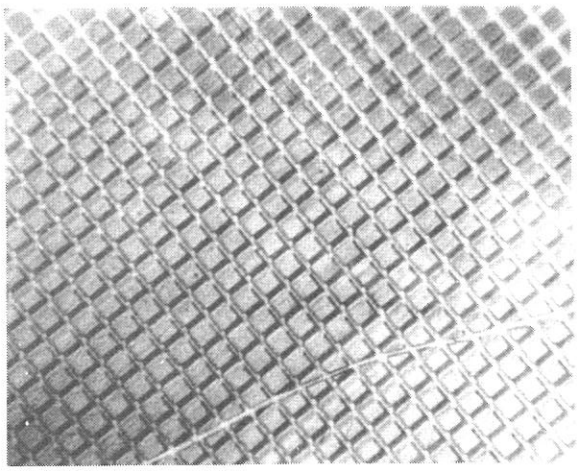

Fig. 1. Micrograph of a Si surface obtained by photo-assisted etching by Cl_2 gas at 0.3 Torr using SR with a Ti filter 500 Å thick. The rectangular lines are due to nickel mesh of 20μm used for an application of negative bias (at 75 V) to the Si sample. The etch depth was measured to be 900 ± 100 Å.

THIN FILM DEPOSITION BY VUV SYNCHROTRON RADIATION

Akira YOSHIDA

Toyohashi University of Technology, Tempaku, Toyohashi, 440

Thin films play a dominant role in solid state electronics. Various CVD (Chemical Vapor Deposition) techniques have been accepted to deposit thin films. The most common deposition methods are "thermal" CVD and plasma-enhanced CVD (PCVD). In recent years, photochemical vapor deposition (Photo CVD) is expected to be one of new low temperature fabricating processes. In most cases, lasers and/or discharge tubes are used as a light source. Many kinds of materials have been deposited by this method. Also, doping, alloying, and fabricating some devices are tried. Recently, SOR excited chemical vapor deposition (SOR CVD) has been proposed. Synchrotron radiation is suitable as a light source in photo CVD process, because of a continuous spectrum from soft X ray to visible light range, large dissociation and ionization cross sections of many reactant gases in the VUV region, and no contamination from the chamber wall in order to obtain a high quality film. Kyuragi and Urisu[1] deposited amorphous hydrogenated silicon and silicon nitride films from the gas source (SiH_4 or $SiH_4 + N_2$). Their experimental results are shown in Fig.1. We have a plan to fabricate thin films from various source gases by using the photo CVD system (Fig.2), characterize the film properties and investigate the film deposition mechanism by photochemical reaction.

1) H.Kyuragi and T.Urisu: Final Program and Late News Abstracts of 17th Conf. on Solid State Devices and Materials, p.16 , Aug. (1985)

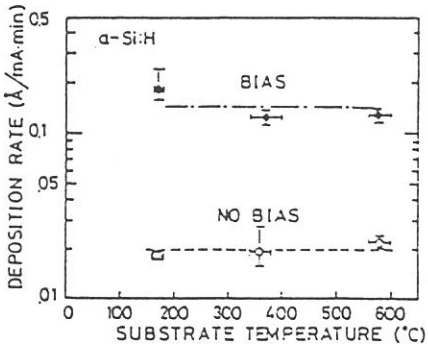

Fig.1[1]

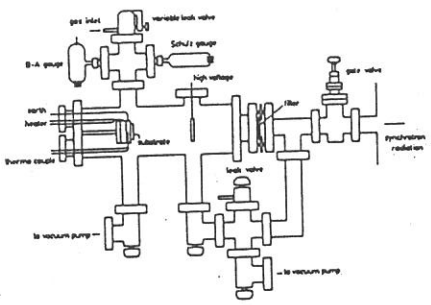

Fig.2

Concluding Remark-"Application of VUV Photons to Organic Chemistry"

Hiroo Inokuchi, Institute for Molecular Science

Since we started the first 'Okazaki Conference' in 1975, a total of 28 Conferences has been held. However, the present one, entitled "Solid State Chemistry with VUV Synchrotron Radiation" is the first Conference on synchrotron radiation research since the UVSOR Facility was constructed. The 5th Conference, entitled "Higher Excited States of Molecules and Molecular Crystals" was held on December 4-7th, 1977 on subjects related to synchrotron radiation research, but at that time our machine was only being planned.

As mentioned by Dr. Saile, UVSOR, a 'chemical machine', is located in the garden of IMS, and therefore it is quite easy for visiting scientists to work on it co-operatively with the in-house staff of our Institute. We would like to extend the co-operative research to new fields, for instance, synthetic chemistry.

Several years ago, during the observations of polarized absorption spectra of an elongated st-1,2-polybutadiene film in the vacuum ultraviolet region using ISSP-SRL, we found a peak at 284.9 $\pm$ 0.2 eV, due the to $\pi^* \longrightarrow C_{1s}$ absorption of oriented vinyl radicals as shown in Figure 1 (Chem. Phys. Lett. 70, 220 (1980)). A similar band was found in the spectrum of polyethylene film, the peak intensity of which increased appreciably with the illumination time of SRL. These findings suggest that the SRL illumination produces double bonds in hydrocarbon chains of single bonds; that is to say, we can rearrange chemical bonds by means of synchrotron radiation. Therefore, we will use the UVSOR as a 'light knife.'

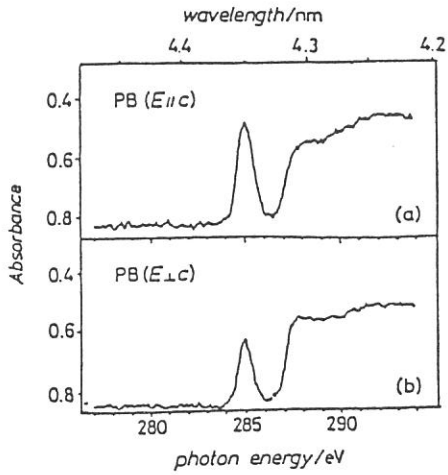

Figure 1. Polarized C_{1s} absorption spectrum of elongated st-1,2-polybutadiene film. a)E // c, b)E $\perp$ c. E: Electric vector of incident light, c: direction of elongation.

LIST OF PARTICIPANTS

F. C. Brown	Department of Physics	University of Illinois	Urbana, IL 61801, USA
S. M. B. Costa	Institute Superior Technico	Lisbon, Portugal	
T. Fujikawa	Faculty of Engineering	Yokohama National University	Hodogaya, Yokohama 240
H. Fujimoto	Inst. for Molecular Science	Myodaiji, Okazaki 444	
K. Fukui	Inst. for Molecular Science	Myodaiji, Okazaki 444	
J. R. Grover	Chemistry Department	Brookhaven National Lab.	Upton, NY 11973, USA
Y. Hatano	Department of Chemistry	Tokyo Institute of Technology	Meguro, Tokyo 152
N. Hayasaka	VLSI Research Center	Toshiba Corporation	Saiwai, Kawasaki 210
H. Hayashi	Inst. for Molecular Science	Myodaiji, Okazaki 444	
A. Hiraya	Inst. for Molecular Science	Myodaiji, Okazaki 444	
N. Hoshino	Inst. for Molecular Science	Myodaiji, Okazaki 444	
A. Ichimiya	Department of Applied Physics	Nagoya University	Chikusa, Nagoya 464
T. Imamura	Inst. for Molecular Science	Myodaiji, Okazaki 444	
T. Inagaki	Osaka Kyoiku University	Tennoji, Osaka 543	
H. Inokuchi	Inst. for Molecular Science	Myodaiji, Okazaki 444	
T. Ishii	Synchrotron Radiation Lab.	ISSP, University of Tokyo	Tanashi, Tokyo 188
T. Ito	College of Arts and Sciences	University of Tokyo	Meguro, Tokyo 153
N. Itoh	Department of Physics	Nagoya University	Chikusa, Nagoya 464
Y. Iwasa	Faculty of Engineering	University of Tokyo	Bunkyo, Tokyo 113
N. Kakuta	Inst. for Molecular Science	Myodaiji, Okazaki 444	
H. Kanamori	Inst. for Molecular Science	Myodaiji, Okazaki 444	
H. Kanzaki	Ashigara Research Laboratories	Fuji Photo Film Co., Ltd.	Minamiashigara, Kanagawa 250-01
K. Kimura	Inst. for Molecular Science	Myodaiji, Okazaki 444	
J. Klein	Centre de Recherches Nucleares	& Universite Louis Pasteur	Strasbourg, France
K. Kobayashi	College of Liberal Arts	Toyama University	Toyama 930
T. Kobayashi	Department of Physics	University of Tokyo	Bunkyo, Tokyo 113
N. Kosugi	Department of Chemistry	University of Tokyo	Bunkyo, Tokyo 113
Masahiro Kotani	Department of Chemistry	Gakushuin University	Toshima, Tokyo 171
Masao Kotani	Inst. for Molecular Science	Myodaiji, Okazaki 444	
I. Koyano	Inst. for Molecular Science	Myodaiji, Okazaki 444	
Y. Maruyama	Inst. for Molecular Science	Myodaiji, Okazaki 444	
H. Masuhara	Kyoto Institute of Technology	Sakyo, Kyoto 606	
T. Matsukawa	College of General Education	Osaka University	Toyonaka, Osaka 560
T. Mitani	Inst. for Molecular Science	Myodaiji, Okazaki 444	
S. Morita	Department of Electronics	Nagoya University	Chikusa, Nagoya 464
I. H. Munro	Synchrotron Radiatio Source	Daresbury Laboratory, SERC	Warrigton WA4 4AD, UK
T. Murata	Kyoto University of Education	Fushimi, Kyoto 612	
S. Nagaoka	Inst. for Molecular Science	Myodaiji, Okazaki 444	
H. Nakagawa	Department of Electronics	Fukui University	Fukui 910

Y. Nakai	Department of Physics	Kyoto University	Sakyo, Kyoto 606
K. Nakamura	Department of Physics	Kyoto University	Sakyo, Kyoto 606
M. Nakamura	Inst. for Molecular Science	Myodaiji, Okazaki 444	
N. Nakashima	Inst. for Molecular Science	Myodaiji, Okazaki 444	
T. Nanba	Department of Physics	Tohoku University	Sendai 980
K. Nasu	Inst. for Molecular Science	Myodaiji, Okazaki 444	
S. Ohtani	Institute of Plasma Physics	Nagoya University	Chikusa, Nagoya 464
T. Okada	Faculty of Engineering Science	Osaka University	Toyonaka Osaka, 560
K. Okuyama	Inst. for Molecular Science	Myodaiji, Okazaki 444	
I. Plazibat	University of Split	Split, Yougoslavia	
V. Saile	HASYLAB, DESY	Notkest. 85, D-2000 Hamburg 52	West Germany
N. Sato	Department of Chemistry	Kumamoto University	Kumamoto 860
S. Sato	Photon Factory	Nat. Lab. for High Energy Phys.	Oho, Ibaraki 305
M. Satoko	Inst. for Molecular Science	Myodaiji, Okazaki 444	
K. Seki	Dept. of Materials Science	Hiroshima University	Naka, Hiroshima 730
T. K. Sham	Chemistry Department	Brookhaven National Lab.	Upton, NY 11973, USA
H. Shiromaru	Inst. for Molecular Science	Myodaiji, Okazaki 444	
K. Shobatake	Inst. for Molecular Science	Myodaiji, Okazaki 444	
P.-S. Song	Department of Chemistry	University of Nebrasaka	Lincoln, NE 68588-0304, USA
R. Stockbauer	National Bureau of Standards	Gaithersburg, Maryland 20899	USA
I. Suzuki	Electrotechnical Laboratory	Sakura, Ibaraki 305	
M. Suzuki	Inst. for Molecular Science	Myodaiji, Okazaki 444	
S. Suzuki	Inst. for Molecular Science	Myodaiji, Okazaki 444	
K. Tabayashi	Inst. for Molecular Science	Myodaiji, Okazaki 444	
Y. Takagi	Inst. for Molecular Science	Myodaiji, Okazaki 444	
T. Takahashi	Department of Physics	Tohoku University	Sendai 980
N. Tamai	Inst. for Molecular Science	Myodaiji, Okazaki 444	
K. Tanaka	Photon Factory	Nat. Lab. for High Energy Phys.	Oho, Ibaraki 305
K. Tohji	Inst. for Molecular Science	Myodaiji, Okazaki 444	
J. Tanaka	Department of Chemistry	Nagoya University	Chikusa, Nagoya 464
M. Taniguchi	Synchrotron Radiation Lab.	ISSP, University of Tokyo	Tanashi, Tokyo 188
K. Tanimura	Department of Physics	Nagoya University	Chikusa, Nagoya 464
Y. Udagawa	Inst. for Molecular Science	Myodaiji, Okazaki 444	
N. Ueno	Faculty of Engineering,	Chiba University	Chiba 260
Y. Wada	Inst. for Molecular Science	Myodaiji, Okazaki 444	
M. Watanabe	Inst. for Molecular Science	Myodaiji, Okazaki 444	
K. Yamamoto	Inst. for Molecular Science	Myodaiji, Okazaki 444	
I. Yamazaki	Inst. for Molecular Science	Myodaiji, Okazaki 444	
T. Yasue	Department of Applied Physics	Nagoya University	Chikusa, Nagoya 464
A. Yoshida	Toyohashi Univ. of Technology	Tempaku, Toyohashi 440	
K. Yoshihara	Inst. for Molecular Science	Myodaiji, Okazaki 444	

APPENDIX

ORGANIZATION

Staff

Director	Hiroo INOKUCHI	Professor
Light Source Group		
	Toshio KASUGA	Associate Professor
	Hiroto YONEHARA	Research Associate
	Toshio KINOSHITA	Engineer
	Masami HASUMOTO	Engineer
Measurement Systems Group		
	Makoto WATANABE	Associate Professor
	Kazutoshi FUKUI	Research Associate
	Kusuo SAKAI	Section Chief Engineer
	Osamu MATSUDO	Unit Chief Engineer
	Jun-ichiro YAMAZAKI	Engineer
	Eiken NAKAMURA	Engineer
Secretary	Takayo OHTE	
Guest Scientists		
	Hisashi KOBAYAKAWA	Adjunct Associate Professor from Nat. Lab. High Enegy Phys. (April 1986 - March 1987)
	Teruo HOSOKAWA	Visiting Research Fellow from NTT (April 1985 - March 1987)

Representative of Beam Lines

BL2A	Kosuke SHOBATAKE	Dept. Molecular Assemblies
BL2B2	Katsumi KIMURA	Dept. Molecular Assemblies
BL3B	Inosuke KOYANO	Dept. Molecular Assemblies
BL8B2	Hiroo INOKUCHI	UVSOR and Dept. Molecular Assemblies
Others	Makoto WATANABE	UVSOR

Steering Committee (June 1986 - March 1988)

Hiroo INOKUCHI	IMS	Chairman
Toshio KASUGA	IMS	
Katsumi KIMURA	IMS	
Inosuke KOYANO	IMS	
Tadayoshi SAKATA	IMS	
Yasuo UDAGAWA	IMS	
Makoto WATANABE	IMS	
Hisashi KOBAYAKAWA	IMS and Nat. Lab. High Energy Phys.	
Yoshihiko HATANO	Tokyo Inst. Tech.	
Takehiko ISHII	Univ. of Tokyo	
Yoshio NAKAI	Kyoto Univ.	
Takeshi NAMIOKA	Tohoku Univ.	
Shunsuke OHTANI	Nagoya Univ.	
Tadashi OKADA	Osaka Univ.	
Taizo SASAKI	Osaka Univ.	

LIST OF PUBLICATIONS (1986)

1)"The UVSOR Facility : Status in 1985"
M.Watanabe
Nucl. Instr. Meth. Phys. Res. A246 (1986) 15.

2)"A Plane-Grating Monochromator for 2 eV $\leq$ hv $\leq$ 150 eV"
K.Seki, H.Nakagawa, K.Fukui, E.Ishiguro, R.Kato, T.Mori, K.Sakai and M.Watanabe
Nucl. Instr. Meth. Phys. Res. A246 (1986) 264.

3)"The TEPSICO-II Apparatus for Use with UVSOR Synchrotron Radiation"
I.Koyano, K.Tanaka, T.Kato, S.Suzuki and E.Ishiguro
Nucl. Instr. Meth. Phys. Res. A246 (1986) 507.

4)"Normal Incidence Monochromator with an Aberration-Corrected Concave Grating for Synchrotron Radiation"
M.Itou, T.Harada, T.Kita, K.Hasumi, I.Koyano and K.Tanaka
Appl. Optics 25 (1986) 2240.

5)"Ion-Clearing System of UVSOR Stroage Ring"
T.Kasuga
Jpn. J. Appl. Phys. 25 (1986) 1711.

6)"Far-Infrared Spectroscopy by Synchrotorn Radiation at the UVSOR Facility"
T.Nanba, Y.Urashima, M.Ikezawa, M.Watanabe, E.Nakamura, K.Fukui and H.Inokuchi
J. Infrared & Millimeter Waves 7 (1986) 1769.

7)"The TEPSICO-II Apparatus at UVSOR and Threshold Electron Spectra of Some Molecules over the Wavelength Range 35-120 nm"
S.Suzuki, S.Nagaoka, I.Koyano, K.Tanaka and T.Kato
Z. Phys. D 4 (1986) 111.

8)"Photon Stimulated Desorption of Positive Ions from LiF"
T.Yasue, T.Gotoh, A.Ichimiya, Y.Kawaguchi, M.Kotani, S.Ohtani, Y.Shigeta, S.Takagi, Y.Tazawa and G.Tominaga
Jpn. J. Appl. Phys. 25 (1986) L363.

9)"$CCl_2(\tilde{A}^1B_1)$ Radical Formation in VUV Photolyses of CCl_4 and $CBrCl_3$"
T.Ibuki, N.Takahashi, A.Hiraya and K.Shobatake
J. Chem. Phys. 85 (1986) 5717.

LOCATION

Ultraviolet Synchrotron Orbital Radiation (UVSOR) Facility, Institute for Molecular Science (IMS) is located at Okazaki. Okazaki (population 280,000) is 260 km southwest of Tokyo, and can be reached by train in about 3 hours from Tokyo via New Tokaido Line (Shinkansen) and Meitetsu Line.

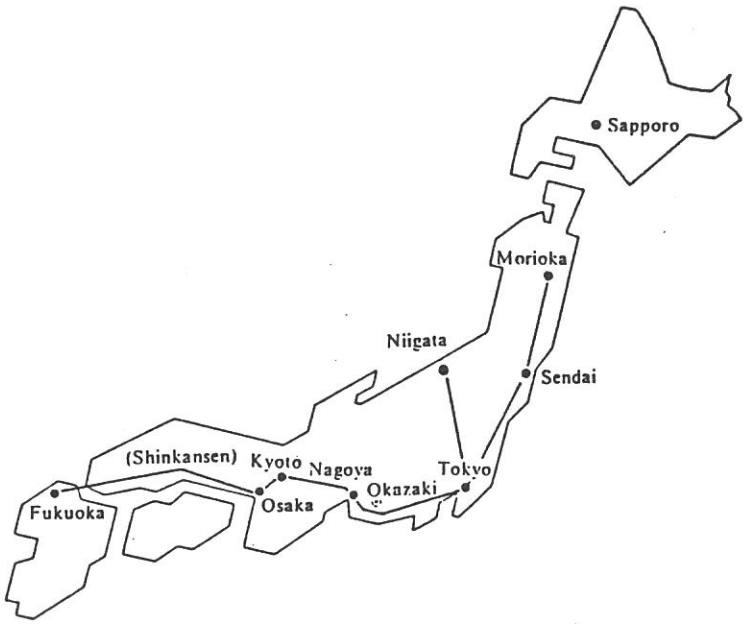

Address is as follows.
UVSOR Facility
Institute for Molecular Science
Myodaiji, Okazaki 444, JAPAN

Telephone : 0564-54-1111 (IMS), ex. 400-409 (UVSOR)
Fax : 0564-54-2254 (IMS)
Telex : 4537475 KOKKEN J (IMS)